

**EVALUATION OF TERRESTRIAL LASER SCANNING AND GROUND  
PENETRATING RADAR FOR FIELD-BASED HIGH-THROUGHPUT  
PHENOTYPING IN WHEAT BREEDING**

A Dissertation

by

SEAN MICHAEL THOMPSON

Submitted to the Office of Graduate and Professional Studies of  
Texas A&M University  
in partial fulfillment of the requirements for the degree of

DOCTOR OF PHILOSOPHY

Chair of Committee,	Dirk B. Hays
Co-Chair of Committee,	Amir M. H. Ibrahim
Committee Members,	Ronald E. Lacey
	Matthew P. Reynolds
	R. Esten Mason
	J. Creighton Miller Jr.
Head of Department,	David D. Baltensperger

August 2014

Major Subject: Plant Breeding

Copyright 2014 Sean Michael Thompson

## ABSTRACT

Targeted adaptive physiological trait introgression, a method by which breeders seek to introduce specific characteristics into breeding germplasm in a specific and targeted manner, is one of the primary methods breeders are using to develop cultivars optimized for performance and yield under heat and drought conditions. In traditional breeding platforms, this is carried out in a stepwise fashion, with the crossing of parental lines and the phenotype-driven selection of offspring.

As with other adaptive physiological traits, rapid field-based high-throughput phenotyping of early season aboveground biomass and ideal root architecture is limited by our inability to accurately and nondestructively characterize these important traits. Terrestrial laser scanning (TLS) and ground penetrating radar (GPR) have the potential to fill this gap by non-invasively estimating biomass and mapping three-dimensional above- and below-ground vegetation.

The research objective was to evaluate the use of TLS to estimate aboveground wheat (*Triticum aestivum* L.) biomass. Linear regressions comparing mean canopy height and total plot forage yield for each experimental plot across four replications was poorly correlated ( $R^2$  0.08). Mean plot normalized difference vegetation index measurements were evaluated against total plot forage biomass with limited correlation ( $R^2$  0.036). The mean value of the TLS elevation points had the highest correlation with both plot

( $R^2$  0.09458) and sub plot ( $R^2$  0.37984) forage yield as compared to traditional platforms.

GPR is a remote sensing technology that has been successfully used in the evaluation of coarse tree root biomass. Incorporating GPR into current crop phenotyping methodologies could potentially provide a long awaited solution to the current inability to efficiently phenotype roots under realistic field conditions. Here, the utility of using GPR to estimate root biomass of wheat was evaluated. GPR ability to predict root presence and absence was tested and GPR was able to differentiate root mass from soil significantly ( $\alpha = 0.95$ ,  $t = 1.96022$ ). Linear regression between Log10 of the mean GPR amplitude return at the 0-3 ns range was compared with agronomic breeding traits. Overall increased amplitude was observed in plots scoring higher with regard to overall yield and yield components.

## **DEDICATION**

This doctoral dissertation is dedicated to the very few that are as good as spring itself.

“When spring came, even the false spring, there were no problems except where to be happiest. The only thing that could spoil a day was people and if you could keep from making engagements, each day had no limits. People were always the limiters of happiness except for the very few that were as good as spring itself.”

(Hemingway, 1964)



## **ACKNOWLEDGEMENTS**

I would like to thank my committee members, Dirk B. Hays, Amir M. H. Ibrahim, Ronald E. Lacey, Matthew P. Reynolds, R. Esten Mason, and J. Creighton Miller Jr. for their guidance and support throughout the course of this research. In addition, I thank Robert A. Washington-Allen for offering his expertise, without this research would not have been possible.

Thanks go to my friends, colleagues, faculty, and staff of the Soil and Crop Sciences Department for making my time at Texas A&M University a wonderful experience. A special thanks goes to Alfredo Delgado for his assistance and input into this research every step of the way.

I would like to extend my gratitude to the International Maize and Wheat Improvement Center (CIMMYT) for supporting my projects and hosting my research in Ciudad Obregon, Sonora, Mexico. I am forever grateful to every member of the CIMMYT team for his or her kind support. Additionally, I thank C. Mariano Cossani for his guidance and direction as both a mentor and friend.

Finally, thanks to both of my mothers, my father, and my brothers for their encouragement and to my wife, Whitney, thank you for your patience and love.

## TABLE OF CONTENTS

	Page
ABSTRACT .....	ii
DEDICATION .....	iv
ACKNOWLEDGEMENTS .....	v
TABLE OF CONTENTS .....	vi
LIST OF FIGURES.....	viii
LIST OF TABLES .....	xvi
CHAPTER I INTRODUCTION .....	1
Crop breeding.....	1
Improving crop breeding.....	2
Wheat a global grain for future environments .....	2
Target adaptive traits.....	4
Phenotyping technologies .....	5
Research .....	6
"Qdlgevkxg"3.....	9
"Qdlgevkxg"4.....	9
CHAPTER II LITERATURE REVIEW .....	10
Facilitating plant breeding.....	10
Plant breeding.....	13
Field-based high-throughput phenotyping .....	18
Target physiological traits for field-based high-throughput phenotyping .....	22
Current phenotyping methodologies .....	27
Target field-based high throughput phenotyping platforms.....	27
Management and analysis: field-based high-throughput phenotyping data.....	31
Forward strategies .....	33
CHAPTER III USE OF TERRESTRIAL LASER SCANNING IN CROP BREEDING FOR EVALUATION OF EARLY GROUND COVER AND FORAGE ..	34
Overview .....	34
Introduction .....	35
Materials and methods .....	40

Results .....	50
Discussion .....	65
Conclusions .....	67
 CHAPTER IV UTILITY OF GROUND PENETRATING RADAR FOR FIELD- BASED HIGH-THROUGHPUT PHENOTYPING OF WHEAT ROOTS.....	 68
Overview .....	68
Introduction .....	69
Materials and methods .....	87
Results .....	95
Discussion .....	120
Conclusions .....	125
 CHAPTER V SUMMARY .....	 127
Field-based high-throughput phenotyping .....	127
Terrestrial laser scanning .....	127
Ground penetrating radar .....	128
 LITERATURE CITED .....	 129
 APPENDIX A .....	 139
 APPENDIX B .....	 141

## LIST OF FIGURES

	Page
Figure 1. Application of high-throughput phenotyping to cultivar development in a wheat breeding program. ....	20
Figure 2. Data collection using a Leica ScanStation 2 terrestrial laser scanner. The Leica ScanStation 2 is shown mounted on a surveyor's tripod collecting data to be compare with traditional biomass measurements. ....	39
Figure 3. Field illustration depicting experimental plot layout and field ranges (1-4) and relative location of terrestrial laser scanning positions. ....	47
Figure 4. Point cloud depicting terrestrial laser scanning data of experimental plot. ...	48
Figure 5. Distribution analysis of plot forage biomass across four replications for the first and second forage biomass sampling events of the growing season. ....	51
Figure 6. Distribution analysis of plot forage biomass across four replications for the third and fourth forage biomass sampling events of the growing season. ....	52
Figure 7. Linear regression comparing sub plot forage yield and total plot forage yield for each experimental plot across four replications.....	53
Figure 8. Linear regressions comparing mean canopy height and total plot forage yield for each experimental plot across four replications.....	55
Figure 9. Linear regressions comparing visual forage biomass score and total plot forage yield for each experimental plot across four replications. ....	55
Figure 10. Linear regressions comparing normalized difference vegetation index (NDVI) and total plot forage yield for each experimental plot across four replications. ....	56
Figure 11. Linear regressions comparing normalized difference vegetation index (NDVI) and wheat plants per square meter for each experimental plot across four replications.....	56

	Page
Figure 12. Linear regressions comparing total terrestrial laser scanner point cloud points collected and total plot forage yield for each experimental plot across four replications.....	58
Figure 13. Linear regressions comparing total terrestrial laser scanner point cloud points collected and sub plot forage yield for each experimental plot across four replications.....	58
Figure 14. Linear regressions comparing terrestrial laser scanner elevation mean point cloud points collected and total plot forage yield for each experimental plot across four replications.....	59
Figure 15. Linear regressions comparing terrestrial laser scanner elevation mean point cloud points collected and sub plot forage yield for each experimental plot across four replications.....	59
Figure 16. Linear regressions comparing terrestrial laser scanner elevation max point cloud points collected and total plot forage yield for each experimental plot across four replications.....	60
Figure 17. Linear regressions comparing terrestrial laser scanner elevation max point cloud points collected and sub plot forage yield for each experimental plot across four replications.....	60
Figure 18. Linear regressions comparing total terrestrial laser scanner point cloud points collected and mean plant canopy height for each experimental plot across four replications. ....	62
Figure 19. Linear regressions comparing total terrestrial laser scanner point cloud points collected and normalized difference vegetation index (NDVI) for each experimental plot across four replications. ....	62
Figure 20. Linear regressions comparing terrestrial laser scanner elevation mean point cloud points collected and mean plant canopy height for each experimental plot across four replications.....	63
Figure 21. Linear regressions comparing terrestrial laser scanner elevation mean point cloud points collected and mean normalized difference vegetation index (NDVI) for each experimental plot across four replications. ....	63

Figure 22. Linear regressions comparing terrestrial laser scanner elevation max point cloud points collected and mean plant canopy height for each experimental plot across four replications.....	64
Figure 23. Linear regressions comparing terrestrial laser scanner elevation max point cloud points collected and mean normalized difference vegetation index (NDVI) for each experimental plot across four replications. ....	64
Figure 24. Illustration of the potential impact of increased root systems on carbon, water and nutrient sequestration. Atmospheric carbon dioxide is reduced by photosynthesis contributing to soil carbon sequestration. Improving crop roots could increase steady-state trapping of carbon, nutrients, and water leading to improved drought- and flooding tolerance, greater biomass yields, and better soil structure. Figure adapted from (Kell, 2011).....	72
Figure 25. Destructive sampling of wheat roots by soil coring. Determining root biomass of wheat plants (A) hydraulic soil core extraction, (B) separation of root material from soil by washing, (C) hand sieving of root material, (D) drying samples, and (E) weighing dried root samples. To evaluate rooting depth the same procedure is followed however core samples are separated into 30 cm segments and treated independently.....	76
Figure 26. Current agricultural geophysical techniques. (A) Resistivity (Image: Veris technologies, Salina, KS, USA). (B) Electromagnetic Induction (C) Groud Penetrating Radar.....	78
Figure 27. Components of a ground penetrating radar system. The ground penetrating radar system is comprised of three main components; (A) control computer, (B) control unit, and (C) the antenna. ....	80
Figure 28. Schematic illustration of ground penetrating radar concept. (A) Ground penetrating radar functions by transmission of radio waves into the ground and detection of their reflected signals from subsurface interfaces separating layers differing relative dielectric permittivity. The antenna functions in both the transmitting and receiving of the radio wave. The radar pulse is timed from the point of transmission into the ground to the interaction with dielectric interface to establish distance to the target. (B) Corresponding radargram representing a series of digitized trace signals equidistantly spaced along the profile axis. ....	82

Figure 29. Ground penetrating radar wave conical radiating pattern. Spreading footprint of ground penetrating radar radio wave increases with distance from transmission antenna.....	85
Figure 30. Ground penetrating radar signal components. (A) Trace signal recorder by the receiver. (B) Digitized signals sampled from trace signal. (C) Multiple digitized samples representing a series of trace signals. (D) Radargram representing a series of digitized trace signals equidistantly spaced along the profile axis. (E) Multiple radargrams are combined spatially to produce a three-dimensionally accurate representation of the subsurface.....	88
Figure 31. Schematic diagram of the study site at the field and plot level. This study was designed in a randomized complete block with four replications of both the waterlogging and control treatments. Plots consisted of seven rows 18 cm apart in a plot area of 1.25 m wide by 6 m long. Red lines indicate the location of ground penetrating radar data collection profiles within each plot. ....	89
Figure 32. Schematic of ground penetrating radar measurement area. Ground penetrating radar profiles (4 total) were collected for each experimental plot for analysis. ....	94
Figure 33. Ground penetrating radar profile. Ground penetrating radar profile from experimental trial. (A) Total ground penetrating radar profile spanning total length of field across eight experimental plots (6 m) and alleyways (1.5 m). (B) Subset ground penetrating radar profile depicting known plot locations. ....	97
Figure 34. Ground penetrating radar amplitude map. Field level distribution of ground penetrating radar amplitude compared with experimental plot distribution.....	98
Figure 35. Students T test comparing root presence and absence. Predictive ability of Ground penetrating radar amplitude return compared with known plot location for root presence and absence.....	99
Figure 36. Linear regression between the Log10 of mean ground penetrating radar amplitude returned for the 0-3 ns range and total plot yield of 28 wheat varieties. ....	101

	Page
Figure 37. Linear regression between the Log10 of mean ground penetrating radar amplitude returned for the 0-3 ns range and average yield of each experimental replication. ....	101
Figure 38. Linear regression between the Log10 of mean ground penetrating radar amplitude returned for the 0-3 ns range and average thousand kernel weight (TKW) of 28 wheat varieties. ....	102
Figure 39. Linear regression between the Log10 of mean ground penetrating radar amplitude returned for the 0-3 ns range and average thousand kernel weight (TKW) of each experimental replication. ....	102
Figure 40. Linear regression between the Log10 of mean ground penetrating radar amplitude returned for the 0-3 ns range and average kernel weight per spike (KWS) of 28 wheat varieties. ....	103
Figure 41. Linear regression between the Log10 of mean ground penetrating radar amplitude returned for the 0-3 ns range and average kernel weight per spike (KWS) of each experimental replication. ....	103
Figure 42. Linear regression between the Log10 of mean ground penetrating radar amplitude returned for the 0-3 ns range and average kernel number per spike (KNS) of 28 wheat varieties. ....	104
Figure 43. Linear regression between the Log10 of mean ground penetrating radar amplitude returned for the 0-3 ns range and average kernel number per spike (KNS) of each experimental replication. ....	104
Figure 44. Linear regression between the Log10 of mean ground penetrating radar amplitude returned for the 0-3 ns range and average normalized difference vegetation index (NDVI) of 28 wheat varieties measured on 3/23/2013. ....	105
Figure 45. Linear regression between the Log10 of mean ground penetrating radar amplitude returned for the 0-3 ns range and average normalized difference vegetation index (NDVI) of each experimental replication measured on 3/23/2013. ....	105
Figure 46. Linear regression between the Log10 of mean ground penetrating radar amplitude returned for the 0-3 ns range and average normalized difference vegetation index (NDVI) of 28 wheat varieties measured on 3/27/2013. ....	106



	Page
Figure 47. Linear regression between the Log10 of mean ground penetrating radar amplitude returned for the 0-3 ns range and average normalized difference vegetation index (NDVI) of each experimental replication measured on 3/27/2013. ....	106
Figure 48. Linear regression between the Log10 of mean ground penetrating radar amplitude returned for the 0-3 ns range and average normalized difference vegetation index (NDVI) of 28 wheat varieties measured on 4/10/2013. ....	107
Figure 49. Linear regression between the Log10 of mean ground penetrating radar amplitude returned for the 0-3 ns range and average normalized difference vegetation index (NDVI) of each experimental replication measured on 4/10/2013. ....	107
Figure 50. Linear regression between the Log10 of mean ground penetrating radar amplitude returned for the 0-3 ns range and average normalized difference vegetation index (NDVI) of 28 wheat varieties measured on 4/19/2013. ....	108
Figure 51. Linear regression between the Log10 of mean ground penetrating radar amplitude returned for the 0-3 ns range and average normalized difference vegetation index (NDVI) of each experimental replication measured on 4/19/2013. ....	108
Figure 52. Linear regression between the Log10 of mean ground penetrating radar amplitude returned for the 0-3 ns range and average normalized difference vegetation index (NDVI) of 28 wheat varieties measured on 4/29/2013. ....	109
Figure 53. Linear regression between the Log10 of mean ground penetrating radar amplitude returned for the 0-3 ns range and average normalized difference vegetation index (NDVI) of each experimental replication measured on 4/29/2013. ....	109
Figure 54. Linear regression between the Log10 of mean ground penetrating radar amplitude returned for the 0-3 ns range and average normalized difference vegetation index (NDVI) of 28 wheat varieties measured on 5/09/2013. ....	110

Figure 55. Linear regression between the Log10 of mean ground penetrating radar amplitude returned for the 0-3 ns range and average normalized difference vegetation index (NDVI) of each experimental replication measured on 5/09/2013. ....	110
Figure 56. Linear regression between the Log10 of mean ground penetrating radar amplitude returned for the 0-3 ns range and average normalized difference vegetation index (NDVI) of 28 wheat varieties measured on 5/24/2013. ....	111
Figure 57. Linear regression between the Log10 of mean ground penetrating radar amplitude returned for the 0-3 ns range and average normalized difference vegetation index (NDVI) of each experimental replication measured on 5/24/2013. ....	111
Figure 58. Linear regression between the Log10 of mean ground penetrating radar amplitude returned for the 0-3 ns range and average normalized difference vegetation index (NDVI) of 28 wheat varieties measured on 5/31/2013. ....	112
Figure 59. Linear regression between the Log10 of mean ground penetrating radar amplitude returned for the 0-3 ns range and average normalized difference vegetation index (NDVI) of each experimental replication measured on 5/31/2013. ....	112
Figure 60. Linear regression between the Log10 of mean ground penetrating radar amplitude returned for the 0-3 ns range and average fresh weight (FW) root biomass collected at 0-30 cm for each wheat variety. ....	114
Figure 61. Linear regression between the Log10 of mean ground penetrating radar amplitude returned for the 0-3 ns range and average fresh weight (FW) root biomass collected at 0-30 cm for each experimental replication. ....	114
Figure 62. Linear regression between the Log10 of mean ground penetrating radar amplitude returned for the 0-3 ns range and average fresh weight (FW) root biomass collected at 30-60 cm for each wheat variety. ....	115
Figure 63. Linear regression between the Log10 of mean ground penetrating radar amplitude returned for the 0-3 ns range and average fresh weight (FW) root biomass collected at 30-60 cm for each experimental replication. ....	115

Figure 64. Linear regression between the Log10 of mean ground penetrating radar amplitude returned for the 0-3 ns range and average fresh weight (FW) root biomass collected at 0-60 cm for each wheat variety. ....	116
Figure 65. Linear regression between the Log10 of mean ground penetrating radar amplitude returned for the 0-3 ns range and average fresh weight (FW) root biomass collected at 0-60 cm for each experimental replication. ....	116
Figure 66. Linear regression between the Log10 of mean ground penetrating radar amplitude returned for the 0-3 ns range and average dry weight (DW) root biomass collected at 0-30 cm for each wheat variety. ....	117
Figure 67. Linear regression between the Log10 of mean ground penetrating radar amplitude returned for the 0-3 ns range and average dry weight (DW) root biomass collected at 0-30 cm for each experimental replication. ....	117
Figure 68. Linear regression between the Log10 of mean ground penetrating radar amplitude returned for the 0-3 ns range and average dry weight (DW) root biomass collected at 30-60 cm for each wheat variety. ....	118
Figure 69. Linear regression between the Log10 of mean ground penetrating radar amplitude returned for the 0-3 ns range and average dry weight (DW) root biomass collected at 30-60 cm for each experimental replication. ....	118
Figure 70. Linear regression between the Log10 of mean ground penetrating radar amplitude returned for the 0-3 ns range and average dry weight (DW) root biomass collected at 0-60 cm for each wheat variety. ....	119
Figure 71. Linear regression between the Log10 of mean ground penetrating radar amplitude returned for the 0-3 ns range and average dry weight (DW) root biomass collected at 0-60 cm for each experimental replication. ....	119
Figure 72. Field soil electrical conductivity map of experimental trial. Differences in electrical conductivity across experimental field trial as predicted by kriging. ....	122
Figure 73. Illustration of the Feekes scale of growth stages in cereals (Large, 1954).....	139

## LIST OF TABLES

	Page
Table 1. Overview of current field-based high-throughput phenotyping (FBHTP) technologies in crop breeding.....	24
Table 2. Overview of common field-based phenotyping techniques.....	75

# **CHAPTER I**

## **INTRODUCTION**

### **Crop breeding**

Crop breeding, improving the heredity of plants for the benefit of man, is based on linking genetic variation to observed phenotypes (Benfey and Mitchell-Olds, 2008). Breeders cross lines with different but complementary genes in hopes of generating progeny able to outperform both parents, a condition termed transgressive segregation (Bernardo, 2010). Individuals that express targeted traits are selected from these high performing progeny. Since genes are the unit of heredity, procedures for gene manipulation and genetic principles allow for accurate prediction of resulting progeny based on analysis of their genetic makeup (Sleper and Poehlman, 2006). In the traditional phenotypic selection driven model, the breeding process is time consuming and limited by the breeder's available resources (Tester and Langridge, 2010). Molecular markers, the association of deoxyribonucleic acids polymorphism with a given phenotype, allow plant breeders to select for phenotypic traits with great efficiency while reducing time and resources (Boopathi, 2013). The effectiveness of marker-assisted selection (MAS) in breeding relies on accurate and cost effective platforms for genotyping and phenotyping (Collard and Mackill, 2008a). Recent technological advances in genotyping have improved accuracy while reducing cost, thus increasing the possible impact of MAS on crop breeding programs (Davey et al., 2011). Accurate

field-based phenotyping is critical to developing molecular markers capable of predicting traits of interest (White et al., 2012).

### **Improving crop breeding**

Molecular markers must be strongly linked with expression of the desired phenotypic trait (Collard and Mackill, 2008a). In combination with only being able to evaluate limited population size and numbers of different populations the current limitation to MAS is the development of phenotyping tools capable of accurately phenotyping responses to a given environment (Poland and Rife, 2012). Field-based high-throughput phenotyping (FBHTP) technologies, tools capable of precise and accurate plant phenotyping at the field level, are needed for rapid, non-destructive phenotypic assessment of breeding populations for traits over physiological development as well those undetectable using traditional methods (White et al., 2012). The ability of plant breeders to dissect and capitalize on genetic traits associated with increased yield and stress tolerance is limited by a lack of FBHTP tools capable of accurate and cost effective characterization of target traits (Araus and Cairns, 2013).

### **Wheat a global grain for future environments**

Cultivated globally, wheat (*Triticum spp.*) is second only to maize in total hectares of cereal production and the primary source of dietary calories for those living in the

poorest countries (Msangi et al., 2009). Wheat is relatively well adapted to dry environments and research has shown steady progress in efforts to increase its performance in heat and drought stressed conditions (Ammar et al., 2008; Trethowan et al., 2002). However, current cultivars grown in temperate regions of the world are limited to an increase in temperature of 1-3°C, beyond which their productivity will be negatively impacted (IPCC, 2007). Wheat grown in tropical and sub tropical regions will be negatively impacted by less (1-2°C) of an increase in temperature (Hodson and White, 2007). Performance of wheat in hot environments, which are often co-associated with dry environments, is not promising and substantial yield losses have been reported (Reynolds et al., 1994; Wardlaw and Wrigley, 1994). In order to achieve the wheat production levels required to feed the world, breeders need to adapt new technologies to enable selection of crop varieties capable of maintaining plant productivity despite the predicted increasing occurrences of heat and drought stress (Tester and Langridge, 2010). Increases in atmospheric temperature and altered patterns of precipitation, the result of elevated carbon dioxide on climate stability, are negatively impacting global food security (Schmidhuber and Tubiello, 2007).

Primary constraints to global wheat production are drought and high temperature stress during the vegetative and reproductive stages (Bita and Gerats, 2013). Increased temperatures during these critical physiological stages reduce both grain weight and grain number, ultimately lowering total yield (Bita and Gerats, 2013; Ferris et al., 1998). Indeed, under abiotic stress, plants undergo a series of changes, including altered gene

expression and adaptive physiological responses, which negatively impact yield (Shinozaki and Yamaguchi-Shinozaki, 2007). Wheat germplasm, adapted and exotic, harbor multiple adaptive traits with the potential to buffer these impacts of high temperatures and drought stress (Reynolds, 2010). Historically, breeding efforts for targeted adaptive traits such as dwarf stature and resistance to biotic and abiotic stressors have mediated eras of global food insecurity (Ronald, 2011).

### **Target adaptive traits**

Early season aboveground biomass is one adaptive trait shown to increase photosynthesis and radiation-use efficiency, ultimately providing the plant a temporal advantage during the growing season (Reynolds et al., 2010). By utilizing the availability of early season moisture, these adapted varieties are better able to establish the photo-assimilates needed to complete grain-fill in stressed environments (Whan et al., 1991). Likewise, greater root elongation can play a critical role in allowing plants to reach deeper soil profiles, allowing access to needed water and nutrients (Bengough et al., 2011). Selection of varieties possessing these beneficial attributes has been hampered because common methodologies for phenotyping early season biomass are limited by their destructive nature (Reynolds et al., 2009). Non-destructive phenotyping tools capable of providing insight into the plant's response to heat and drought stress from emergence through harvest are needed to understand this adaptive trait. Use of remote sensing tools such as normalized difference vegetation index (NDVI) have



shown great promise and are quickly being adapted to breeding programs (Pask et al., 2012). However, NDVI can only be used in early physiological growth stages; as the crop canopy closes, the predictive ability of the sensor becomes limited (Aparicio et al., 2000). In the case of roots, although non-destructive root characterization is possible, current root phenotyping platforms such as minirhizotron cameras are far too costly, time-consuming, and limited in scope to be utilized in a breeding program (Box, 1993). As these facts indicate there is a need for new tools capable of phenotypically evaluating above- and below-ground plant biomass for use in FBHTP.

### **Phenotyping technologies**

Previous research has shown that remote sensing technologies including terrestrial laser scanning (TLS) and ground penetrating radar (GPR) are capable of non-invasively estimating biomass both above and below ground (Butnor et al., 2003; Hosoi and Omasa, 2009). TLS is a ground based light detection and ranging system capable of high-resolution mapping (Lemmens, 2011). Previous work has demonstrated the use of TLS in wheat to derive plant area density correlations with manual measurements of dry weight (Hosoi and Omasa, 2009). TLS has the potential to non-destructively evaluate early season biomass of wheat. Likewise GPR has been successfully used in characterizing belowground root biomass and architecture in trees (Butnor et al., 2003). GPR functions by transmitting a radio signal into the ground (Goodman and Piro, 2013). Measuring signal attenuation and signal return time, GPR is able to detect different

dielectric properties of unique belowground materials (Freeland et al., 1998). Returned signals can be quantified and rendered, allowing for visualization and quantification of belowground root biomass (Novo et al., 2013). GPR also has the potential to map root architecture, a trait many see as central to higher yields (Gewin, 2010).

## **Research**

This research evaluates the use of TLS and GPR to phenotypically evaluate above- and below-ground plant biomass, respectively, for use in FBHTP. TLS and GPR were evaluated for their non-destructive sampling capabilities against traditional destructive methodologies. The research aim is to develop phenotyping tools capable of accurate non-destructive sampling allowing for data collection across physiological development and during response to crop stress to be utilized in future development of molecular markers capable of streamlining the use of MAS for these needed traits.

The ***long-term goal*** is to aid in development of new cultivars through a focused program of optimized phenotyping and packaging of multiple drought and heat tolerance adaptive traits utilizing breeding and nursery scale remote sensing technologies. These technologies would allow for rapid, non-destructive assessment of populations and selection for traits undetectable by traditional methods (Butnor et al., 2003; Hosoi and Omasa, 2009). The ***primary objective of this research*** was to define the capability of TLS and GPR as FBHTP tools for above ground crop biomass and root biomass

respectively. The **central hypothesis** was that FBHTP tools such as TLS and GPR can be employed to accurately phenotype plants in the field with precision. In this context, TLS and GPR can be used for developing molecular markers, phenotypic selection in breeding nurseries, and in evaluation of exotic germplasm for introgression. As such, TLS and GPR can serve as powerful phenomics tools for defining the genetic loci that regulate ideal traits in the context of performance during stress, while allowing plant breeders to screen larger populations while decreasing cost and error. The hypothesis was tested using the following specific objectives.

### Objective 1

Early season biomass is correlated with increased yield in wheat and other crop production systems under water limiting conditions (Whan et al., 1991). However, using current methods, aboveground biomass can only be quantified destructively limiting the ability to understand a trait that is highly correlated with yield. *It was hypothesized that TLS can be used to quantify aboveground biomass non-destructively over time allowing for insight into the trait's impact on yield.*

## Objective 2

F gvgto kpg'vj g'cdkklv "qh'I RT'vq's wcpvkc vkg n{ 'o gcwtg'tqqv'dkqo cuu'cpf 'f gr vj 0

Root biomass can be correlated with increased yield in wheat and other crop production systems under water limiting and heat stress conditions (Bengough et al., 2011).

Currently, root biomass can only be quantified destructively, limiting our ability to understand this highly yield correlated trait. *It was hypothesized that GPR can be used to quantify root biomass non-destructively over time allowing for insight into the traits impact on yield.*

In response to predicted climate change, plant breeders have increased their efforts to adapt crops to heat and drought stressed environments (Araus and Cairns, 2013).

Increasing early season aboveground biomass and root biomass are a principal focus.

However, non-destructive selection for these traits is not yet feasible at a breeding scale due to the high cost of current methodologies and a lack of high throughput tools (Pask et al., 2012). Incorporating remote sensing technologies into breeding platforms could facilitate the needed knowledge for introgression of critical adaptive traits needed during stress events. Use of TLS and GPR in current crop phenotyping methodologies could potentially provide a long awaited method for high throughput non-invasive phenotyping of early season biomass and roots under realistic field conditions. This research is *innovative* because it will identify the capability of TLS and GPR to assist plant breeders in meeting the future demands of agriculture. We expect that TLS and GPR could

provide a new look at plant breeding, allowing breeders to revolutionize current processes. Without these FBHTP tools, breeders are unable to bridge the gap between genotype and phenotype thus constraining future advances in yield potential.

## **CHAPTER II**

### **LITERATURE REVIEW**

#### **Facilitating plant breeding**

Predicted population growth and future climatic conditions require a need for preemptive agricultural strategies to avoid global hunger. The global population as estimated by the United Nations exceeded seven billion in October of 2011. Current estimates project global population growth to nine billion people by the year 2050 (Msangi et al., 2009). Avoiding a global food crisis and ensuring food security for nine billion people will require the adaptation of crop varieties to projected conditions, including increased climactic temperatures and drought (IPCC, 2007). In order to achieve the crop production levels required to feed the world, plant breeders will need to adapt new technologies enabling the selection of crop varieties capable of maintaining plant productivity under drought and heat stress conditions (Mba et al., 2012).

Agriculture has faced confounded hardships before and prevailed. Historically, breeding efforts for targeted adaptive traits such as dwarf stature and resistance to biotic and abiotic stressors have mediated eras of global food insecurity (Ronald, 2011). Increased population needs during the 1940s through late 1960s were met through the work of plant breeder, Norman E. Borlaug, father of “The Green Revolution”. Borlaug was thought to have saved a billion lives through introduction of high-yielding, semi-dwarf,

disease resistant wheat (*Triticum spp.*) varieties he developed using traditional plant breeding strategies. Borlaug's success came through a willingness to utilize new agronomic strategies coupled with elite varieties developed to optimize overall crop production. Borlaug's breeding efforts in selecting adaptive traits for target environments while pairing his adapted wheat with modern agricultural production technologies were thought worthy of the 1970 Nobel Peace Prize. Dr. Borlaug was strategic in his fight against hunger. He developed the varieties needed to feed a hungry world, and with that seed he shared the technology that cultivated their impact. Wheat yields in Mexico, where Borlaug did his breeding work, transitioned from roughly two tons per hectare in 1960 to over three by early 1970 and have continued to increase by 25% over the past 2 decades (Lobell et al., 2005).

Wheat is cultivated globally and second only to maize in total hectares worldwide. It was estimated in 2010 that bread and durum wheat production occupied 200 million ha producing over 646 tons, making it the most widespread cereal in terms of area planted (FAO, 2013). Wheat is the primary source of dietary calories for those living in the poorest countries and has played a key role in global food security (Msangi et al., 2009). Wheat germplasm, adapted and exotic, harbors multiple adaptive traits with the potential to buffer the impact of climate change (Reynolds, 2010). Wheat is relatively well adapted to dry environments and research has shown steady progress in efforts to increase its performance under heat and drought stressed conditions (Ammar et al., 2008; Trethowan et al., 2002).

Today, plant breeders stand on the front lines of this rapidly shifting war on hunger, but are armed with the same tools utilized for many centuries. Time has diversified and expanded the problem of food security, and breeders cannot win this battle without diversifying and expanding breeding strategies. To date, plant breeders have been able to stand their ground, protecting crop yields and ultimately shielding the global population from hunger. In order to keep pace with changing global conditions, there is a need to employ new technologies focused on optimizing current breeding processes.

Tools such as genomic selection have the potential to facilitate the needed advances in plant breeding. Constraints to genomic selection are manifested in the time and cost of phenotypic data generation and analysis. Recent advances have made genotyping economically feasible for breeding populations, allowing access to valuable genetic information. However, this information is only half of the story; to utilize it fully we must understand the phenotype encoded by it must be understood. Although phenotyping at the field level has seen some improvement in recent years, it is still costly and time-consuming; factors that make it poorly suited for the breeding pipeline. Linking genotype to phenotype would allow breeders to make selections based on genomic information, thus speeding their ability to adapt crops to future environments. This can only be done through development of tools allowing breeders access to phenotypic information at the same level of precision, accuracy, speed, and cost as current genomic tools.



This review focuses on efforts to increase the efficiency of wheat breeding by developing phenotyping tools to exploit marker assisted selection (MAS) within the breeding pipeline. Current methodologies of field-based high-throughput phenotyping (FBHTP) of wheat are discussed. Target physiological traits of above- and below-ground biomass and height/depth for future predicted high temperature and drought stressed environments is presented with regard to current and needed phenotyping platforms. In addition, terrestrial laser scanning (TLS) for aboveground biomass and height as well as ground penetrating radar (GPR) for belowground biomass and rooting depth are discussed as potential FBHTP tools. Field spatial variability, data management, and analysis are presented for consideration in future breeding strategies.

### **Plant breeding**

Plant breeding is the term for the process of, selecting individuals possessing desirable traits or superior performance, to improve varieties of crops. Traditionally, this is achieved by the careful screening of progeny derived from a cross between two elite parents. Ideally, those progeny displaying exceptional performance are selected and that performance is passed on to the next generation; in time, this can give rise to a new variety. However, this process is contingent on the fact that the selected performance is linked to a unit of heredity, the gene. Only phenotypes which are genetic in nature are suitable for selection, making the ability to discern genetic variability between individuals the key to successful plant breeding. By separating genetic variation in

performance from variability caused by the environment and other factors, breeders are best able to make selections and improve the crop.

Technological improvements in both crop breeding and agricultural platforms have sustained a linear increase in global food production at around 32 million metric tons per year (Tester and Langridge, 2010). However, the declaration of the World Food Summit on Food Security has called for a 70% increase by 2050 to meet future population needs (FAO et al., 2013). Agriculture will need to see an annual increase of 44 million metric tons per year to feed the world in 2050 (Tester and Langridge, 2010). Increasing crop yields to meet these demands will depend upon a breeder's ability to utilize crops' adaptive capacity. Selection of traits capable of limiting the impact of drought and high temperature stress in addition to those for increased yield and disease resistance will be required based on predicted future climatic conditions (Wang, 2005). However, drought and high temperature tolerance adaptive traits are challenging to phenotype, thus making it difficult to identify genetic loci for marker-assisted breeding and selection (Passioura, 2012). The pressing bottleneck for modern plant breeding in understanding these adaptive traits is accurate field and whole nursery scale plant phenotyping (Haro von Mogel, 2013). The selection of improved crop varieties is dependent on the ability of breeders to discern and quantify differences in plant phenotypes linked to improved performance. The effectiveness of plant breeding is therefore enhanced by high-throughput phenotyping: the use of tools able to rapidly identify differences in plants with accuracy superior to that of the biased human eye or of existing technologies.

FBHTP are capable of collecting data non-destructively in vivo allowing for multiple measurements of the same plant across physiological growth.

### ***Traditional breeding methodologies***

The sexual process of plant breeding involves crossing parental lines to unlock genetic diversity, the basis of all plant improvement. The progeny in all cases are guaranteed to be different but not always better than the parents, a challenge for breeders. To understand genetic diversity, plant breeders have traditionally had to observe breeding nurseries over multiple years and locations. Through complex statistical designs and replication within trials, breeders are able to understand trait heritability and environmental influences on a given phenotype. Through this process, plant breeders have protected yield performance from changing disease pressures while feeding a growing population. Despite this valiant effort, the pace of crop adaptation to meet future needs has fallen behind the rate required by our changing environment, population growth, and depletion of needed resources.

### ***Molecular breeding tools***

Technological advances in molecular genetics over the past decade have made great strides in cereal genomics, providing insight into genes linked to agronomically important traits. Mapping of quantitative trait loci has led to the ability to utilize MAS in breeding populations. This process was thought to replace the slow more traditional

applied plant breeding approach. However, many of the initial markers did not work, the maps were poorly constructed, the process was time consuming, and cost far too much to be practical in any breeding program (Collard and Mackill, 2008b). Today, on the other hand, the technology has improved to the point where markers provide the ability to select phenotypes a plant breeder is incapable of, maps are constructed with statistical accuracy, and the process can be done in a fraction of the time required for growing plants in the field. The key to the successful utilization of MAS is accurate genotypic and phenotypic information.

Molecular markers, the association of polymorphisms in deoxyribonucleic acids with a given phenotype, allow plant breeders to select for phenotypic traits with great efficiency while reducing the required time and resources (Boopathi, 2013). The effectiveness of MAS in breeding relies on accurate and cost effective platforms for genotyping and phenotyping (Collard et al., 2005). Recent technological advances in genotyping have improved accuracy while reducing cost, increasing the possible impact of MAS on crop breeding programs (Davey et al., 2011). Accurate field-based phenotyping is a required partner to this improvement in genotyping, and is critical to developing molecular markers capable of identifying traits of interest (White et al., 2012). Molecular markers must be strongly associated with the expression of the desired trait (Collard et al., 2005). The current limitation to MAS is the development of tools capable of accurately phenotyping responses to a given environment (Poland and Rife, 2012). FBHTP technologies, tools capable of precise and accurate plant phenotyping at the field level,

are needed for rapid, non-destructive phenotypic assessment of breeding populations for traits over physiological development as well as for those undetectable using traditional methods (White et al., 2012).

Combining complementary scientific disciplines has yielded genomic selection as a powerful tool to identify offspring capable of outperforming parental lines. The advantage of genomic selection over traditional MAS strategies is based on an improved efficiency and time. Decreases in the sequencing costs of genomic information have resulted high-throughput phenotyping becoming the current limitation in genomic selection.

### ***Improving the breeding pipeline throughput***

Understanding and capitalizing on the link between genetic variation and phenotype is the basic foundation of plant breeding. Unlike sequencing information, phenotypic information changes during the course of physiological development in response to environmental conditions. As such, by coupling time series phenotypic information to genomic data we may be able to understand the genotype-phenotype relationship, potentially allowing insight into complex traits such as yield.

Yield is the primary target for improvement by crop breeding. Like other agronomic traits, yield is challenging to manipulate due to its polygenetic inheritance as well its

susceptibility to environmental influence. To make matters worse, environmental stresses, such as high temperature and drought in particular, have very complex effects on overall yield and make it difficult to measure accurately. Genomic selection has the potential to allow breeders insight into these complex traits with the possibility of increasing yield potential to meet current and future needs. Previous success of genomic selection has been inhibited by the necessity of both highly accurate genotypic and phenotypic characterization. Genotypic characterization is now economically feasible for plant breeding due to recent technological advances. However, current phenotyping technologies are still limited in their accuracy and ability to be applied to large scale breeding populations. As such, there is a critical need in plant breeding for the development of FBHTP tools capable of rapidly and accurately characterizing plant phenotypes. Development of FBHTP platforms comparable in accuracy and economic ability to current genomic analysis tools should establish a platform for breeding capable of dissecting complex traits accurately and efficiently, allowing breeders the ability to utilize genomic selection to its fullest potential.

### **Field-based high-throughput phenotyping in breeding**

FBHTP can be defined as a system capable of in situ, non-invasive, automated phenotype assessment of quantitative plant traits. This definition requires (1) that the physiological trait be measured in the field to ensure the response is characteristic of the environment. (2) That the physiological measurement be non-invasive to allow for

measurement of the same plant across the entire lifecycle. (3) That the process must be automated, from data acquisition, to data storage, and analysis. (4) That the physiological trait being measured is quantitative in nature.

Physiological traits can be used as a basis for selection criteria in plant breeding (Figure 1). In wheat, progeny are typically self pollinated through the first several generations in an attempt to fix traits. Additionally, progeny resulting from a cross will segregate in the first several generations, meaning the genetics driving the phenotypes of the progeny are not equal. This results in differentiation or segregation for traits, as they progress in further generations these traits become fixed. Individual progeny are phenotypically evaluated in and selected for target traits. This selection can happen at the whole plant level or by single head. With whole plant selection, typically there is a further head selection in subsequent generations. To increase the chance of identifying those rare recombinants expressing the desired phenotype, breeders have to screen large populations and selectively reduce the numbers in testing until only optimal candidates remain. This requires starting with a large population, which becomes smaller as selection pressure is applied. One of the strengths of the FBHTP platform for early generation selection is the ability to look at larger volumes of potential progeny than in traditional breeding approaches.

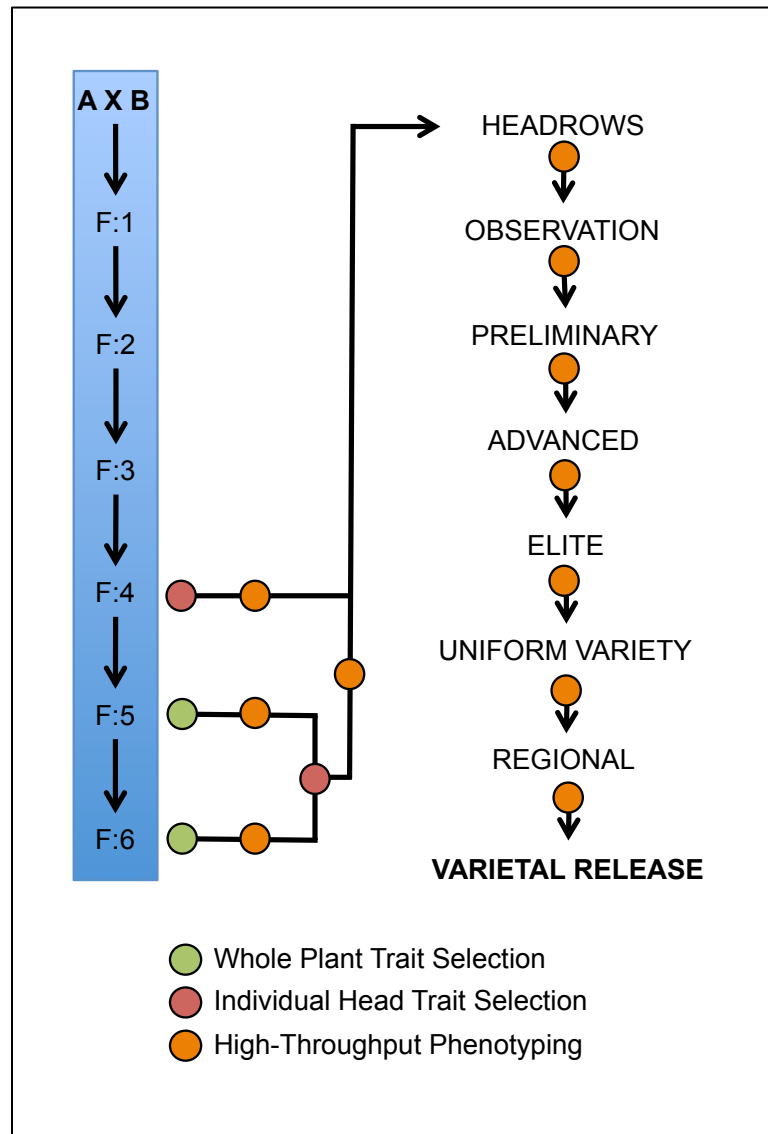


Figure 1. Application of high-throughput phenotyping to cultivar development in a wheat breeding program.



In most cases breeder's nursery size is the limiting factor in the amount of material they are capable of screening. FBHTP allows breeders the ability to screen for traits in early generation they typically would have to consider later in the breeding pipeline, thus limiting the amount of material being screened in later generations. Once selected progeny have been advanced to evaluation nurseries, they can be highly scrutinized by FBHTP platforms. Early generation (F:4) evaluation nurseries are grown in more than one environment, allowing the breeder to assess any interaction potentially impacting the target phenotype, however, limited replication limits needed phenotypic confidence. In addition, multiple locations and replications are used to confirm that the phenotype is authentic, allowing the breeder to select advanced lines. Advanced lines are evaluated in multiple environments, typically geographically distant from one another. This poses a logistical complication in the breeders' ability to evaluate traits. Phenotypes are evaluated at different growth stages and under different constraints or biases due to the need for a breeder to rely on other's interpolations of the physiology. FBHTP evaluates lines identically regardless of logistical location under the same constraints, allowing for direct comparison of data and isolating only the response by the line to the environment. This is especially true in multi-region trials leading to the development of better adapted material. Uniform data collection using FBHTP can provide breeders with historical performance information as well, which can be utilized in selection of parental lines for deriving new populations.

FBHTP platforms are currently being evaluated for an ability to characterize physiological traits associated with heat and drought tolerance in crop breeding systems (Cabrera-Bosquet et al., 2012). FBHTP tools can be classified based on the impact of their physiological traits being measured and their association to yield. In some cases FBHTP tool can be used to understand multiple phenotypes adding to the value of FBHTP measurements. Utilizing these tools could provide breeders the needed insight for optimized selection in addition to the ability to screen larger populations in multiple environments. Highly heritable physiological traits, such as early vigor or rapid ground cover, are considered easy for a breeder to identify and are able to be accurately predicted across multiple environments. These traits are being considered for physiological breeding of wheat, and may additionally prove valuable in other crop systems as well. Indeed, the adaptive physiological mechanisms being exploited in drought and heat stressed environments for wheat are often conserved across multiple species and can be applied to other agricultural crops as well (Reynolds, 2010).

### **Target physiological traits for field-based high-throughput phenotyping**

To start, traits associated with performance must be identified and the heritability of the traits and their response to selection must be estimated. To define target traits associated with performance, one must define the target growing area and traits that are relevant to environmental conditions. To be suitable target for breeding, physiological traits need to possess significant genetic variability across available germplasm as well, as described

by the proposed selection criteria. Selection for the target trait needs to be cost effective with regard to the payoff. Choosing appropriate genotypes best suited for the study should be based on how well they are adapted to the target environment.

### ***High temperature and drought stress***

Increased temperature can modify the developmental growth of the crop. Higher temperatures result in reduced canopy and green area duration. Early vigor in canopy development can equate to increased aboveground biomass and can be easily evaluated using several FBHTP tools (Table 1). Stay-Green traits are those delaying senescence, allowing photosynthesis to continue. Stay-Green can be characterized individually or in concert with other canopy phenotypes using FBHTP platforms (Lopes and Reynolds, 2010).

Wheat is most susceptible to high temperature and drought stress during the reproductive development and grain filling physiological growth stages. Increased temperatures and drought during these critical stages can result in reduced grain weight and number leading to yield loss. Improved wheat varieties cultivated in the US Great Plains from 1874-1994 were able to withstand high temperature stress, leading to increased yields (Assad and Paulsen, 2002). However, current varieties grown in the US Great Plains lack the required yield stability and grain quality under high temperature stress (Hays et al., 2007). Breeders are selecting cultivars optimized for performance and yield under heat and drought conditions using targeted adaptive physiological trait introgression.

Table 1. Overview of current field-based high-throughput phenotyping (FBHTP) technologies in crop breeding.

<b>FBHTP Technology</b>	<b>Physiological Trait</b>	<b>Trait Value</b>	<b>FBHTP Advantage</b>	<b>Reference</b>
Ceptometer	Light Interception: Light intercepted by the crop canopy.	Allows calculation of canopy green area index and extinction coefficient.	Relative measurement of canopy accurate.	(Pask et al., 2012; Reynolds et al., 2012)
Digital Imaging	Crop ground cover: Early vigor (green area and aboveground biomass).	Early interception of radiation; early estimate of reduction in soil moisture evaporation.	Quick, easy and cheap to measure; integrative.	(Pask et al., 2012; Reynolds et al., 2012)
Electrical Resistivity Tomography	Root biomass: Root biomass distribution. Soil water availability.	Association of roots with water and nutrient uptake.	Measurement of root distribution.	(Durlleser and Stanjek, 1997)
Ground Penetrating Radar	Root biomass: Root biomass distribution and architecture.	Association of roots with water and nutrient uptake.	Measurement of root distribution and architecture.	(Butnor et al., 2003; Guo et al., 2012; Hruska et al., 1999)
Infrared Thermometer	Canopy temperature: Evaporative cooling from the canopy surface.	Linked to many physiological factors: stomatal conductance, plant water status, root an yield performance under a range of environments.	Integrative; quick, easy, and cheap to measure; non-destructive; remote.	(Pask et al., 2012; Reynolds et al., 2012) Lopes and Reynolds, 2010
Hyperpectral Imaging	Disease infection.	Quantification of disease infection.	Rapid assessment of plant disease.	(Bauriegel et al., 2011)11
Normalized Difference Vegetation Index	Normalized Difference Vegetation Index: Canopy size, vegetative greenness.	Estimation of early cover, pre-anthesis biomass, nitrogen content, post-anthesis stay-green.	Quick, easy and cheap to measure; integrative.	(Pask et al., 2012; Reynolds et al., 2012)
Ultrasonic Sensor	Plant height: Height of overall canopy from ground level.	Photo protective adaptive trait to heat/drought stress; provides information on crop canopy archetecture; lodging risk.	Quick, easy and cheap to measure; integrative.	(Sui et al., 2012)
Spectral Radiometer / Spectrometer	Spectral reflectance: Vegetative, pigment and water indices.	Estimation of green biomass, leaf area index, photosynthetic potential, and plant water status.	All indices available from a single repeated measurement; integrative.	(Pask et al., 2012; Reynolds et al., 2012)
Terrestrial Laser Scanning	Vertical plant area density and canopy growth parameters.	Early interception of radiation; early estimate of reduction in soil moisture evaporation.	Crop canopy structure.	(Hosoi and Omasa, 2009)
Thermal Imaging	Canopy temperature: Evaporative cooling from the canopy surface.	Diagnosis and quantification of pant response to water stress.	Rapid assessment of plant stress.	(Jones et al., 2009)

### ***Physiological response impacting production and yield***

Physiological traits linked to improved performance in stressed environments are identified based on their impact on yield potential (YP) (Lumme et al.). The YP of a crop is defined as the yield when grown in environments for which it is adapted, with abundant water and nutrients, and effective control of biotic stress (Evans and Fischer, 1999). YP can be expressed as a function of light interception (LI) and radiation use efficiency (RUE), where the product is biomass and the partitioning of biomass to yield, i.e. harvest index (HI) (Cossani and Reynolds, 2012).

$$YP=LI \times RUE \times HI$$

Increasing HI has driven progress in wheat YP by introgression of dwarfing genes (Evans and Fischer, 1999). However, progress in breeding to increase HI has been limited since the mid 1980s (Sayre et al., 1997). LI traits such as stand establishment and delayed maturity are easily selected for, suggesting little relationship to increased yield. Improvement of RUE could increase biomass and positively impact YP. Recent developments in FBHTP technologies have allowed for characterization of several physiological traits associated with drought and high temperature stress.

Target LI traits for improving crop performance under heat and drought stress are canopy establishment and architecture. Increased temperature can modify developmental growth of the crop, with higher temperatures resulting in reduced canopy

and green area duration. Early vigor in canopy development can equate to increased aboveground biomass. RUE, which is the result of gross carbon assimilation less that required for growth and maintenance, will impact crop biomass given that LI has been optimized. Improving photosynthetic capacity and efficiency are physiological traits capable of positively impacting overall yield in stressed environments. Target physiological traits impacting RUE are photosynthesis, photorespiration, and respiration.

### ***Adaptation to high temperature and drought stress***

Plants have developed different mechanisms to facilitate their existence in suboptimal environments. The ability of plants to utilize their surroundings and adapt to biotic and abiotic stress only demonstrates their true phenoplasticity. Plant adaptations to heat and drought stress include but are not limited to: early season biomass, osmotic adjustment, increased root elongation, and increased root membrane permeability. The primary drivers of yield are; water uptake, water use efficiency, and HI (Reynolds et al., 2012). This defines a need for WU in producing higher yields. Better understanding the relationship between plants and the environment could provide insight into reduction of water stress by optimal early season root growth, architecture, or exploration of deeper soils with higher water potential. Deep early season roots could play a role in reduction of crop stress. In addition to increased water sequestration, breeding for deeper-rooted crops has a potential to increase nutrient uptake (Kell, 2011).

## **Current phenotyping methodologies**

Current phenotyping tools for above and below ground biomass are limited by their reliability and cost limited sample size, negatively impacting our understanding.

Research has been able to establish methods capable of defining both above and below ground biomass growth parameters; however they are destructive and labor intensive.

This means that above- and below-ground biomass have primarily been destructively characterized by traditional study techniques, and that today's knowledge in above- and below-ground biomass physiology has been possible only by the determination of researchers willing to exert substantial amounts of time and physical effort. To understand adaptation of crops in stressed and changing environments, researchers need non-destructive phenotyping tools that can characterize responses over time in situ.

## **Target field-based high throughput phenotyping platforms**

Early season above-ground biomass is one adaptive trait shown to increase photosynthesis and radiation use efficiency, ultimately providing the plant a timely advantage during the growing season (Reynolds et al., 2010). Utilizing the available early season moisture, these adapted varieties are better able to establish the photo-assimilates needed to complete grain-fill under stressed conditions (Whan et al., 1991). Likewise, greater root elongation can play a critical role in allowing the plant to reach deeper soil profiles, allowing access to nutrients and needed water (Bengough et al.,

2011). Common methodologies for phenotyping early season biomass are limited by their destructive nature (Pask et al., 2012). Non-destructive phenotyping tools capable of providing insight into the plant's response to heat and drought stress from emergence through harvest are needed to understand this adaptive trait. Use of remote sensing tools, such as normalized difference vegetation index, have shown great promise and are quickly being adapted to breeding programs (Pask et al., 2012). NDVI can only be used in early physiological growth stages, as the crop canopy closes the predictive ability of the sensor becomes limited (Aparicio et al., 2000). Non-destructive root characterization is possible; however current root phenotyping platforms such as minirhizotron cameras are far too costly, time-consuming, and limited in scope to be utilized in a breeding program (Box, 1993).

### ***Terrestrial laser scanning for aboveground biomass and plant height***

As with other ideal adaptive physiological traits, rapid FBHTP of early season aboveground biomass and height is limited by our inability to accurately and nondestructively characterize these traits. TLS is a ground based light detection and ranging system capable of high-resolution mapping (Lemmens, 2011). Previous work has demonstrated the use of TLS in wheat to derive plant area density correlations with manual measurements of dry weight (Hosoi and Omasa, 2009). TLS has the potential to non-destructively evaluate early season biomass of wheat.



Time of flight TLS operates as a photons sec<sup>-1</sup> laser light emitting device estimating time of flight for point to distance interpretation and provides non-destructive three-dimensional (3D) point cloud renderings of varietal plots. The laser spot resolution is in the range of 4.5mm increasing as the beam is emitted further from the source. The system provides >0.5mm spacing between return points, and is capable of ranges of measurement from 0-300m radius through 360 degrees in the horizontal and 270 degrees in the vertical. Positioning targets allow for multiple 3D data sets of point clouds to be aligned creating a virtual environment for repeated measurement. Each intercepted point by the TLS is a record of x,y,z, (position and range, i.e., distance to target).

TLS has been used to estimate vertical plant area density profiles as well as growth parameters (Hosoi and Omasa, 2009); however, the study was limited in scope and did not address the application of the technology. Reviews of other technologies have been assessed and considered for contrast to this technology. Some information such as spectral data can be attained using tools like green seeker. These tools use the reflectance of light emitted off the plant to calculate levels of health or stress. One limitation of these technologies is that they do not take into account YP, which is determined by the amount of incident solar radiation, temperature, and plant density (Cassman et al., 2003). It is understood that density is a driver in the incidence of solar radiation and the temperature of the plant. Using TLS, plant structural characteristics can be derived. Biomass characteristics are primary drivers of physiological plant traits that are associated with plant health. The ability of TLS to characterize and quantify leaf

number, density, tillering, branching, and plant architecture would provide information necessary for selection in population studies.

### ***Ground penetrating radar for belowground biomass and depth***

GPR, a geophysical impulse radar system designed to image subsurface features, has successfully been used in coarse root detection and quantification (Guo et al., 2012). GPR transmits short pulse electromagnetic energy (EM) into the ground in the radio spectrum through an antenna. Transmitted pulses consist of a spectrum of wave frequencies above and below the transmitted central frequency of the selected antenna. Subsurface interfaces separating layers of differing relative dielectric permittivity (RDP), a measurement of how well EM energy is transmitted through a medium, reflect back a portion of the energy from the pulse, while the remaining energy continues to the next interface. Received signals are sampled and digitized, converted into a reflection trace, and stored for processing. The RDP contrast between the neighboring soil and the roots determines the strength of the reflected energy. The higher water content in roots compared to the surrounding soil provides the required contrast that allows for root detection by GPR. Measuring signal attenuation and signal return time; GPR is able to detect different dielectric properties of unique belowground materials (Freeland et al., 1998). Returned signals can be quantified and rendered allowing for visualization and quantification of belowground root biomass (Novo et al., 2013).

To date, GPR has been used successfully for non-destructive in situ characterization of tree root biomass (Butnor et al., 2001). In addition, GPR has been used in situ to characterizing tree root architecture with some limitations (Hruska et al., 1999). Incorporating GPR into current crop phenotyping methodologies could potentially provide a long awaited solution to high throughput phenotyping for roots under field conditions. GPR has the potential to offer insight into stress adaptive traits and possible identification of quantitative trait loci linked to improved stress tolerance for use in marker-assisted selection. Incorporating GPR into current crop phenotyping methodologies could potentially provide a long awaited solution to high throughput phenotyping for roots under realistic field conditions.

### **Management and analysis: field-based high-throughput phenotyping data**

Recently, FBHTP has gained popularity with both crop physiologists and plant breeders alike based on the potential impact these technologies could have on future crop yields. FBHTP has a strong appeal to many due to its highly accurate dense data sets. However, in most cases, the scientific community awaits results validating these cutting edge tools and technologies. Adapting FBHTP platforms is time consuming, filled with trial and error. In addition, many of these tools require breeders and physiologists to step beyond their areas of expertise, slowing the overall process of innovation. Successful adaptation of FBHTP platforms will be achieved through collaboration between multiple disciplines. Agricultural engineers, crop modelers, programmers, and remote sensing

specialists will all be needed to facilitate and optimize the FBHTP platform.

Agricultural engineering can play a key role in the logistics of data collection. Many of the tools utilized in FBHTP were not initially designed for field applications and need to be adapted to fit field constraints. The logistics of passing a sensor through the field in a standardized system of measurement can be challenging. Engineering equipment capable of meeting both the needs of the sensor and the growing environment is typically the first step in developing a FBHTP tool. Data collection can be a daunting task depending on the FBHTP platform and how it is designed, this component is one typically preformed by the breeder or physiologist. This requires a working knowledge of the system being used as well the experimental design and objectives. Data must be collected in a format that can easily be interpolated, allowing remote sensing specialists who have worked in this type data to offer guidance and facilitate data analysis. Crop modelers and software programmers can be useful in understanding the collected data. In most cases, the sensors being used in FBHTP collect vast amounts of data. Crop modelers have been working with these large dense data sets for some time and can offer guidance toward understanding the collected information. In most cases, software is not available with the capabilities of breaking down the collected data into a format usable by the breeder. Having a team member capable of developing software able to interoperate collected data is an essential element, as there is typically limited time for data analysis.

## **Forward strategies**

In response to predicted climate change, plant breeders have increased their efforts to adapt crops to heat and drought stressed environments (Araus et al., 2008). Increasing early season shoot growth and root biomass are a principal focus. However, non-destructive selection for these traits is not yet feasible at a breeding scale due to the high cost of current methodologies and a lack of high throughput tools (Pask et al., 2012). Incorporating remote sensing technologies into breeding platforms could facilitate the needed knowledge for introgression of critical adaptive traits needed during stress events.

# **CHAPTER III**

## **USE OF TERRESTRIAL LASER SCANNING IN CROP BREEDING FOR EVALUATION OF EARLY GROUND COVER AND FORAGE**

### **Overview**

Recent literature suggests new technologies are available for deriving non-destructive wheat biomass estimations. Currently, development of wheat (*Triticum spp.*) cultivars, capable of early season groundcover (increased forage production) is limited by the inability to accurately and nondestructively phenotype individual lines in breeding systems. Terrestrial Laser Scanning (TLS) is a non-destructive method to capture changes in the aboveground three-dimensional (3D) structure and distribution of wheat. Consequently, our objective was to evaluate the use of TLS to estimate aboveground biomass. Using a Leica Scan Station 2 time of flight TLS we surveyed a 23m x 46m site at 1cm point spacing resolution and a range of 30m. The site consisted of 25 nitrogen treatments on one forage wheat variety replicated four times for a total of 100 subplots each at 1.5m x 6.0m. We expected differences in biomass based on N treatments within the subplots. The survey data was collected at the four corners and midpoints of the two outer lengths of the plot boundary. The TLS data was processed to generate 3D visualizations of plant, height, and point density within each subplot. Whole plot biomass was destructively measured in each subplot using an Alfalfa-Omega flail type forage harvester. Linear regressions comparing mean canopy height and total plot

forage yield for each experimental plot across four replications was poorly correlated ( $R^2$  0.08). Mean plot normalized difference vegetation index measurements were evaluated against total plot forage biomass with limited correlation ( $R^2$  0.036). The mean value of the TLS elevation points had the highest correlation with both plot ( $R^2$  0.09458) and sub plot ( $R^2$  0.37984) forage yield as compared to traditional platforms.

## **Introduction**

Dual-purpose wheat (*Triticum spp.*) production (grazing livestock on winter wheat during vegetative growth) is common in the Southern Great Plains region of the United States. Grazing winter wheat provides a unique opportunity for producers in Colorado, Kansas, Oklahoma, New Mexico, and Texas to utilize production acreage and costly inputs to their maximum benefit. Dual-purpose wheat is typically seeded in summer and grazed through the fall and winter seasons providing a timely resource for the livestock industry, as availability of quality forage becomes limited. Winter wheat is typically managed in the Southern Great Plains for use in grain production, forage production, and dual-purpose (grazing of forage through the jointing stage). Annually, 20 million acres in this region are seeded to wheat with an estimated 30 to 80 percent being utilized for grazing (Pinchak et al., 1996).

In wheat, grain and forage production systems, early ground cover is associated with higher yield both in forage biomass and grain yield making it a desirable trait for

selection in breeding programs. Increased ground cover (percent of soil covered by plant foliage) increases light interception, and as such early establishment and vigor are keys to increased productivity. Early ground cover is best characterized by fast development of leaf area and increased biomass. Genotypes capable of early groundcover increase grain yield production, not only due to intercept light interception, but also by decreasing soil water evaporative potential and increasing water use efficiency. Early ground cover also is a desirable trait in dual-purpose (forage and production) systems, while decreasing weeds through competition.

Current destructive methodologies used in phenotyping biomass provide information on growth rate and partitioning between the canopy components. Breeders are better able to select cultivars adapted for early season biomass by selecting those with early vigor, or the ability to produce a full canopy early in the growing season. Increased canopy allows for better radiation use efficiency, which can be calculated by partitioning the harvested samples. Plants with early vigor have a larger canopy thus increasing the amount of light that can be intercepted and converted to photosynthates available to mobilize during grain fill. Traditional destructive sampling is time consuming and costly, however the information yielded is of great value.

Two digital methods include digital camera image analysis and the normalized difference vegetation index (NDVI). Digital camera image analysis quantifies the total area differences between leaf tissue and soil for a given plot based on pixel color. NDVI



is a spectral photometric derived vegetative index that has proven to be a useful tool prior to canopy closure. Digital analysis and NDVI are quantitative measures removing the subjectivity however they the ability to resolve phenotypes within a breeding program is just as critical.

Terrestrial laser scanner (TLS) is a relatively new technology, developed for the industrial sector, has a potential to be used as a non-destructive field-based high-throughput phenotyping tool in phenotyping early season forage biomass (Lemmens, 2011). TLS is a light detection and ranging system developed for ground use (Lemmens, 2011). The TLS operated by a laser light source is transmitted from the scanner, once intercepted by an object the light is reflected back to the scanner (Figure 2). Time of flight is calculated for the light signal and converted to distance (Pesci and Teza, 2008). This allows the TLS to define position in an X, Y, and Z coordinate to be reconstructed in a three-dimensional (3D) representation (Hofle and Pfeifer, 2007).

Several tools have been developed for assessing early ground cover. The most common is a visual score, where experimental plots are visually rated for early biomass. In most cases this consist of simply comparing one plot to another, multiple times over the course of vegetative growth, to rank the total soil area covered. This low cost visual assessment is inexpensive, however it is subjective and may lack the resolving ability to differentiate phenotypes, a critical requirement in breeding programs.

Studies have shown TLS can be used to predict dry weight biomass in wheat by correlation of TLS derived plant area density and manual destructive biomass measurements under controlled growing conditions (Hosoi and Omasa, 2009). In addition, TLS has been utilized in evaluation of wheat plant height measurements for yield estimation. TLS has also been used to evaluate foliar nitrogen and chlorophyll (Eitel et al., 2010).

A TLS is a photons/sec laser light emitting device that by estimating time of flight for point to distance interpretation it can provide non-destructive 3D point cloud renderings of varietal plots at varying light wavelengths. The laser spot resolution is in the range of 4.5mm increasing as the beam is emitted further from the source. The system provides >0.5mm spacing between return points, and is capable of ranges of measurement from 0-300m radius through 360 degrees in the horizontal and 270 degrees in the vertical. Positioning targets allow for multiple 3D data sets of point clouds to be aligned creating a virtual environment for repeated measurement. Each intercepted point by the TLS is a record of X, Y, and Z, (position and range, i.e., distance to target), intensity (maximum reflectance) information that is unique to every object the laser contacts (Antonarakis et al., 2010).



Figure 2. Data collection using a Leica ScanStation 2 terrestrial laser scanner. The Leica ScanStation 2 is shown mounted on a surveyor's tripod collecting data to be compare with traditional biomass measurements.

## **Materials and methods**

### ***Plant material***

The wheat cultivar ‘Fannin’ was used for this study. ‘Fannin’ is classified as a hard red winter wheat (AgriPro, Berthoud, CO, USA). Fannin was selected for its forage quality as well resistance to rust (*Puccinia*) and powdery mildew (*Erysiphe*). Wheat seed was treated prior to planting with the labeled rate of Gaucho XT (Bayer Crop Sciences, Research Triangle Park, NC, USA) to control for possible confounding factors such as seedling disease and insect damage.

Plots were drill seeded at a rate of 100 kg/ ha based on forage production recommendations specific to Texas. Using a Hege 500 small plot seed drill (Hege Equipment Inc. Colwich, KS, USA) each experimental plot consisted of seven rows 16.5 cm apart and a plot area of 1.5 m wide by 4.5 m long. The trial was sown on September 21, 2010. Following seedling emergence, 1.5 m alleys between experimental plots were seeded with ‘Fannin’ to control for plot edge effects resulting from bank alleys.

### ***Description of study area***

Plots were established at the Texas A&M AgriLife Extension Experimental Station, in Burleson county Texas (30° 30’ 36.57’’ N latitude / 96° 25’ 07.14’’ W longitude / 66 m

elevation above sea level). The study site is within the Brazos River flood plain. Site soils were Belk clay (fine, mixed, thermic entic hapluderts) and described as being well drained, very slowly permeable, and having a high water holding capacity. Belk clay soils are typical of those found on flood plains. The soil capability classification for dry land Belk clay soils is 3S. Belk clay soils are formed in calcareous clayey sediments underlain by loamy sediments. Soil present exhibited a 0 to 1% slope.

This trial of 5 pre-plant (0, 45, 67, 90 and 112 kg/ha) and 5 top-dress (0, 22, 45, 67, and 90 kg/ha) nitrogen treatments and one control plot, was established in a split-plot (pre nitrogen main plot and post nitrogen sub plot) randomized block design replicated four times (26 plots total per replication).

### ***Production practices***

The trial field location was prepared for sowing in August of 2010 using disk cultivation. Soil samples were collected to a depth of 90 cm and separated in 30 cm increments (0-15 cm, 15-30 cm, 30-60 cm, and 60-90 cm) for routine soil and a stratified soil nitrate analysis to determine residual soil nutrients. Composite soil samples were submitted to the Texas A&M AgriLife Soil, Water, and Forage Testing Lab (College Station, Texas, USA) for analysis. Considering the first 15 cm of soil sampled and analyzed, triple super phosphate (0-46-0) was applied to meet standard agronomic recommendations using a

pendulum-type spreader. The applied phosphate was incorporated into the soil by harrow cultivation prior to sowing.

Mechanical and chemical pest control was administered on an as need basis during the growing season. Chemical weed control included the application of 2, 4-D (0.5 l ha<sup>-1</sup>), Finesse Grass and Broadleaf herbicide (52 g/ha, chlorosulfuron and flucarbozone sodium), and Huskie (1.1 l/ha, pyrasulfotol, bromoxynil octanoate, and bromoxynil heptanoate). Greenbug (*Schizaphis graminum*), bird cherry-oat aphid (*Rhopalosiphum padi*), and army worm (*Pseudaletia unipuncta*) were observed and controlled by application of dimethoate (0.25 l/ha).

The study site was equipped with a linear irrigation system designed to deliver low rates of water to reduce nutrient runoff (Valley Industries, Valley, NE, USA). During the course of this study 50 mm total irrigation was applied in addition to 88 mm of rainfall received over the growing season. Irrigation water was analyzed and shown to have no significant nutrient input to the experimental trial.

### ***Nitrogen treatments***

Pre-planting nitrogen treatments (5 total) were established for each plot by considering the residual nitrogen identified by the soil nitrate test results of the first 15 cm of soil. Plot nitrogen treatments were calculated to establish each pre planting treatment (0, 45, 67, 90 and 112 kg/ha). Pre planting nitrogen treatments were of urea ammonium nitrate

(32-0-0) were applied using a calibrated hand boom sprayer following field preparation and prior to sowing. Post planting nitrogen treatments (5 total) of urea ammonium nitrate (32-0-0) were applied using a calibrated sprayer hand boom to establish each post planting treatment (0, 22, 45, 67 and 90 kg/ha) following sowing. Post-planting nitrogen treatments were applied at Feeks 2.0 growth stage (Appendix A, Figure 72).

### ***Crop agronomic measurements***

#### **Visual biomass rating**

Visual ratings were assigned to each plot ranging from 1 (low biomass) to 9 (high biomass) relative to all plots evaluated within the field. To ensure separation within the evaluation, only odd values were assigned.

#### **Canopy height**

Canopy height was measured from soil surface to the tip of the flag leaf using a ruler and recorded to the nearest cm. Plants were selected for measurement at the base to avoid bias in evaluation. Measurements within each plot were used to establish a mean canopy height value representative of the whole plot.

### **Normalized difference vegetation index**

A GreenSeeker crop sensing system (Trimble Navigation Limited, Sunnyvale, CA, USA) was used to measure NDVI. Using reflectance measurements of the red and near infrared spectrum converted the response to NDVI ( $NDVI = (NIR - Red) / (NIR + Red)$ ). Data was collected using the active sensor by passing over the crop canopy at a height of approximately 1.5 m above the canopy. Reflectance readings for each plot were then averaged for a mean plot response representative of each plot.

### **Forage biomass**

Destructive sampling was done at the sub plot level to ensure accuracy within the data. Interior rows within the plot were selected for hand harvest to avoid possible plot edge effects. Forage biomass was harvested using shears and collected into a marked paper bag. In total 30.5 cm lengths of three selected rows were harvested, all plant material above the height of 1.5 cm was collected for analysis. Fresh weight of the forage biomass sample was recorded for all three samples.

Whole plot destructive sampling was done using a flail type forage harvester equipped with an Alfalfa-Omega weigh scale (R-Tech Industries Ltd, Homewood, MB, CAN). Whole plot forage remaining following hand harvest sampling was collected and



weighed for fresh weight biomass using the onboard scale to determine whole plot fresh weight forage biomass.

Forage biomass dry weight was determined for all samples. Following harvest, samples were placed in a commercial dryer at 65°C for 48 hours to remove all moisture.

Following drying, the samples were weighed to obtain dry weight biomass. Using the fresh weight and dry weight we were able to determine total dry matter forage biomass for each plot.

### ***Terrestrial laser scanner measurements***

#### **Terrestrial laser scanner data acquisition**

TLS data was acquired from six scans positions within the experimental trial, one from each of the four corners and two from the boundary midpoint (Figure 3). The data was collected during wheat vegetative growth. TLS scans were acquired at a height of 1.65 m to ensure consistent vertical angles for each scan (Hofle and Pfeifer, 2007). Scans were all acquired with a fixed resolution of 2 cm by 2 cm.

Corner scans were collected at 90° angles with a range of 40 m. Boundary midpoint scans were collected at 180° angles with a range of 40 m. Multiple scans were collected to reduce the impact of line of sight interference. All scans were collected just prior to

forage sampling and immediately following biomass harvest. Three target poles were placed in the trial to allow for accurate registration while combining all six of the individual scans for data analysis.

### **Terrestrial laser scanner data processing**

Collected data is then used to construct digital, three-dimensional models useful for a wide variety of applications. Six individual scans are combined into one point cloud for data analysis using HDS Cyclone (Leica Geosystems, St, Gallen, CHE). Overlapping data points between the scans were removed using HDS Cyclone (Leica Geosystems, St, Gallen, CHE). Data was then visualized using Quick Terrain Modeler (Applied Imagery, Silver Spring, MD, USA) (Figure 4). Laser time of flight to and from the TLS to the intercepted target defines distance from the scanner. Data is captured using cartesian coordinates with respect to the position of the TLS scanning unit and established height (Lemmens, 2011). Position and height of each target point are recorded. TLS uses the scanner vertical elevation as the reference datum defining the elevation values below the scanner in negative values. These negative height values are transformed into an adjusted height value for each intercept point collected by the scanner.

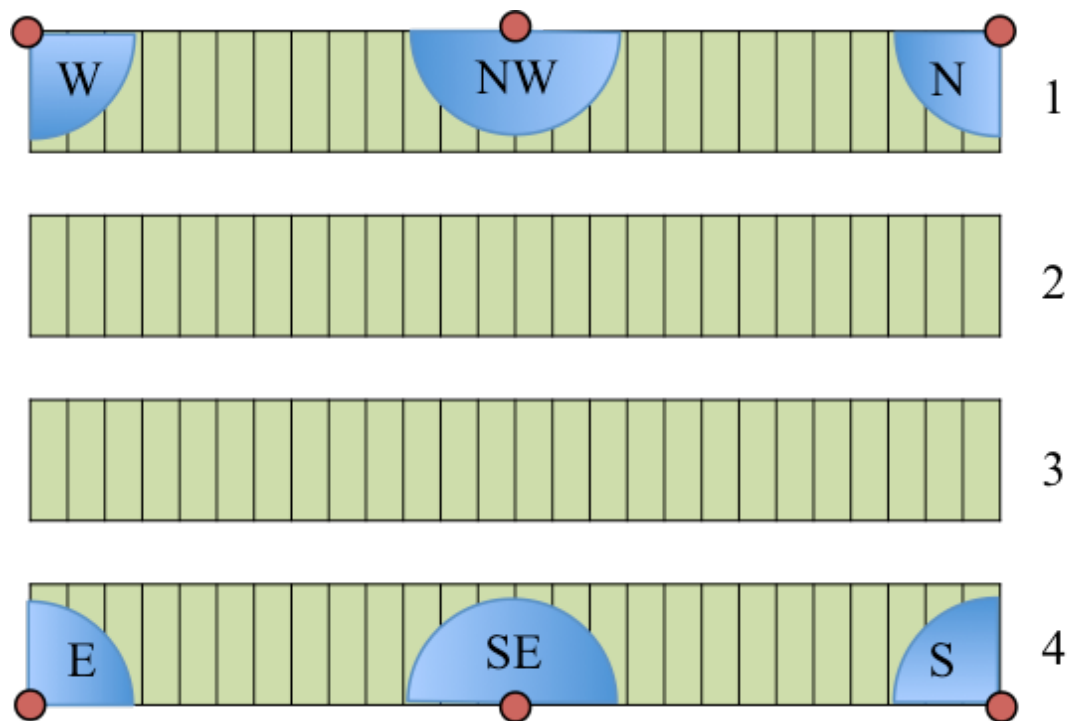


Figure 3. Field illustration depicting experimental plot layout and field ranges (1-4) and relative location of terrestrial laser scanning positions.

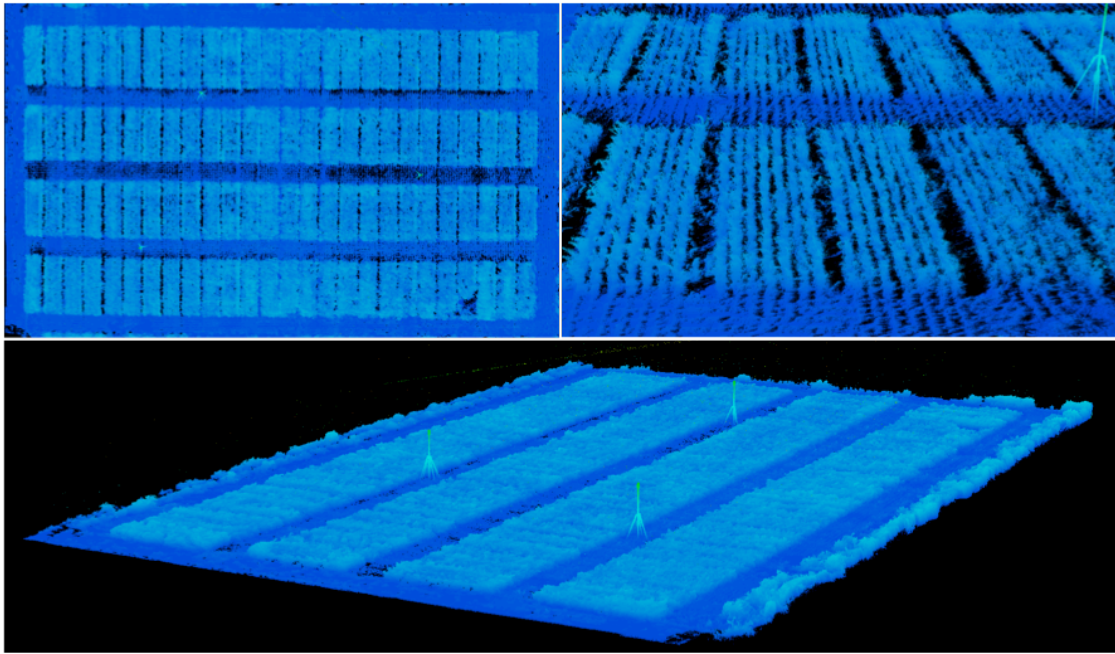


Figure 4. Point cloud depicting terrestrial laser scanning data of experimental plot.

Point cloud data representing the plot vegetation was selected by removal of the soil background. To remove the soil all values with an elevation within the point cloud of less than 0.05 m the data was transformed to a zero value, all data points above the 0.05 m plane were used in further analysis. Data was sorted to remove all zero values from the analysis.

Point cloud data was then parsed into subsets representing each experimental plot within the trial using HDS Cyclone (Leica Geosystems, St, Gallen, CHE). Data was then gridded using Quick Terrain Modeler (Applied Imagery, Silver Spring, MD, USA). Gridded data was then classified and exported using ArcGIS (ESRI, Redlands, CA, USA). Subset plot data representing point cloud density for each plot was separated into 10 cm horizons for evaluation.

### ***Statistical analysis***

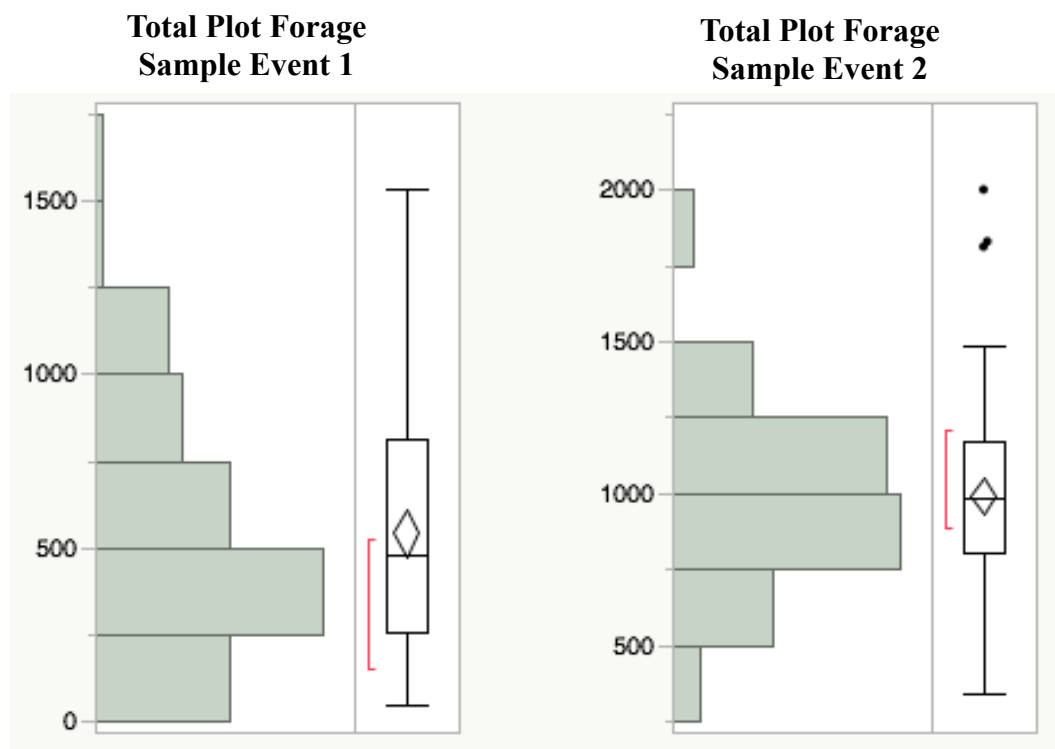
Statistical analysis of the data was performed using JMP Pro version 11 (SAS Institute Inc., Carry, NC, USA). Data presented in the results are from the 2010 growing season. We used a general linear model to calculate analysis of variance. Least squares means were correlated using Pearson's correlation to determine if relationships existed. A probability value of 0.05 or less was considered to be statistical significant.

## Results

### *Destructive forage measurements*

Forage biomass was collected a total of four times during the growing season with variability in the data collected being highest during the first sampling event (CV 62.8) then improving for the second event (CV 30.0) and third event (CV 18.2) then increasing for the fourth and final harvest (CV 37.7) (Figure 5; 6). The standard deviation and the standard error mean for the data both decreased from the first to the fourth sampling event. The data discussed within this study is representative of the fourth sampling event.

Forage biomass was evaluated at the full plot level as well at a sub plot level. Linear regression comparing sub plot forage yield and total plot forage yield for each experimental plot across the four replications correlated poorly ( $R^2 = 0.10579$ ) (Figure 7).



Mean	541.921
Std Dev	340.45549
Std Err Mean	34.045549
Upper 95%	609.47475
Lower 95%	474.36725
N	100
CV	62.823822

Mean	992.6829
Std Dev	298.39114
Std Err Mean	29.839114
Upper 95%	1051.8902
Lower 95%	933.47562
N	100
CV	30.05906

Figure 5. Distribution analysis of plot forage biomass across four replications for the first and second forage biomass sampling events of the growing season.

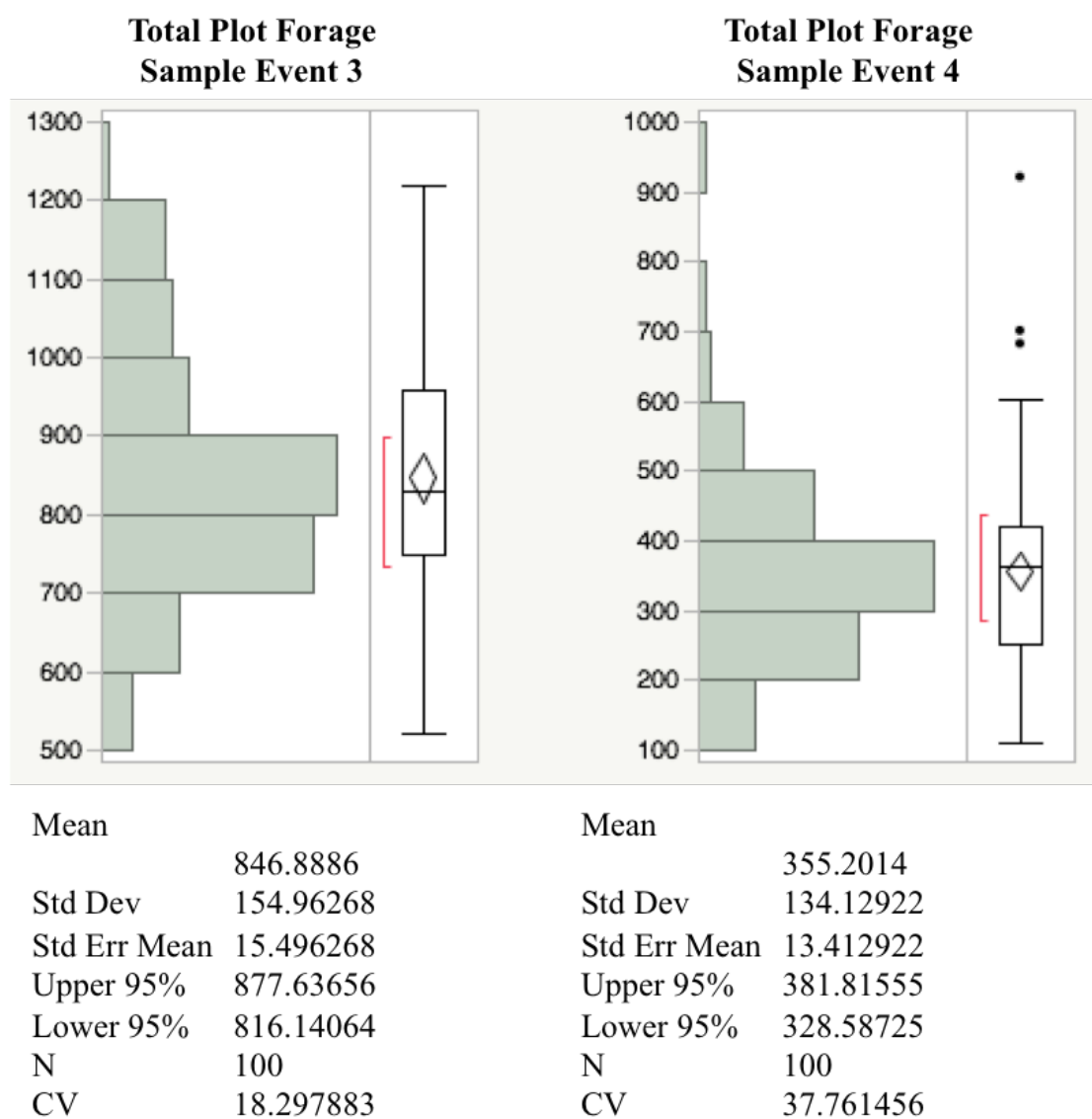


Figure 6. Distribution analysis of plot forage biomass across four replications for the third and fourth forage biomass sampling events of the growing season.



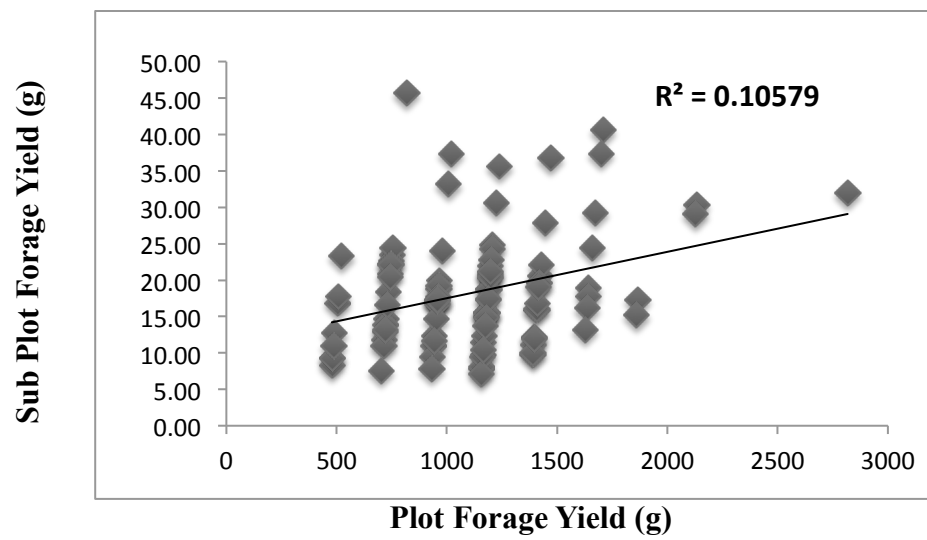


Figure 7. Linear regression comparing sub plot forage yield and total plot forage yield for each experimental plot across four replications.

### *Non-Destructive forage measurements*

Non-destructive forage measurements were evaluated against established destructive techniques. Data presented was collected during the fourth harvest event only. Linear regressions comparing mean canopy height and total plot forage yield for each experimental plot across four replications was poorly correlated ( $R^2$  0.08) (Figure 8). Additionally, total forage yield for each experimental plot was compared with the visual biomass scores with even less predication ability ( $R^2$  0.02) (Figure 9). The data representing the visual biomass score was grouped based on the limited possible classifications.

Mean plot NDVI measurements were evaluated against total plot forage biomass with poor correlation ( $R^2$  0.036) (Figure 10). Wheat forage plants per meter square at the plot level were measured and linear regression to mean NDVI values was poor ( $R^2$  0.056) (Figure 11). NDVI mean values for the experimental plots were largely grouped with limited distribution as were the number of plants per square meter.

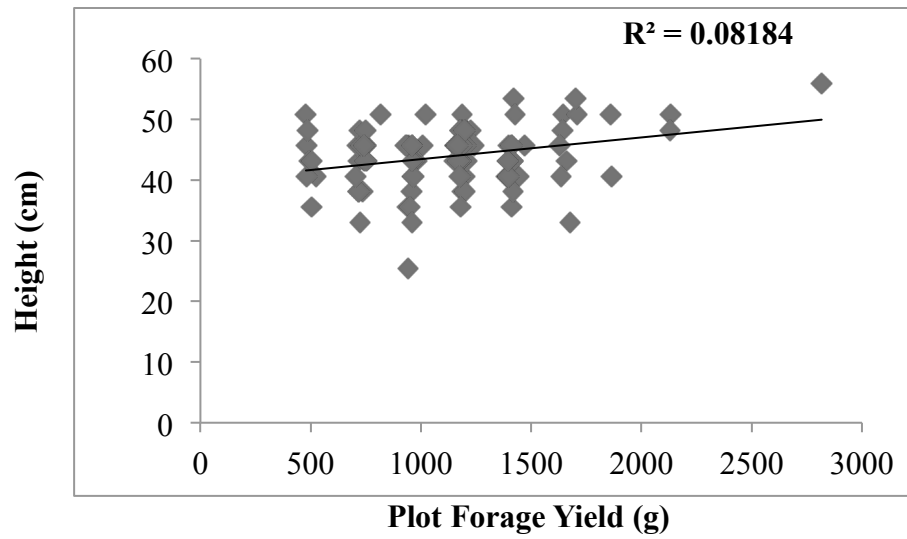


Figure 8. Linear regressions comparing mean canopy height and total plot forage yield for each experimental plot across four replications.

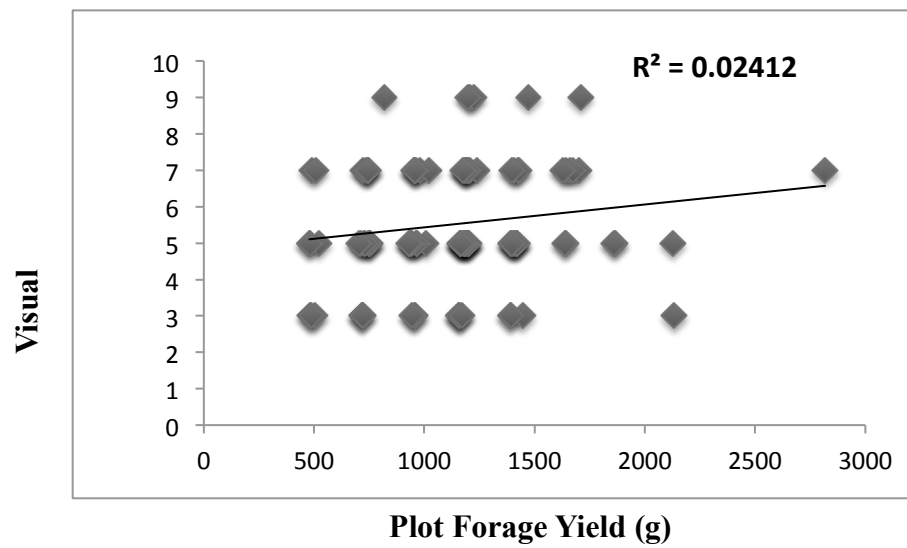


Figure 9. Linear regressions comparing visual forage biomass score and total plot forage yield for each experimental plot across four replications.

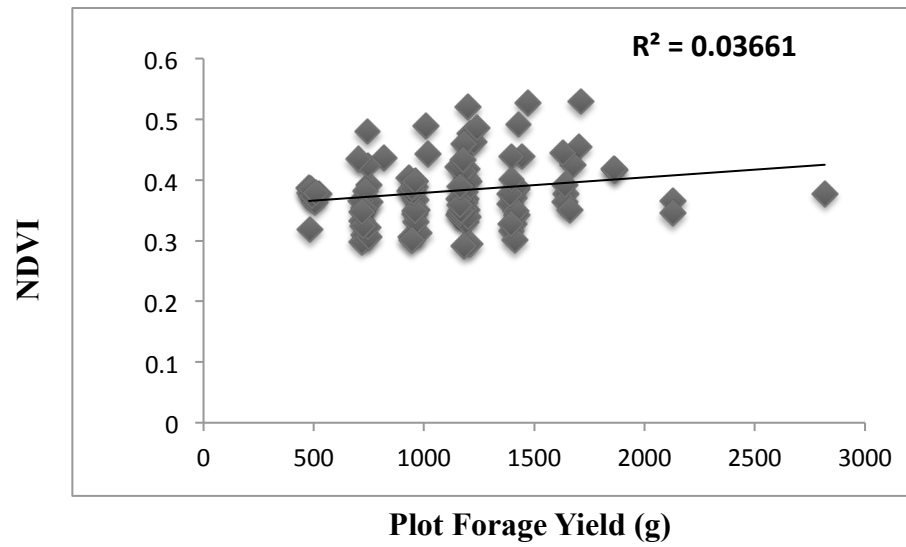


Figure 10. Linear regressions comparing normalized difference vegetation index (NDVI) and total plot forage yield for each experimental plot across four replications.

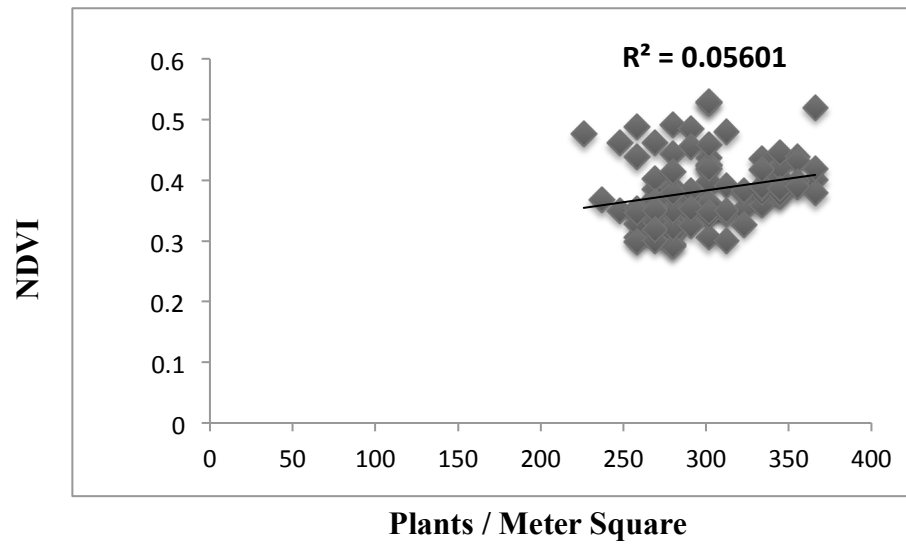


Figure 11. Linear regressions comparing normalized difference vegetation index (NDVI) and wheat plants per square meter for each experimental plot across four replications.

TLS data evaluated against total plot forage biomass and sub plot forage biomass. TLS plot data was parsed into 10 cm horizons for evaluation of the mean number of returns. Each horizon was evaluated using both total plot forage biomass as well the sub plot value representing a mean of 3 samples. Poor to no correlation was found for the individual TLS data horizons.

Total mean TLS data points returned for a given plot were tested for a linear relationship with little success to total plot forage yield ( $R^2$  0.000) (Figure 12) . Evaluation of the total mean TLS data points for each plot as compared to the sub plot forage harvested yielded a negative relationship ( $R^2$  0.039) (Figure 13).

The mean value of the TLS elevation points had a higher correlation with both plot ( $R^2$  0.09458) and sub plot ( $R^2$  0.37984) forage yield (Figure 14; 15). Using the elevation maximum value for TLS plot data a comparison to plot ( $R^2$  0.05842) and sub plot ( $R^2$  0.09607) forage yield was made (Figure 16; 17).

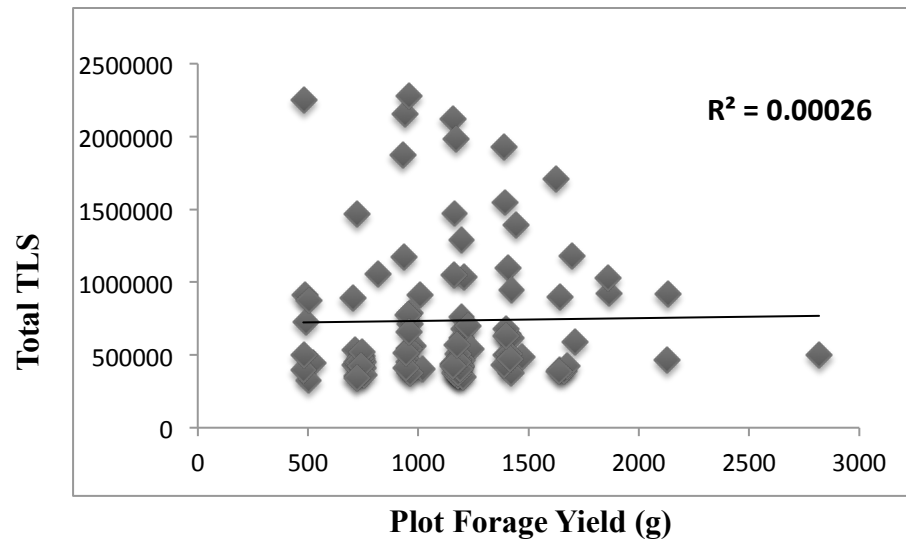


Figure 12. Linear regressions comparing total terrestrial laser scanner point cloud points collected and total plot forage yield for each experimental plot across four replications.

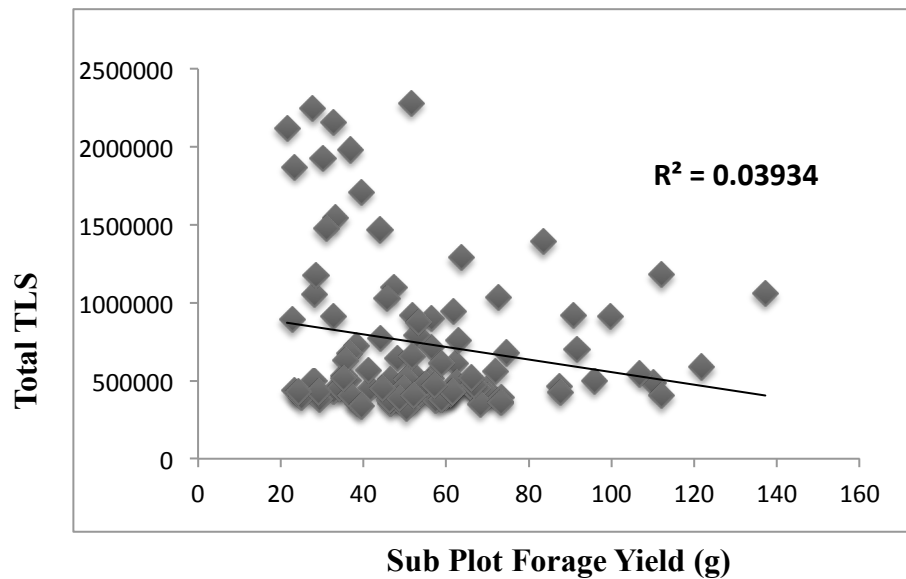


Figure 13. Linear regressions comparing total terrestrial laser scanner point cloud points collected and sub plot forage yield for each experimental plot across four replications.

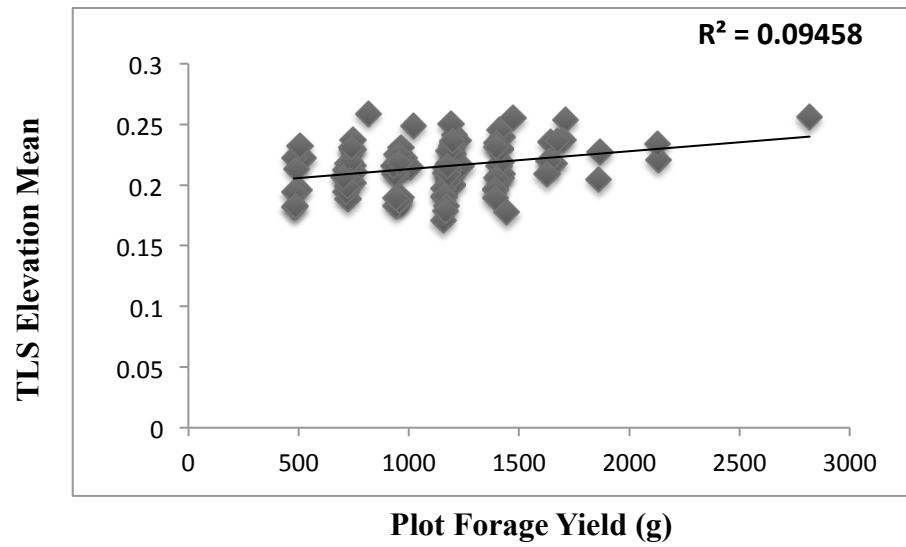


Figure 14. Linear regressions comparing terrestrial laser scanner elevation mean point cloud points collected and total plot forage yield for each experimental plot across four replications.

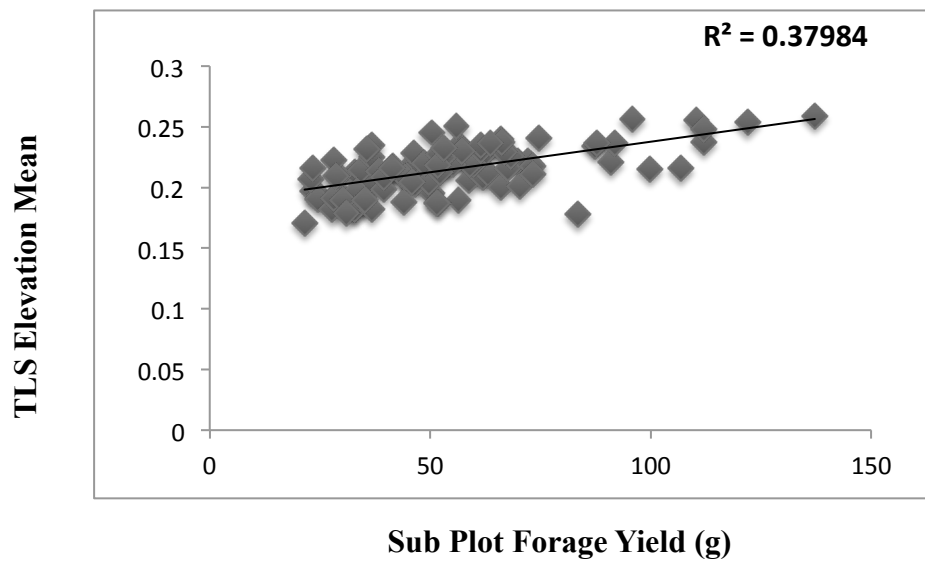


Figure 15. Linear regressions comparing terrestrial laser scanner elevation mean point cloud points collected and sub plot forage yield for each experimental plot across four replications.

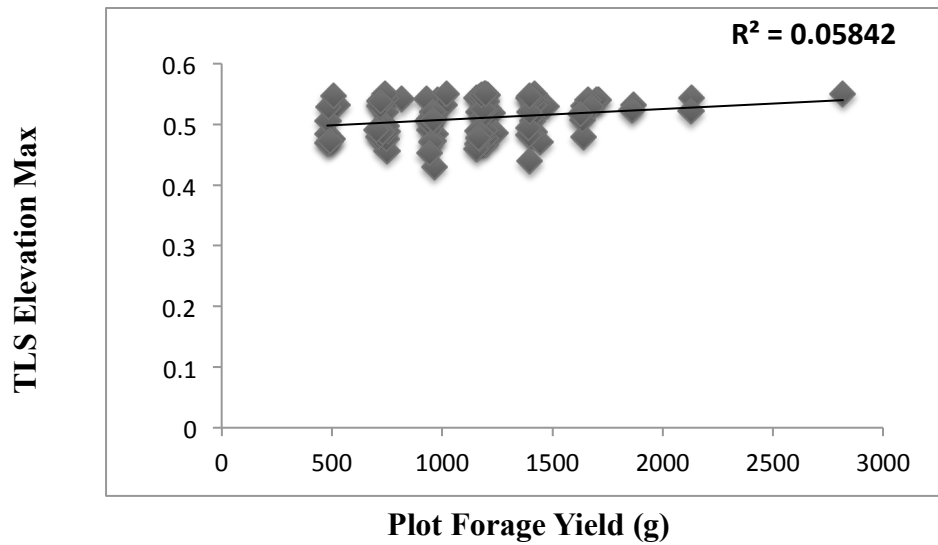


Figure 16. Linear regressions comparing terrestrial laser scanner elevation max point cloud points collected and total plot forage yield for each experimental plot across four replications.

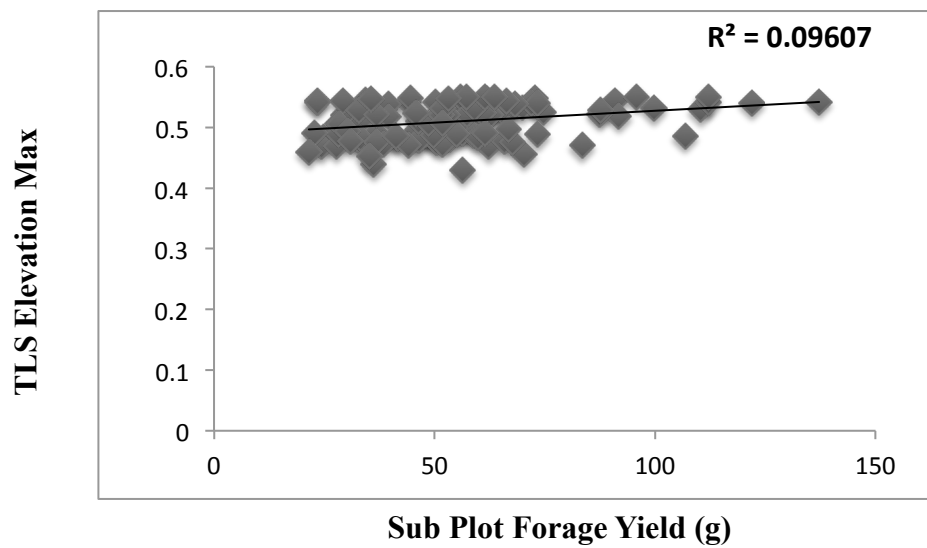


Figure 17. Linear regressions comparing terrestrial laser scanner elevation max point cloud points collected and sub plot forage yield for each experimental plot across four replications.



Total mean TLS data points returned for a given plot were tested for a linear relationship against plant canopy height ( $R^2$  0.00112) (Figure 18). Total mean TLS data points for each plot as compared to mean NDVI measurements produced weak relationship ( $R^2$  0.01764) (Figure 19).

The mean value of the TLS elevation points had a weak yet better correlation with both plant canopy height ( $R^2$  0.11831) and NDVI ( $R^2$  0.08837) (Figure 20; 21). TLS data representing the elevation mean value was clustered with little variability. Using the elevation maximum value for TLS plot data a comparison to plant canopy height ( $R^2$  0.07601) and NDVI ( $R^2$  0.05395) was made (Figure 22; 23). Data representing the mean NDVI values was poorly distributed and lacked variation.

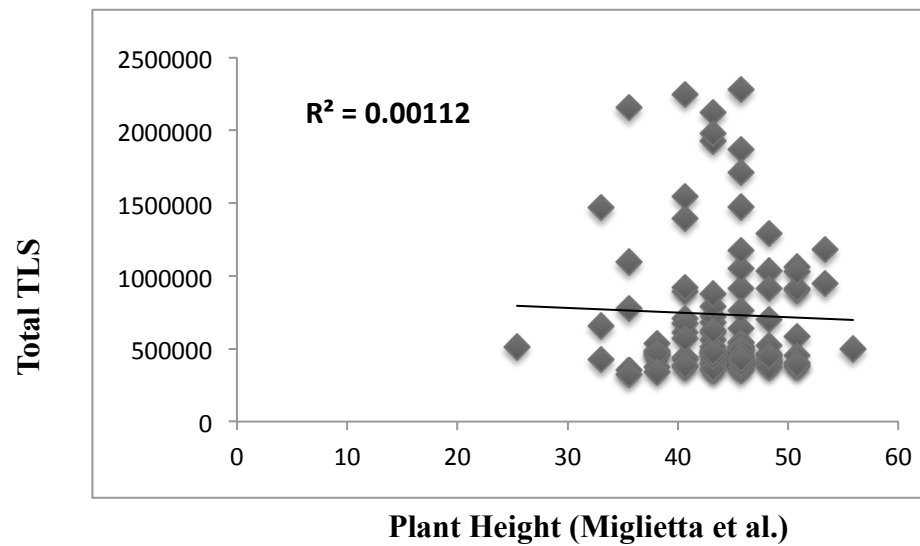


Figure 18. Linear regressions comparing total terrestrial laser scanner point cloud points collected and mean plant canopy height for each experimental plot across four replications.

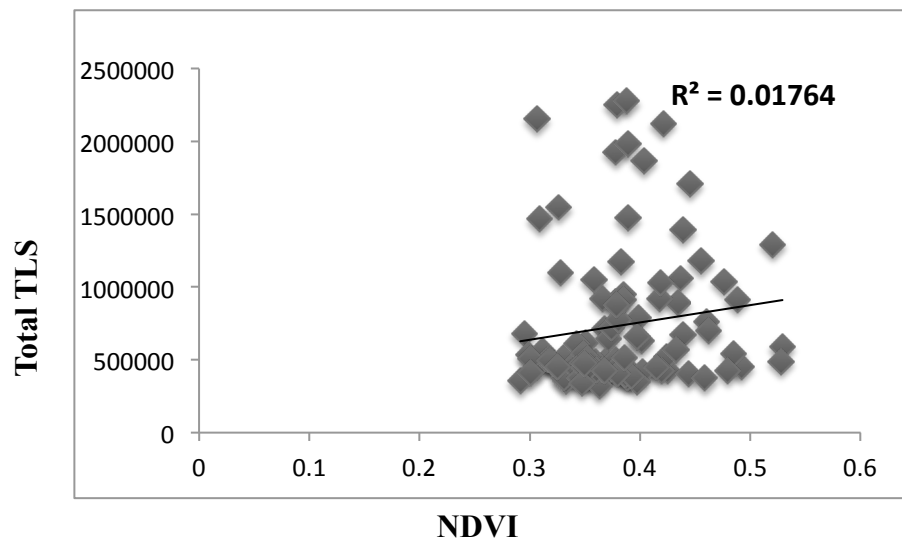


Figure 19. Linear regressions comparing total terrestrial laser scanner point cloud points collected and normalized difference vegetation index (NDVI) for each experimental plot across four replications.

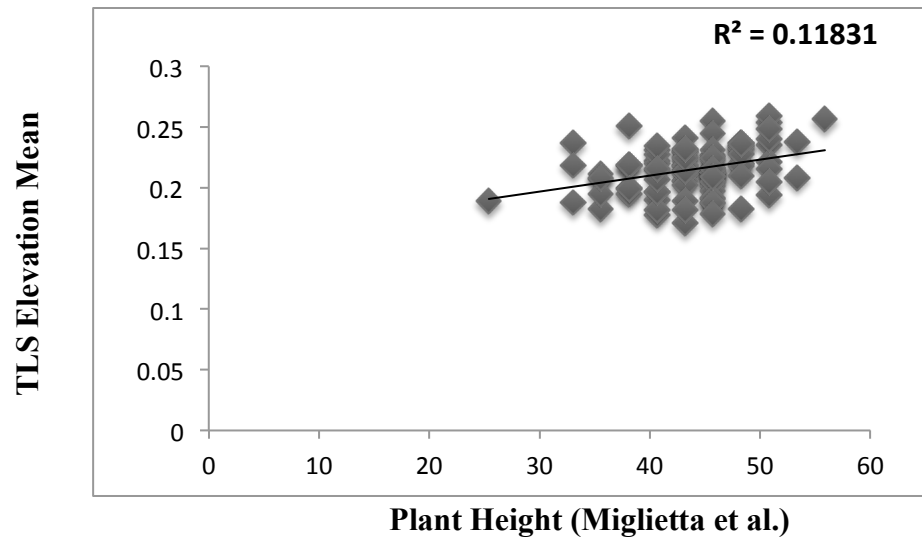


Figure 20. Linear regressions comparing terrestrial laser scanner elevation mean point cloud points collected and mean plant canopy height for each experimental plot across four replications.

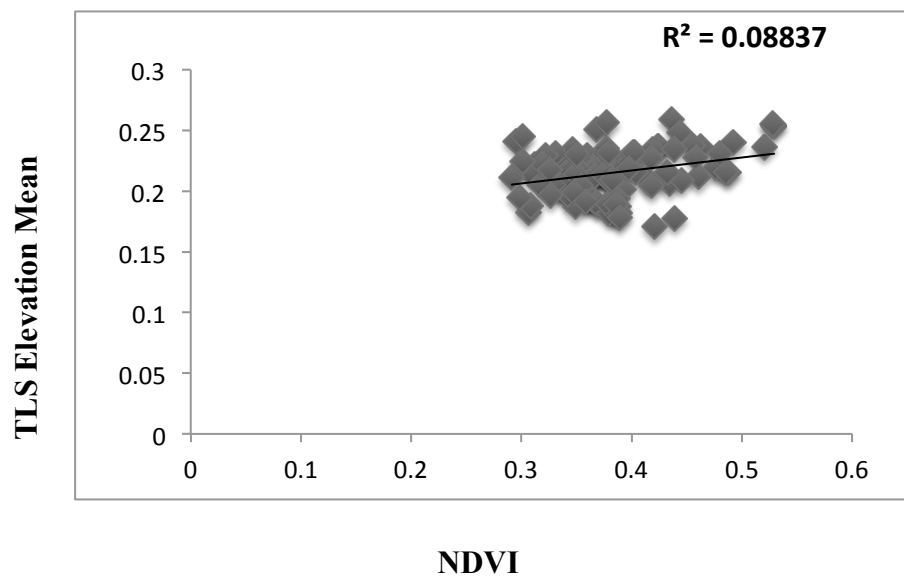


Figure 21. Linear regressions comparing terrestrial laser scanner elevation mean point cloud points collected and mean normalized difference vegetation index (NDVI) for each experimental plot across four replications.

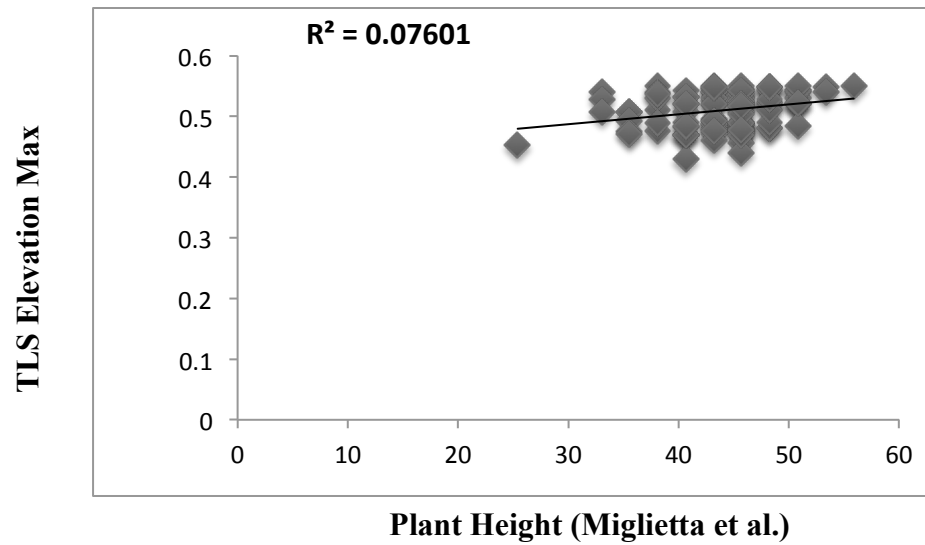


Figure 22. Linear regressions comparing terrestrial laser scanner elevation max point cloud points collected and mean plant canopy height for each experimental plot across four replications

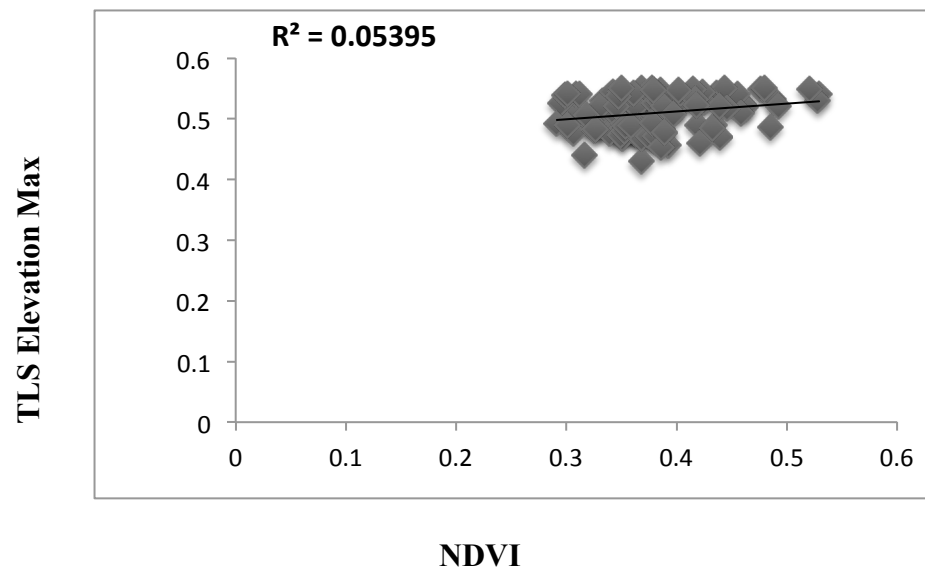


Figure 23. Linear regressions comparing terrestrial laser scanner elevation max point cloud points collected and mean normalized difference vegetation index (NDVI) for each experimental plot across four replications.

## **Discussion**

This experimental trial was conducted in parallel with another study assessing nitrogen pre and post planting application rates to maximize wheat forage production (Franks, 2013). Experimental plot forage was collected across the growing season a total of four times. This study was conducted on the last of four harvest events. Using full plot harvest data across replications analysis of yield distribution for each of the sampling events reveals the mean standard error and standard deviation both decrease from the first to the fourth cutting. Nitrogen treatments were expected to provide sufficient differentiation between plots for forage biomass. Differences were seen in the early cuttings however as the study progressed the treatment effect was less prevalent (Franks, 2013). The limited differentiation between nitrogen treatments in the fourth harvest event may contribute to the poor correlation between total plot forage and the TLS and even sub-plot forage yield.

Comparing full plot harvested forage and the average of three sub-plot samples produced a poor correlation. This could be in part to the limited differentiation seen between nitrogen treatments. In addition, the overall plot yield was less across the trail as expected late in the growing season making the small volume of forage challenging for the onboard weighing system of the harvester to evaluate. The limited correlation seen between the full and sub plot forage harvest data limits the ability of this study to evaluate the non-destructive forage sampling platforms.

The lack of data classification options for both plant height and visual score along with limited variability between treatments was evident when comparing them to total plot forage yield. The height data was clearly grouped based on treatment with some outliers. The classification in canopy height data (30-50 cm) was closely grouped and displayed little variation, as did the visual score. The visual score was limited to forage classification within 4 groups making it even harder to separate small differences. The limited number of classifications the data can be grouped into using these techniques is a limitation even when evaluated against treatments differing in forage yield.

Poor correlation between NDVI and plot yield was expected due to the limited reliability of the measurement following canopy closure. The variability of plants per meter square in each plot was limited, this can be seen by the close association of the data making this a challenging correlation in comparison to NDVI. NDVI measurements from earlier forage harvest events had stronger correlation however were not used in this study as TLS data was only collected prior to the fourth forage harvest.

We compare total and 10 cm horizontal TLS points collected for each experimental plot across all four replication to total forage plot and sub plot yield and found no improvement in correlation using the TLS horizontal data as compared to the total TLS points. Thus, we compared total TLS points collected, the elevation mean, and the elevation maximum for each experimental plot across all four replication to total forage plot and sub plot yield. Poor correlation was seen across methods however, using the

elevation mean TLS value there was a significant increase in correlation suggesting this as a target TLS measurement. Using this approach, total TLS points collected, the elevation mean, and the elevation maximum for each experimental plot across all four replication we tested the linear correlation with plant height and NDVI. Poor correlation was again seen however the relationship between TLS elevation mean and plant height was strongest in comparison.

### **Conclusions**

This study provides limited information as to the capability of TLS in non-invasive forage biomass evaluation. Forage yield variability seen in earlier harvest events would have provided a better opportunity to test TLS. Correlation between sampling methods seen in earlier harvest events were lacking in this experimental trial suggesting the limited relationship observed with TLS could improve if compared to earlier sampling events. Use of the elevation mean value for TLS points collected within an experimental plot has shown potential as a target value for evaluation in future studies.

## CHAPTER IV

### UTILITY OF GROUND PENETRATING RADAR FOR FIELD-BASED HIGH-THROUGHPUT PHENOTYPING OF WHEAT ROOTS

#### Overview

Ground penetrating radar (GPR) is a remote sensing tool that has been successfully used in evaluation of coarse tree root biomass. Incorporating GPR into current crop phenotyping methodologies could potentially provide a long awaited solution to high throughput phenotyping for roots under realistic field conditions. This work tested the utility of using GPR as a tool to estimate root biomass of wheat (*Triticum spp.*). Here a replicated field trial of wheat genotypes with differing aboveground physiology was agronomically evaluated then correlated with GPR returned signals. Plants were grown in standard field conditions and under simulated waterlogging stress for comparison. GPR profiles were collected at 50 cm intervals, using a 1.6 GHz antenna. Plots were subsequently evaluated destructively by root coring to determine root biomass. GPR return signal was processed using GPR-SLICE v7.0 software. GPR ability to predict root presence and absence was tested and GPR was able to differentiate root mass from soil significantly ( $\alpha = 0.95$ ,  $t = 1.96022$ ). Linear regression between Log10 of the mean GPR amplitude return at the 0-3 ns range was compared with agronomic breeding traits. Overall increased amplitude was observed in plots scoring higher with regard to overall yield and yield components.



## **Introduction**

The capacity of agriculture to feed a predicted population of 9 billion in the year 2050 will be challenged by predicted infrequent and intense precipitation events combined with increases in atmospheric temperatures and carbon dioxide (CO<sub>2</sub>) levels. Climatic instability will limit future global food security (Schmidhuber and Tubiello, 2007).

These predictions define drought and heat stress as the most challenging limitations to future agricultural production (Lipiec et al., 2013). Efforts in adapting crops for future production environments will need to be focused on breeding for reduced susceptibility to heat and drought stress as well increased productivity with limited input. High temperature stress often exacerbates the negative impact of drought by limiting crop growth and production (Reynolds, 2010). Under abiotic stress plants respond with a series of changes including altered gene expression and adaptive physiological response negatively impacting yield (Shinozaki and Yamaguchi-Shinozaki, 2007). Crop roots and root-soil interactions have potential to mediate the negative impact of drought and heat stress on overall yield (Lipiec et al., 2013).

## ***Root architecture***

Optimal root biomass and penetrating depth are target traits that function in the extraction of water from surrounding soils (Garrigues et al., 2006). In addition to unlocking needed water, roots function in nutrient and carbon sequestration (Kell, 2011).

Atmospheric CO<sub>2</sub> is reduced by photosynthesis contributing to soil carbon sequestration and stabilization (Figure 24).

Breeding crops with improved roots could increase steady-state trapping of carbon, nutrients, and water leading to improved drought- and flooding tolerance, greater biomass yields, and better soil structure (Kell, 2011). Likewise, greater root elongation can play a critical role in allowing the plant to reach deeper soil profiles allowing access to nutrients and needed water (Bengough et al., 2011). Adaption of agricultural crops to future growing environments will require plant breeders to select cultivars with optimal root traits (Gewin, 2010).

Historically, breeding efforts for targeted adaptive traits such as dwarf stature and resistance to biotic and abiotic stressors have mediated eras of global food insecurity (Ronald, 2011). Utilizing aboveground traits, plant breeders have made substantial improvement in adapting varieties to heat and drought stress. Belowground traits have largely been neglected due to a lack in ability to accurately and nondestructively phenotype roots, this lack of selection pressure on root traits has maintained the needed genetic variation available today. Root phenotypes have long been economically out of reach for breeding programs. Development of field-based high-throughput phenotyping (FBHTP) tools capable of characterizing roots non-destructively and cost effectively remains a bottleneck for future breeding advances.

### ***Breeding global grains***

Cultivated globally, wheat (*Triticum spp.*) is second only to maize in total hectares of cereal production and the primary source of dietary calories for those living in the poorest countries (Msangi et al., 2009). Wheat is relatively well adapted to dry environments and research has shown steady progress in efforts to increase its performance in predicted heat and drought stressed conditions (Trethowan et al., 2002). Wheat germplasm, adapted and exotic, harbor multiple adaptive traits with the potential to buffer the impact high temperature and drought stress (Reynolds et al., 2010). However, current cultivars grown in temperate regions of the world are limited to an increase in atmospheric temperature (1-3°C), beyond which their productivity will be negatively impacted (IPCC, 2007). Wheat grown in tropical and sub tropical regions will be negatively impacted by even less of an increase in temperature (1-2°C) (Hodson and White, 2007). Performance of wheat in hot environments, often co-associated with dry environments, is not promising and substantial yield losses have already been reported (Reynolds et al., 1994; Wardlaw and Wrigley, 1994).

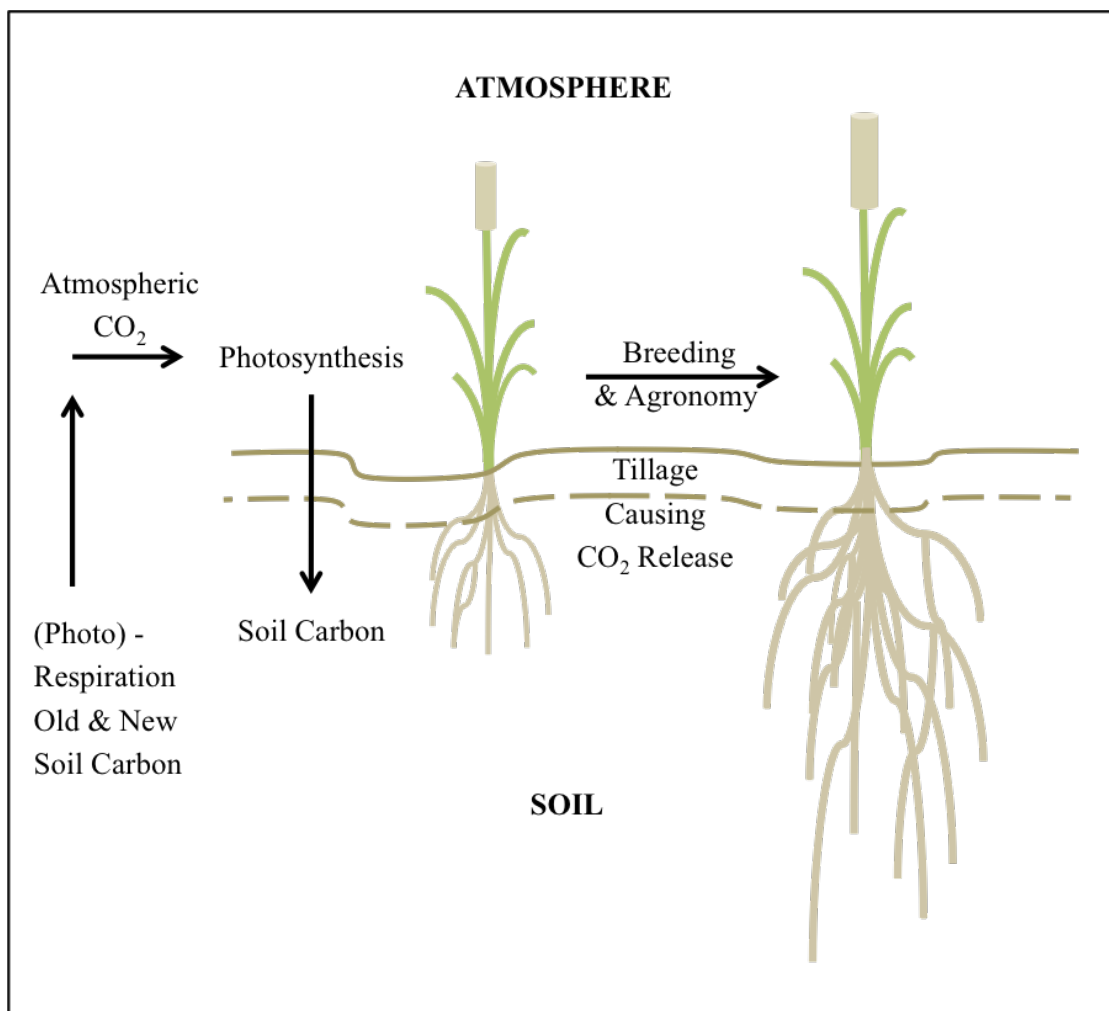


Figure 24. Illustration of the potential impact of increased root systems on carbon, water and nutrient sequestration. Atmospheric carbon dioxide is reduced by photosynthesis contributing to soil carbon sequestration. Improving crop roots could increase steady-state trapping of carbon, nutrients, and water leading to improved drought- and flooding tolerance, greater biomass yields, and better soil structure. Figure adapted from (Kell, 2011).

Breeders are selecting cultivars optimized for performance and yield under heat and drought conditions using targeted adaptive physiological trait introgression. Current breeding platforms operate stepwise, by crossing parental lines followed by selection of offspring.

Evaluation of canopy temperature using a hand held infrared thermometer, has increased selection speed and accuracy of wheat varieties best suited for drought and heat stress environments highlighting the need for additional FBHTP tools (Mason and Singh, 2014). The ability of plant breeders to dissect and capitalize on genetic traits associated with increased yield and stress tolerance is limited by a lack of FBHTP tools capable of accurate and cost effective characterization of target traits (Araus and Cairns, 2013).

### ***Root phenotyping***

Roots have been traditionally overlooked in crop improvement programs due to their highly complex interaction with the soil environment as well the cost and effort required for accurately phenotyping. Traditional methodologies (Table 2) have for the most part been destructive in nature or at the very least influential on root growth and development.

Roots are inherently challenging to study because of their physiological complexity and phenotypic interaction with the soil environment. Techniques for studying roots have

been developed however each method has unique limitations that must be considered. The destructive nature and economic cost of root characterization has limited our ability to capitalize on root traits in breeding programs. Soil coring is a proven technique that has been utilized to study roots in a host of different crops. This method in comparison to other techniques provides the most accurate measurement of root length, and mass (Reynolds et al., 2012). However, soil cores provide a limited view of the rhizosphere requiring sampling replication increasing time and cost (Pierret et al., 2005). Soil cores can be excavated by hand however uses of hydraulic systems have increased accuracy as well reduced sampling time. Root biomass and depth can be evaluated by soil coring methods. Following extraction the cores are washed and the roots removed from the soil then separated from organic debris before analysis (Figure 25). This time consuming process can be improved by use of a root washing machine however it is still considered labor intensive.

The application of a FBHTP to plant breeding for improved roots would require a platform capable of non-destructive evaluation across physiological development. Root phenotyping cost and time must be the primary considerations in developing new tools capable of accurately characterizing roots in large breeding populations and diverse growing environments. Geophysical techniques offer a potential platform for FBHTP of roots considering their non-destructive and high-throughput nature.

Table 2. Overview of common field-based phenotyping techniques.

TECHNIQUE	METHOD	ADVANTAGE	DISADVANTAGE	REFERENCES
<b>Mini-Rhizotrons</b>	Observation of roots through transparent tube inserted into soil. Roots physiology observed by video imaging.	Repeated observations of large numbers of roots over time providing detailed root production and mortality information.	Underestimate root density in upper soils and overestimate in lower soils. Only net changes in growth of roots can be followed. Static representation.	(Bragg et al., 1983; Majdi and Nylund, 1996; Polomski et al., 2002)
<b>Profile Wall (Trenching)</b>	Direct root observation by excavation of neighboring soil. Root distribution mapped on surface of trench wall.	Estimated quantity and development of vertical and horizontal fine and coarse roots.	Partial characterization of root system. Lacks structural information. Root and plant associations problematic.	(Bohm, 1979; Polomski et al., 2002; Rutherford and Curran, 1981)
<b>Pulling Force</b>	Resistance to vertical pull on root crown reflecting root number, depth, and strength.	Rapid and inexpensive. Capable of evaluating lodging resistance and root pest resistance.	Destructive in nature. Indirect measure unable to evaluate individual root traits.	(Easson et al., 1995)
<b>Rhizotrons</b>	Direct observation of roots through transparent viewing plates from subterranean tunnel.	Continuous measurement over root physiological development of the same plant.	Expensive to build. Artifacts, root growth against glass wall may not be representative. Static representation.	(Polomski et al., 2002)
<b>Root Window</b>	Direct observation of roots through transparent viewing panes installed in soil.	Root morphological development, physiological changes, and root lifespan mortality.	Limited replications. Static representation. Artifacts, root growth against glass wall may not be representative.	(Neumann et al., 2009; Polomski et al., 2002)
<b>Shovelomics</b>	Roots excavated using soil cylinder (40cm x 25cm) with plant root crown in center.	Effective in phenotyping root crown.	Laborious, requires multiple sampling replication. Extensive processing of samples is required	(Trachsel et al., 2010)
<b>Soil Coring</b>	Soil cores extracted by depth intervals. Cores are washed to separate roots from soil.	Estimate of root depth and distribution	Laborious, requires multiple sampling replication. Extensive processing of samples is required	(Schroth and Kolbe, 1994)

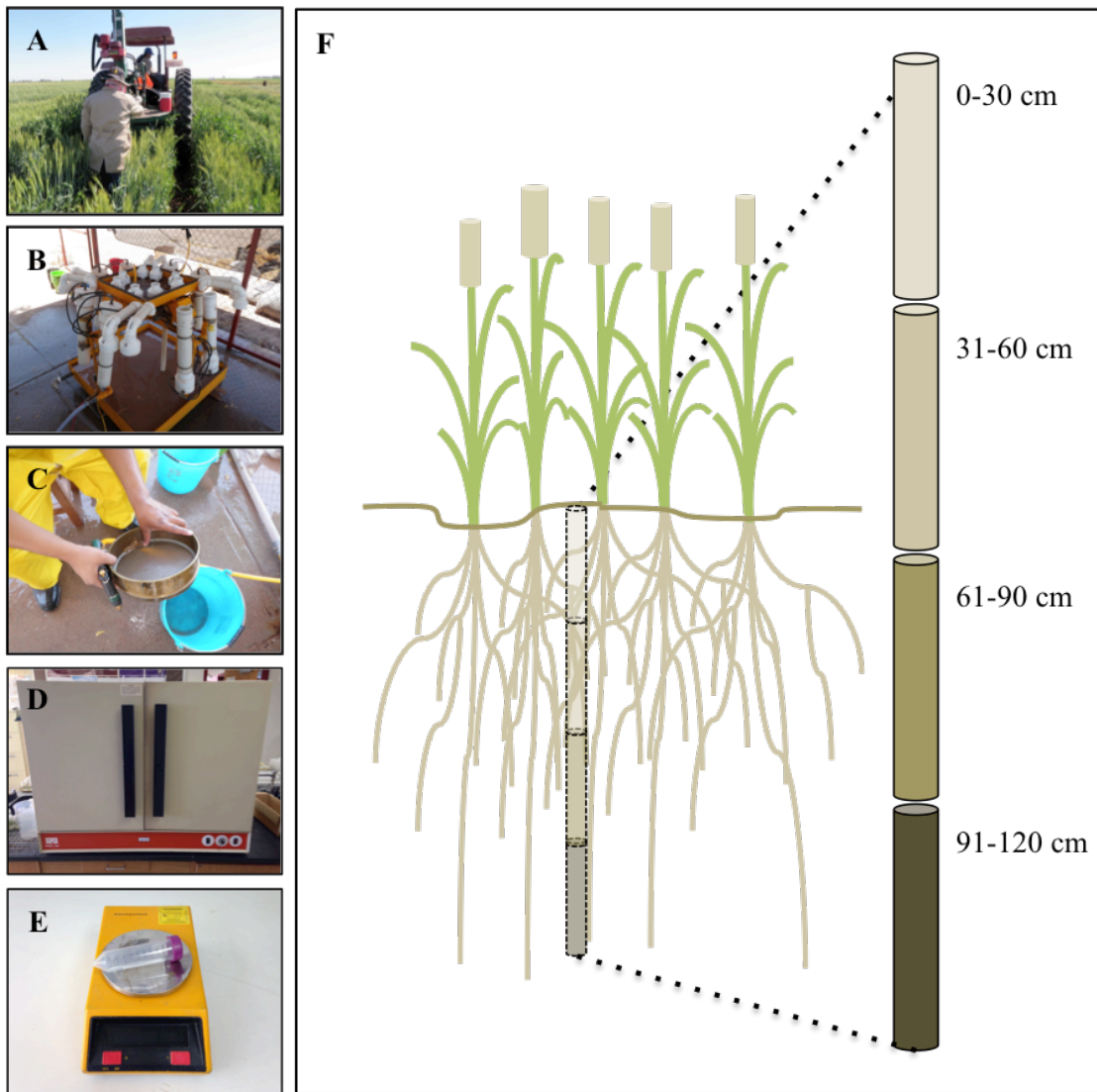


Figure 25. Destructive sampling of wheat roots by soil coring. Determining root biomass of wheat plants (A) hydraulic soil core extraction, (B) separation of root material from soil by washing, (C) hand sieving of root material, (D) drying samples, and (E) weighing dried root samples. To evaluate rooting depth the same procedure is followed however core samples are separated into 30 cm segments and treated independently.



### *Agricultural geophysical methods*

Geophysical methods are being utilized in several different areas of agriculture targeting shallow sub surface features within the soil profile. The most common being used are resistivity, electromagnetic induction (EMI), and ground penetrating radar (GPR) (Figure 26). Resistivity can be used for rapid evaluation of soil water content. Soil salinity is easily mapped in comparison to traditional techniques using EMI techniques as well GPR has also been used in soil survey mapping to aid precision farming's understanding of soil spatial variation. Geophysical methods have become standard in the evaluation of soil hydrology, identification of soil horizons, soil nutrient monitoring, crop and tree root biomass, subsurface drainage monitoring and detection, and in many other applications. Uses of geophysical methods have ultimately increased speed and accuracy of traditional means of measure and thus increased the productivity of agriculture as a whole.

<b>GEOPHYSICAL METHOD</b>	<b>PHYSICAL PRINCIPALS</b>	<b>APPLICATION</b>	<b>REFERENCES</b>
<b>(A) Resistivity</b>	Electrical capacitance of an equivalent parallel resistance-capacitance circuit formed by the interface between soil water and the root surface.	Soil drainage class mapping; Small soil crack imaging	(Amato et al., 2009; Leucci, 2010)
<b>(B) Electromagnetic Induction</b>	Measure of apparent electrical conductivity of soil.	Identification of clay pan depth; Soil nutrient monitoring; soil salinity assessment	(Eizenberg, 2005)
<b>(C) Ground Penetrating Radar</b>	Electromagnetic technique detecting changes in the relative dielectric permittivity within the shallow subsurface.	Tree and crop root biomass assessment; Identification of subsurface flow pathways	(Butnor et al., 2001; Butnor et al., 2003; Guo et al., 2012; Hruska et al., 1999; Leucci, 2010)



Figure 26. Current agricultural geophysical techniques. (A) Resistivity (Image: Veris technologies, Salina, KS, USA). (B) Electromagnetic Induction (C) Groud Penetrating Radar.

GPR has proven useful in non-destructive subsurface characterization in archeology, geology, military, and forensic applications (Daniels, 2000; Goodman and Piro, 2013). Cross discipline use of this rapid noninvasive technique has driven the development of data acquisition platforms and software capable of high-resolution three-dimensional (3D) visualization capabilities (Goodman and Piro, 2013; Novo et al., 2013). GPR has been used successfully in coarse tree root detection and quantification (Guo et al., 2012). GPR could serve as a powerful tool for phenotyping ideal root traits in the context of performance during stress, while allowing plant breeders to screen large populations.

### ***Ground penetrating radar principle***

The GPR system is comprised of three basic components; a control computer, the control unit, and antenna containing both the transmitter and receiver (Figure 27). The control unit generates and synchronizes the radar pulse from the antenna while providing received data to the control computer. Distance traveled along a profile can be recorded by use of a global positioning system (GPS), total scan station (TSS), and or an attached odometer wheel.

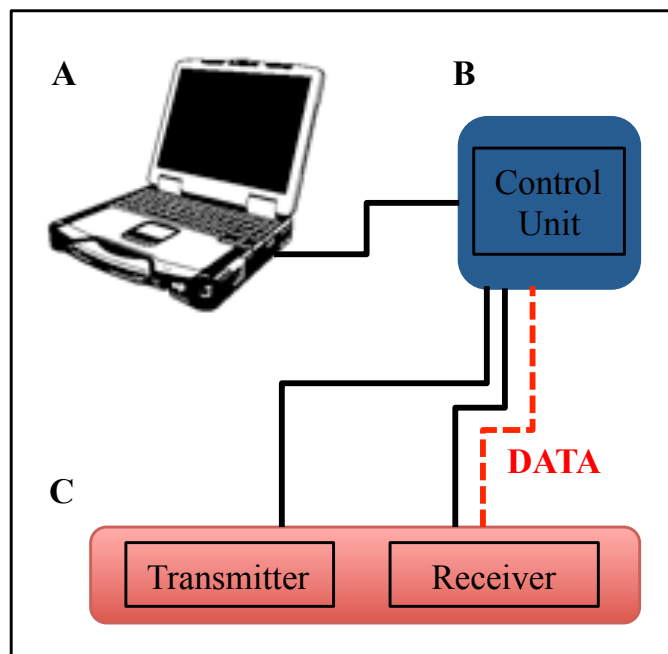


Figure 27. Components of a ground penetrating radar system. The ground penetrating radar system is comprised of three main components; (A) control computer, (B) control unit, and (C) the antenna.

GPR functions by transmitting short pulse, high frequency electromagnetic (EM) energy into the ground in the microwave band of the radio spectrum (Neal, 2004). Transmitted pulses consist of a spectrum of wave frequencies above and below the transmitted central frequency (TCF) of the selected antenna. Subsurface interfaces separating layers of differing relative dielectric permittivity (RDP), a measurement of how well EM energy is transmitted through a medium, reflect back a portion of the energy from the pulse while the remaining energy continues to the next interface (Attia al Hagrey, 2006). The GPR antenna functions in both the transmitting and receiving of the EM pulse (Figure 27). The radar pulse is timed, from the point of transmission into the ground to the interaction with belowground targets or dielectric interfaces, until the reflections are received back at the surface antenna (Figure 28). Antenna position, during signal transmission and reception, can be logged by use of the odometer wheel, GPS, TSS, or any combination of systems.

GPR profiles are two-dimensional data visualized as radiograms. Radar pulses received are recorded by then digitized and converted into a reflection trace. Radiograms comprise of a series of combined reflection traces evenly spaced along a profile (Figure 28). The contrast of RDP between neighboring subsurface targets determines the strength of the reflected energy (Goodman, 1994). GPR pulses are recorded as the antenna moves along a defined transect allowing the data to be represented spatially to belowground anomalies (Figure 28).

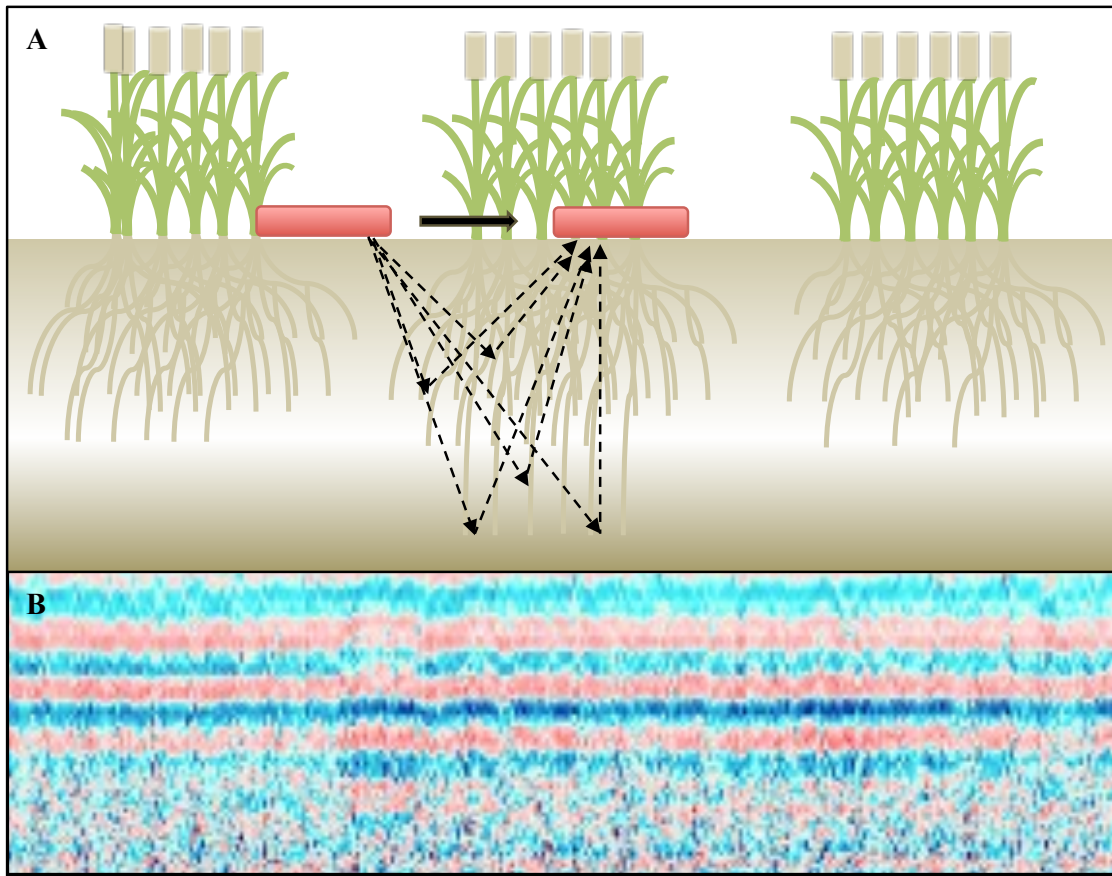


Figure 28. Schematic illustration of ground penetrating radar concept. (A) Ground penetrating radar functions by transmission of radio waves into the ground and detection of their reflected signals from subsurface interfaces separating layers differing relative dielectric permittivity. The antenna functions in both the transmitting and receiving of the radio wave. The radar pulse is timed from the point of transmission into the ground to the interaction with dielectric interface to establish distance to the target. (B) Corresponding radargram representing a series of digitized trace signals equidistantly spaced along the profile axis.

### *Ground penetrating radar considerations*

GPR resolution and depth depend on three key factors: (1) antenna TCF (2) soil electrical conductivity (EC) how strongly a material resist electrical conductivity (3) soil RDP the later is defined by the capacity of a material to store a charge when an electrical field is applied. Resolution refers to the ability to discriminate between two neighboring subsurface features of the minimum size of detection. GPR antennae generate energy pulses that travel in an elliptical cone, with increasing depth the cone expands, as does the footprint or scanned area reducing the resolving power of the sensor (Figure 29). Resolution increases with decreased wavelength. High-frequency antennae (1.6 GHz) have shorter wavelengths, time to complete signal attenuation, and provide increased resolution or a smaller subsurface footprint as compared to those with a lower TCF (400 MHz). Thus, resolution increases with decreasing wavelengths. However, higher frequency antennae have less penetrating depth in comparison to low frequency antennae. Antenna TCF selection is based on predicted target depth and size considering the tradeoff of resolution for depth limitations of the GPR. Depending on the soil conditions and structure as well the target depth antenna choice can be optimized. Soil EC is primarily controlled by water content. High EC can make radar signal penetration difficult. In addition, high soil EC can reduce the overall subsurface footprint of the antenna. Low EC soils allow for a higher resolution. Clay materials with a high cation exchange capacity increase attenuation and decrease depth. Soil EC can only be controlled by trial location.

Increasing transmission power can increase exploration depth. However, when attenuation limits exploration depth, power must increase exponentially with depth. Governments regulate the level of radio emissions that can be generated. Should the GPR signal become too large it can interfere with other interments, TV's, radios, and cell phones. RDP is classified in a range from 1 to 81, with air having an RDP of 1 and water 81. Soil RDP is highly characteristic of the water content present. Differences in RDP between adjacent materials through which the radar wave propagates will cause portions of the radar energy to sheer and return to the surface. The strength of the reflection or amplitude returned is controlled by the contrast of RDP between the adjacent materials.



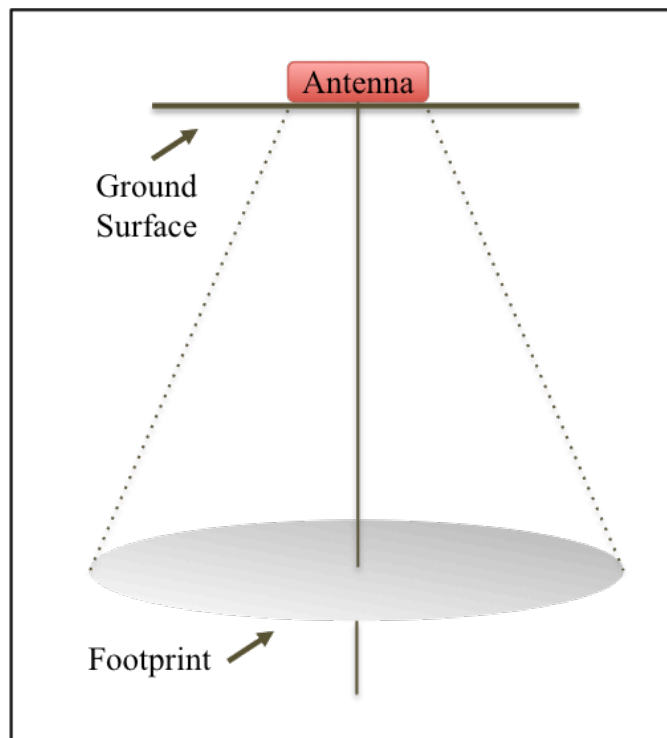


Figure 29. Ground penetrating radar wave conical radiating pattern. Spreading footprint of ground penetrating radar radio wave increases with distance from transmission antenna.

### *Ground penetrating radar signal processing*

GPR radargrams must be combined and interpreted to characterize geometrical information of belowground targets. GPR signal analysis techniques for coarse tree root mapping and detection have been developed (Butnor et al., 2003). These post-processing steps include radargram standardization, noise filtering, signal amplification, migration and Hilbert transformation (Guo et al., 2012). Radargram standardization and noise filtering correct for variations in radar reflection times, while the later corrects for background noise generated by external signals and signals generated by an uneven interface between the soil and GPR antennas. Signal amplification corrects for reduction in the radar signal (Guo et al., 2012). Radargrams portray a distorted image of subsurface objects as point reflections, or in the case of roots, as a hyperbolic reflection. These distortions can be corrected by amplifying migration, tracing the hyperbolic reflections, and collapsing the hyperbolic arms to their apices (Goodman, 1994).

3D images can be obtained by collecting parallel profiles; the profiles are then combined into a 3D volume (Figure 30). Software packages have been developed that integrate these and other data functions allowing the volume to be sliced allowing integration of defined areas and depths. Depth can be estimated knowing the velocity of wave propagation within the soil allowing horizontal slices at target depths to be evaluated.

In previous studies to locate and quantify root biomass, researchers were able to identify roots from the surrounding soils by identify the apex location of hyperbolic patterns within the data. In addition to identifying the location of the root, knowing the intensity of the amplitude returned allows for estimation of size and or biomass. Limitations to this technique are clear, subsurface features crossed by the GPR antenna at angels less than a 45° do not produce distinct hyperbolas (Chow and Hodgson, 2009).

## **Materials and methods**

### ***Study site***

We used a panel of 28 soft winter wheat cultivars and advanced breeding lines selected for heading date and plant height at physiological maturity to eliminate unwanted pleiotropic effect on trait measurement. The trial was conducted at the University of Arkansas, Rice Research and Extension Center (Stuttgart, AR). The study was designed using a randomized complete block with four replications. Plots were drill seeded at a rate of 118 kg of seed per hectare, consisting of seven rows 18 cm apart in a plot area of 1.25 m wide by 6 m long (Figure 31). Fertilizer was applied at a rate of 30 kg of nitrogen per hectare pre sowing and 30 kg of nitrogen was applied at Feeks 3 to 4 (Appendix A). Field waterlogging was simulated through use of dikes and controlled flooding for a period of 28 days.

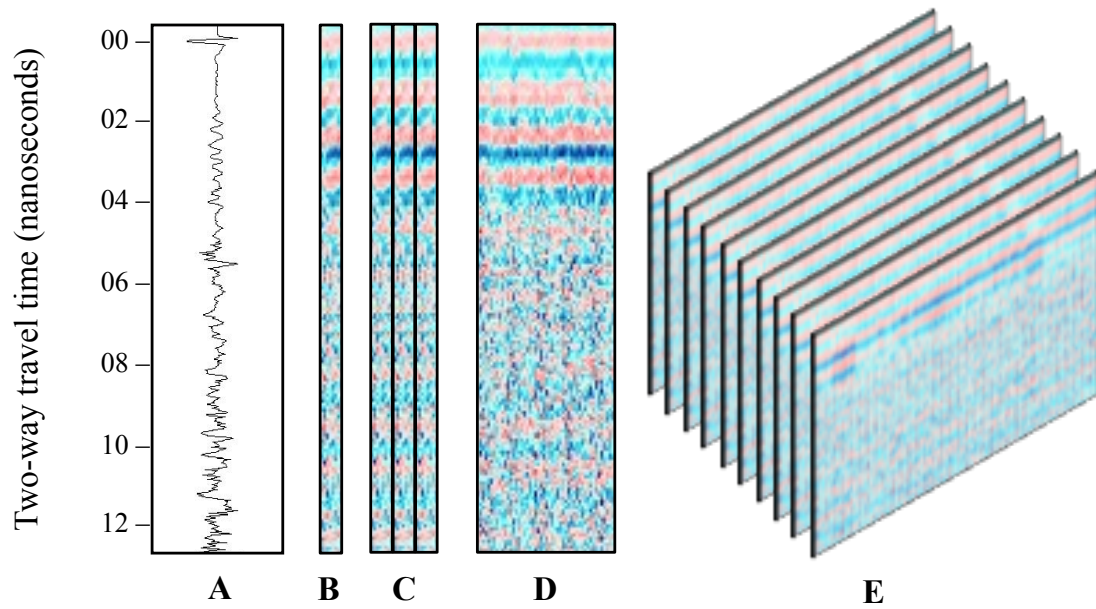


Figure 30. Ground penetrating radar signal components. (A) Trace signal recorder by the receiver. (B) Digitized signals sampled from trace signal. (C) Multiple digitized samples representing a series of trace signals. (D) Radargram representing a series of digitized trace signals equidistantly spaced along the profile axis. (E) Multiple radargrams are combined spatially to produce a three-dimensionally accurate representation of the subsurface.

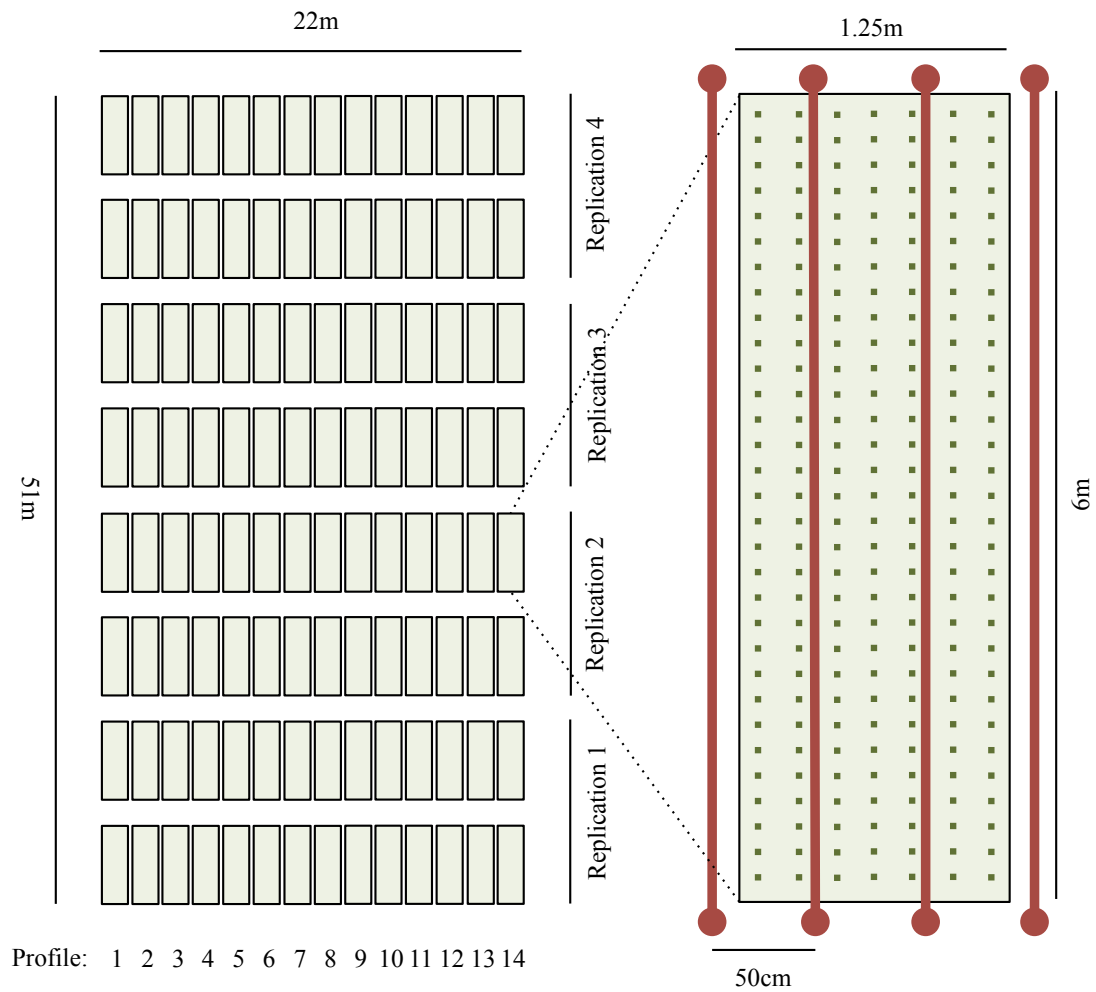


Figure 31. Schematic diagram of the study site at the field and plot level. This study was designed in a randomized complete block with four replications of both the waterlogging and control treatments. Plots consisted of seven rows 18 cm apart in a plot area of 1.25 m wide by 6 m long. Red lines indicate the location of ground penetrating radar data collection profiles within each plot.

The site soils are classified by the National Cooperative Soil Survey as stuttgart series and described as very deep, moderately well drained to somewhat poorly drained slowly permeable soils formed in silty and clayey alluvium (Appendix B). The surface layer of silt loam and slow permeability of the clayey subsoil make the site ideal for evaluation of roots under simulated waterlogging conditions.

### ***Wheat agronomic measurements***

#### **Plot yield, biomass, and yield components**

At maturity, 50 spikes bearing culms were hand-harvested at ground level, dried, and weighed to determine biomass. The 50 culms were then threshed and the seed weight in combination with a measurement of 1000 kernel weight was used to extrapolate harvest index, weight per spike and kernel number per spike. Whole plots were harvested with a plot combine equipped with a HarvestMaster system (Juniper Systems Inc, Logan, UT, USA) for determination of plot yield and calculated yield. Whole plot yield and the seed weight of the 50 culms were used to determine spike density. Plant biomass was determined by hand-harvesting a one meter row section of each plot. Samples were weighed, oven dried and reweighed to determine dry weight.

### **Spectral reflectance (normalized difference vegetation index)**

Canopy spectral reflectance was measured using a handheld GreenSeeker (Trimble Sunnyvale, CA, USA). The active sensor utilizes red and near infrared wavelengths. Measurements were taken over the canopy at 0.9 m above the canopy at a rate of 10 reading per second. The field of view was adjusted to approximately 60 cm perpendicular to the plots. In total 8 measurements were taken per plot across physiological development and maturation. Normalized difference vegetation index (NDVI) was calculated by  $(R_{780}-R_{670})/(R_{780}+R_{670})$ .

### **Root characteristics**

To evaluate rooting depth and morphology, soil cores measuring 6 cm in diameter and 60 cm in length were collected using a Giddings soil probe and plastic soil liners. Core samples were taken post waterlogging. Cores were divided into 0-30 and 30-60 cm sections, roots rinsed free of debris, dried at 75°C for 24 hours and weighed to assess root depth, depth distribution, and biomass.

### ***Electrical conductivity mapping***

Bulk soil EC measurements were made of the study site using a Geonics Limited EM38 terrain meter (Geonics Limited, Mississauga, Ontario, CAN). The EM38 measures soil EC by transmitting a signal through the soil, inducing a magnetic field that is detected by the receiver (Durlleser and Stanjek, 1997). The ratio of the transmission signal to the received signal allows the EC of the soil to be quantified. EC was measured using an EM38 in concert with a differential global positioning system (DGPS) to map soil variability. Using the EM38 in the vertical mode measures EC from soil surface to approximately 1.5m in depth (Durlleser and Stanjek, 1997). The Allegro field computer logged data output from the EM38 and the DGPS simultaneously. Data collected was mapped spatially using DGPS information.

### ***Ground penetrating radar equipment***

A Geophysical Survey System Incorporated (GSSI) (North Salem, NC, USA) subsurface interface radar system 20 (SIR-20) GPR was used. The SIR-20 consisted of a digital control unit, Panasonic CF-30 ToughBook laptop computer, RADAN v6.6 software, and a GSSI model number 5100 antenna with a TCF of 1.6 GHz. Scanning time for this study was 20 ns. Radar profiles were collected using RADAN v6.6 (GSSI).

GPS measurements were collected using a Trimble GeoXH handheld GEO Explorer 2008, model number 70950-00 (Trimble, Sunnyvale, CA, USA). Using a Trimble Zephyr



RTK antenna we were able to log global information systems positions during data collection. GPS data was post processed using Pathfinder software (Trimble, Sunnyvale, CA, USA). Post processing was done to increase accuracy of GPS data to an estimated 2-3cm of actual field position.

### ***Ground penetrating radar field procedures***

Field data collection was done post 2013 growing season. Wheat plots were harvested 60 days prior to GPR data collection. No precipitation in the area was recorded from time of wheat harvest to GPR data collection. Plant stubble was mowed within 10cm of soil surface and all cut plant material was removed from plots. GPR profiles were recorded at 50 cm spacing from east to west with a total of 4 profiles collected in each plot (Figure 32). GPR data was collected using a calibrated survey wheel attached to the system as well; GPS data was collected simultaneously using a Trimble Geo XH handheld GPS utilizing real time kinematic corrections. GPR surveys were conducted using a GSSI SIR-20 equipped with a 1.6GHz antenna.

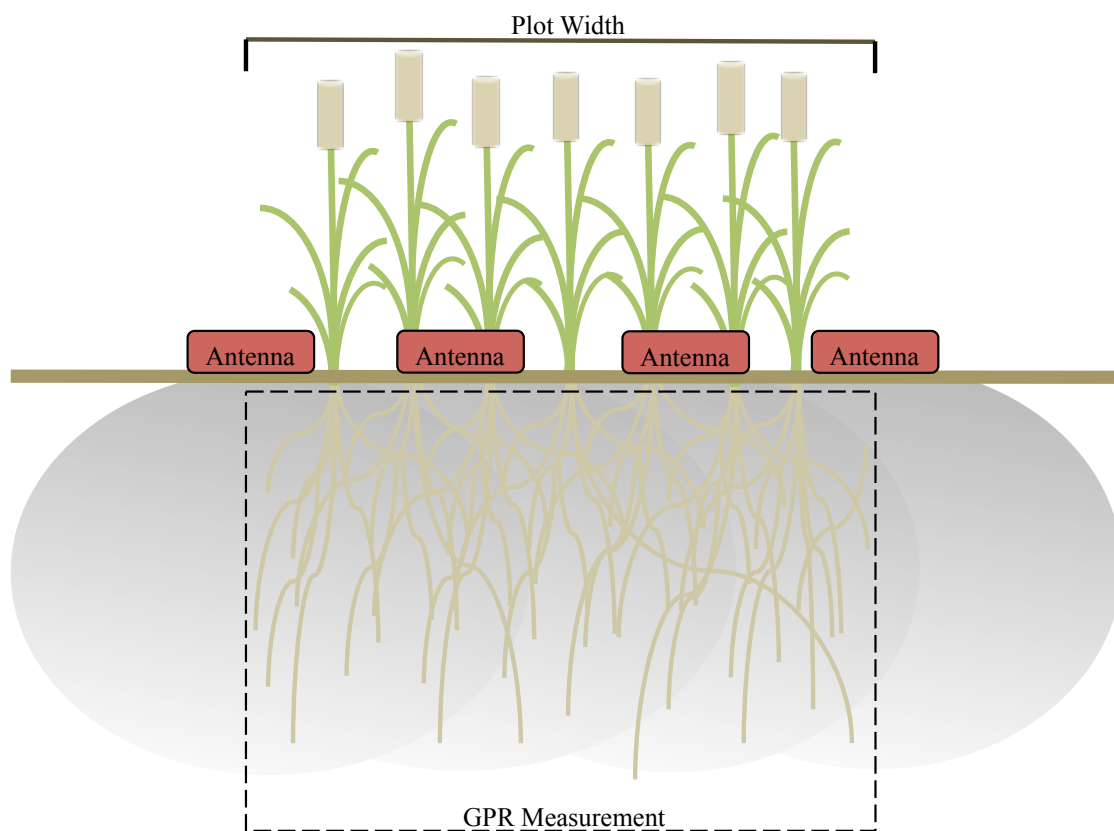


Figure 32. Schematic of ground penetrating radar measurement area. Ground penetrating radar profiles (4 total) were collected for each experimental plot for analysis.

### ***Ground penetrating radar data processing***

Radar data was processed using GPR-Slice v1.0 (Geophysical Archaeometry Laboratory, Woodland Hills, CA, USA). Plot radar data was then analyzed using Surfer12 (Golden Software, Golden, CO, USA) 3D mapping software.

### ***Statistical analysis***

Statistical analysis of the data was performed using JMP Pro version 11 (SAS Institute Inc., Carry, NC, USA). Pearson's correlation coefficient was used to compare GPR data to wheat agronomic and root core data. Standard ANOVA procedures were used in gage impact of block and treatment. A probability value of 0.05 or less was considered to be statistical significant.

## **Results**

### ***Subsurface mapping by ground penetrating radar***

Using a 1.6 GHz antenna we were able to non-invasively map the subsurface features of within a spatial context. GPR was able to identify the subsurface root zones associated for each wheat plot within the experimental trial. Root zone interactions were clearly evident in the collected GPR radargrams within the 0-3 ns range (Figure 33). Plot and

alleyway length, as identified by the GPR radiograms, were consistent with known plot dimensions across the experimental trail as well all collected GPR profiles. The location identified by the GPR was consistent with known plot areas and plant growth was controlled by herbicide in the alleyways.

### ***Wheat root discrimination by ground penetrating radar***

Combined GRP radargrams for each series within a run were compared in the 0-3 ns range and displayed a clear differentiation between known plot and ally location based on intensity of amplitude return (Figure 34). GPR ability to predict root presence and absence was tested using a Students T test comparing know plot presence and absence with amplitude return intensity for each position within the experimental trail. GPR was able to differentiate root mass from soil significantly ( $\alpha = 0.95$ ,  $t = 1.96022$ ) (Figure 35).

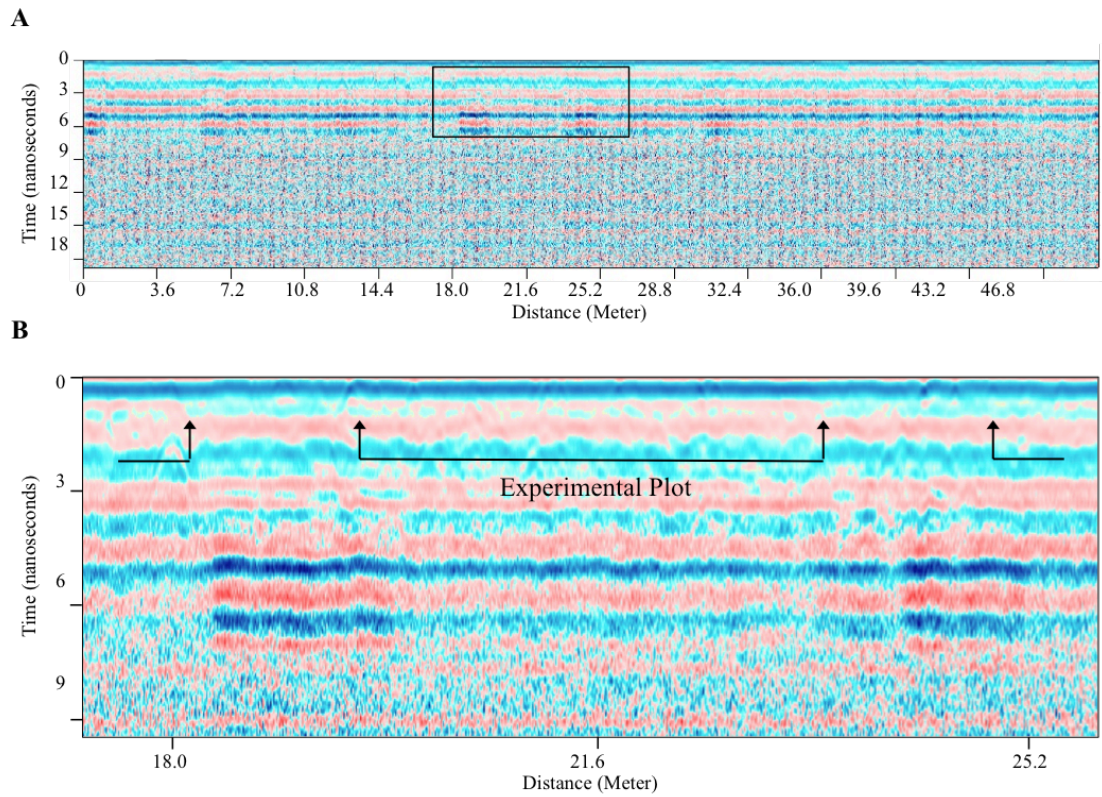


Figure 33. Ground penetrating radar profile. Ground penetrating radar profile from experimental trial. (A) Total ground penetrating radar profile spanning total length of field across eight experimental plots (6 m) and alleyways (1.5 m). (B) Subset ground penetrating radar profile depicting known plot locations.

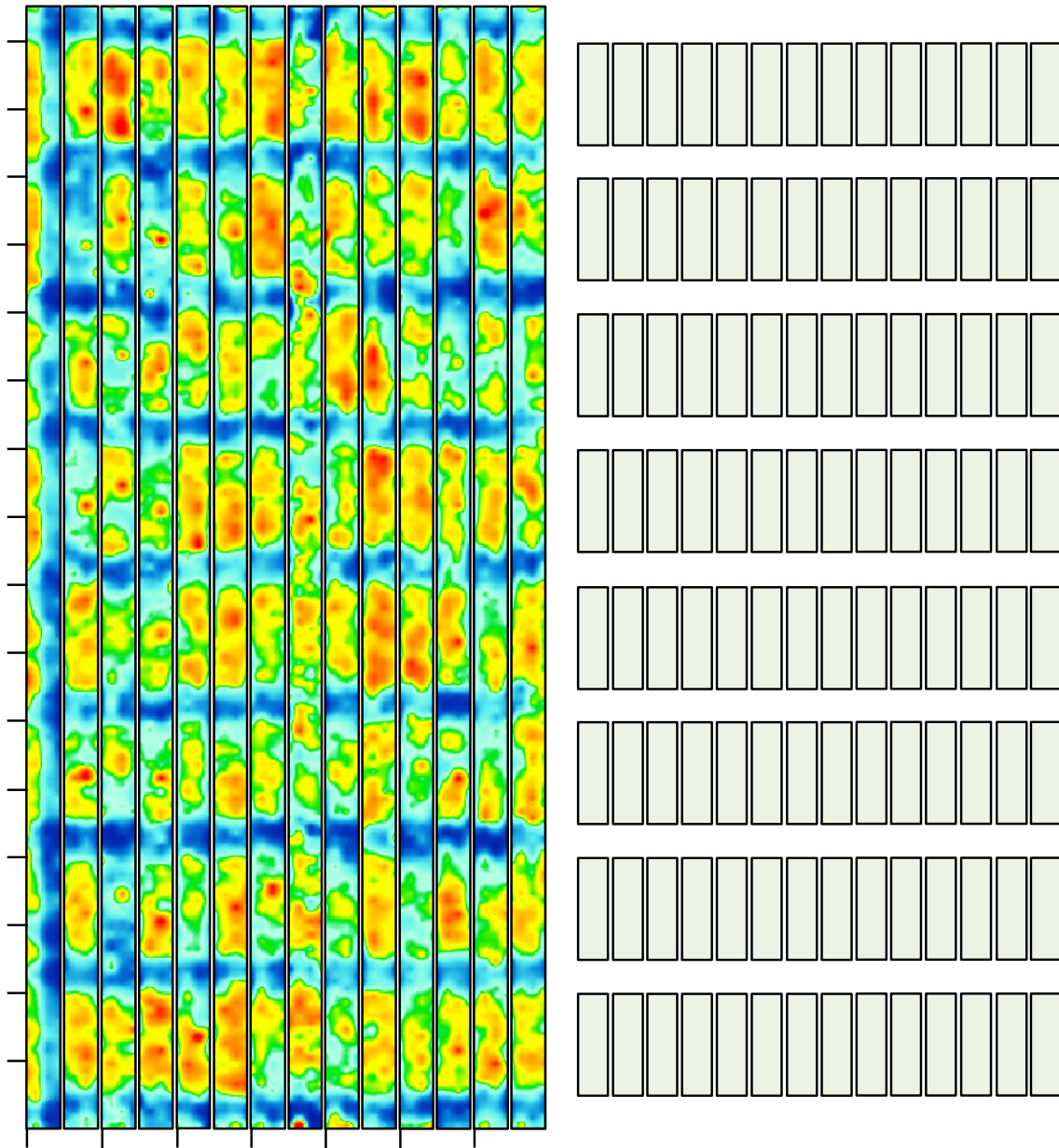


Figure 34. Ground penetrating radar amplitude map. Field level distribution of ground penetrating radar amplitude compared with experimental plot distribution.

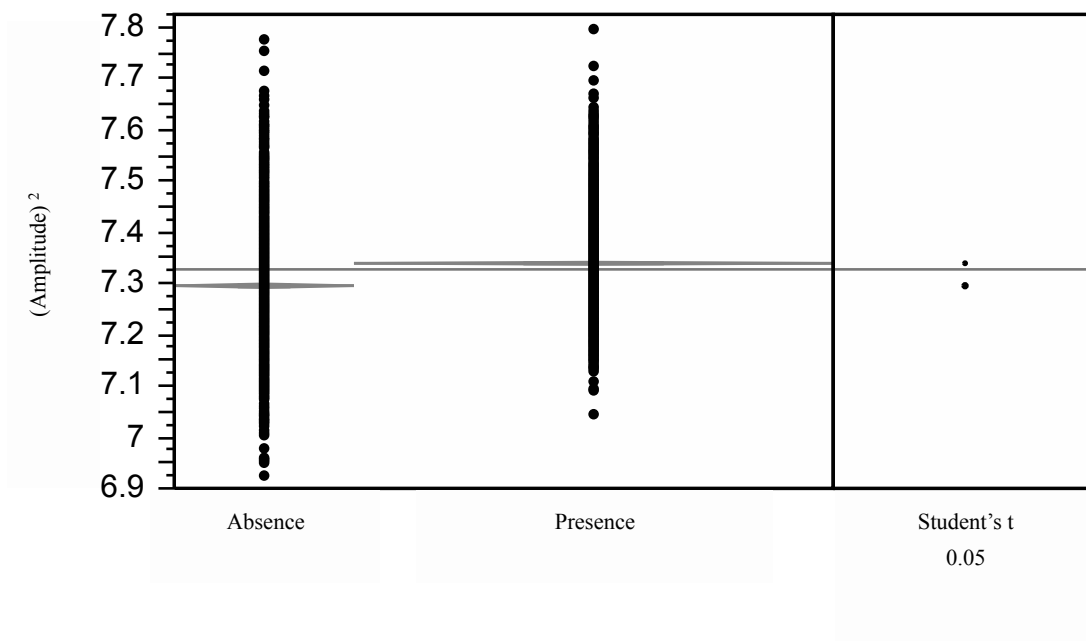


Figure 35. Students T test comparing root presence and absence. Predictive ability of Ground penetrating radar amplitude return compared with known plot location for root presence and absence.

### *Agronomic and physiological measurements*

Linear regression between Log10 of the mean GPR amplitude return for each plot at the 0-3 ns range was compared with agronomic breeding traits. Each trait was evaluated by comparison of the mean of four replications for each of the 28 wheat entries as well each trait was evaluated with by the mean of all entries within each of four replications.

Total plot yield (Yield) (Figure 36; 37), thousand kernel weight (TKW) (Figure 38; 39), kernel weight per spike (KWS) (Figure 40; 41), and average kernel number per spike (KNS) (Figure 42; 43) were all evaluated.

Linear regression between Log10 of the mean GPR amplitude return for each plot at the 0-3 ns range was compared with NDVI across physiological development. Each trait was evaluated by comparison of the mean of four replications for each of the 28 wheat entries as well each trait was evaluated with by the mean of all entries within each of four replications. NDVI collected on 3/23/2013 (Figure 44; 45), 3/27/2013 (Figure 46; 47), 4/10/2013 (Figure 48; 49), 4/19/2013 (Figure 50; 51), 4/29/2013 (Figure 52; 53), 5/09/2013 (Figure 54; 55), 5/24/2013 (Figure 56; 57), and 5/31/2013 (Figure 58; 59), were evaluated.



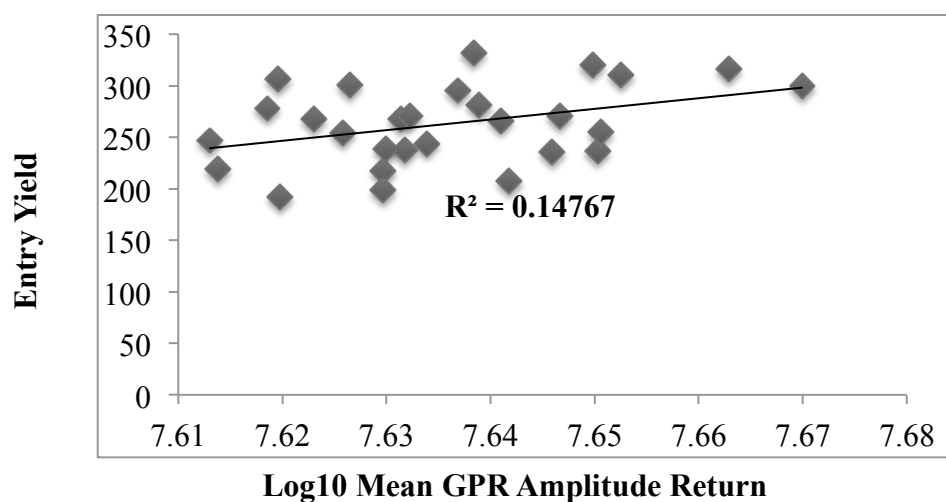


Figure 36. Linear regression between the Log10 of mean ground penetrating radar amplitude returned for the 0-3 ns range and total plot yield of 28 wheat varieties.

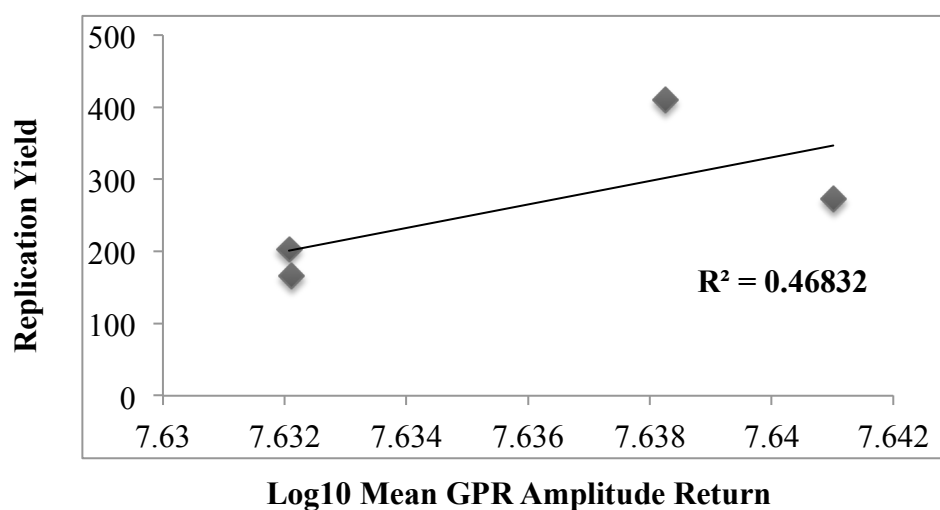


Figure 37. Linear regression between the Log10 of mean ground penetrating radar amplitude returned for the 0-3 ns range and average yield of each experimental replication.

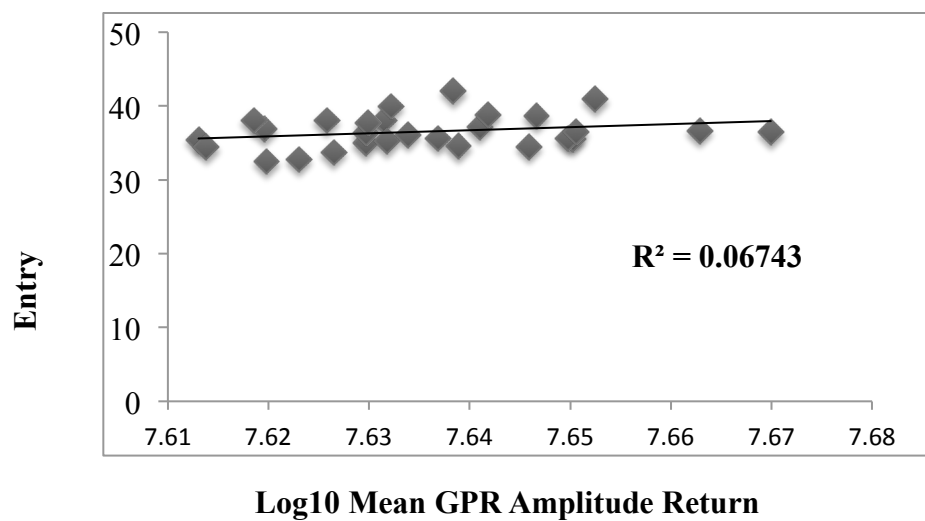


Figure 38. Linear regression between the Log10 of mean ground penetrating radar amplitude returned for the 0-3 ns range and average thousand kernel weight (TKW) of 28 wheat varieties.

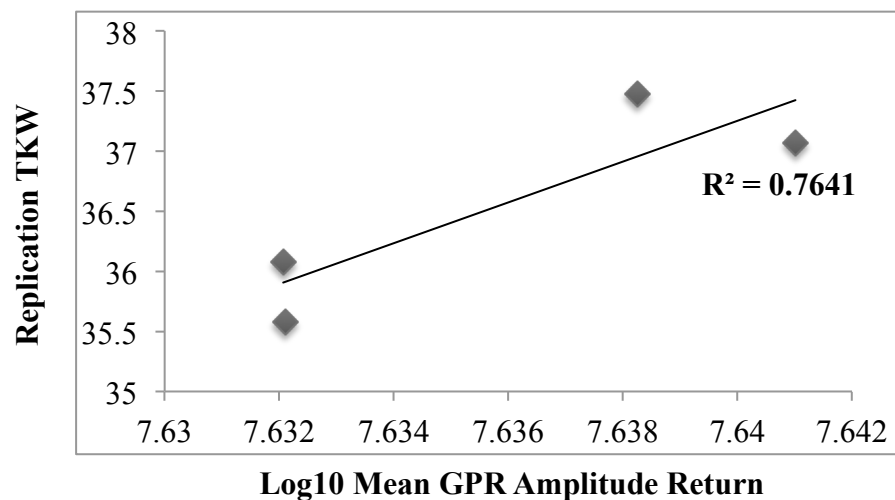


Figure 39. Linear regression between the Log10 of mean ground penetrating radar amplitude returned for the 0-3 ns range and average thousand kernel weight (TKW) of each experimental replication.

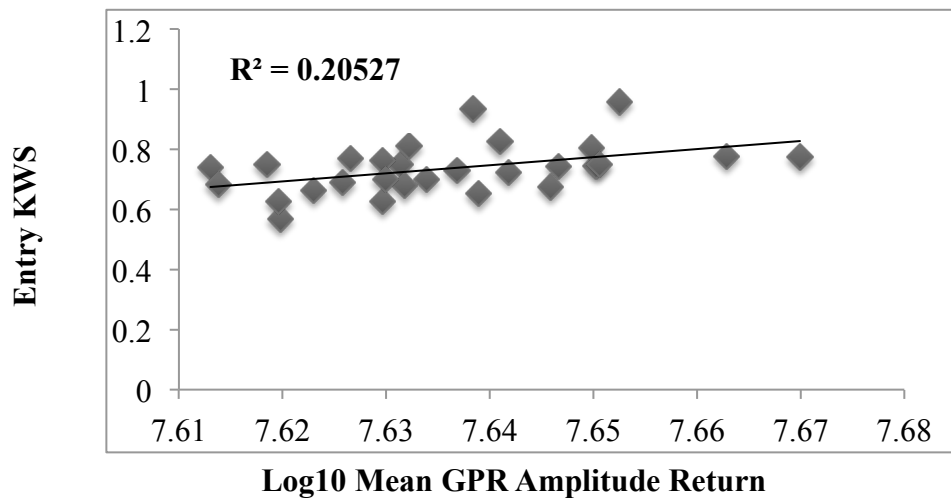


Figure 40. Linear regression between the Log10 of mean ground penetrating radar amplitude returned for the 0-3 ns range and average kernel weight per spike (KWS) of 28 wheat varieties.

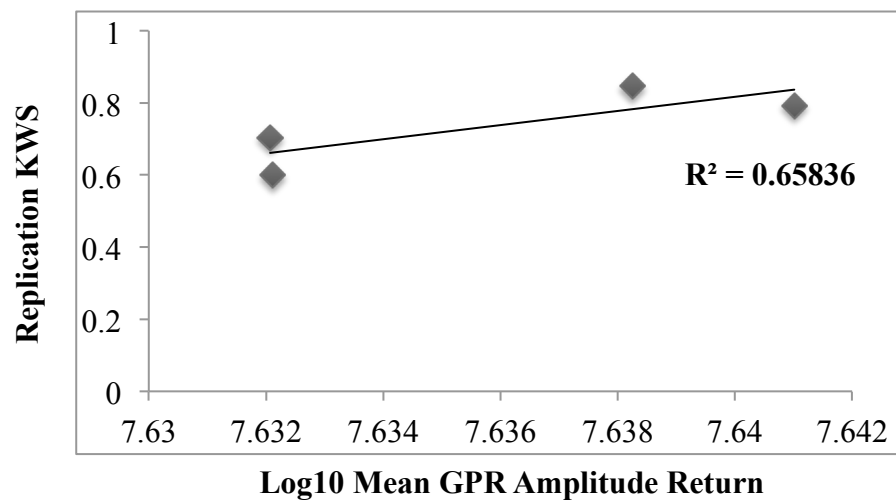


Figure 41. Linear regression between the Log10 of mean ground penetrating radar amplitude returned for the 0-3 ns range and average kernel weight per spike (KWS) of each experimental replication.

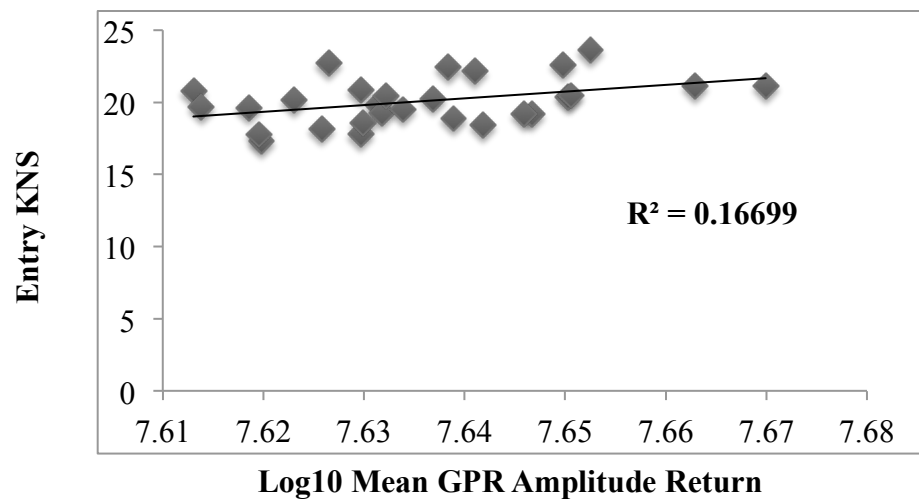


Figure 42. Linear regression between the Log10 of mean ground penetrating radar amplitude returned for the 0-3 ns range and average kernel number per spike (KNS) of 28 wheat varieties.

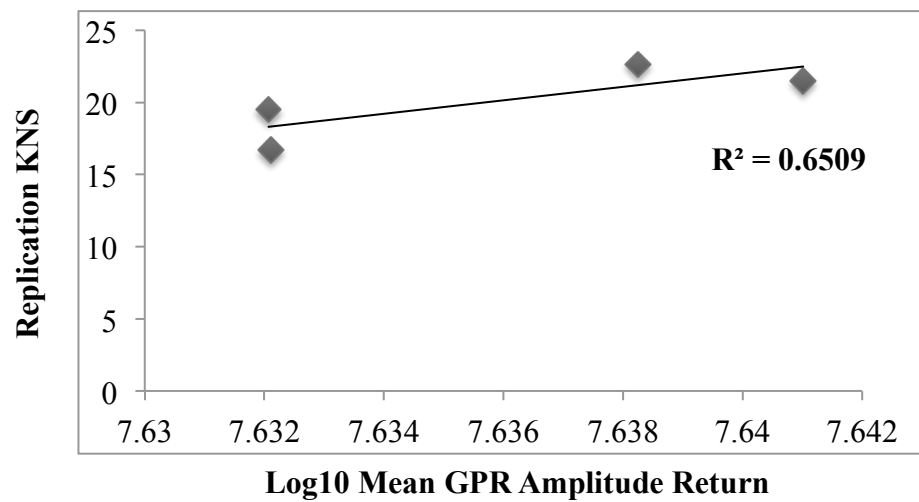


Figure 43. Linear regression between the Log10 of mean ground penetrating radar amplitude returned for the 0-3 ns range and average kernel number per spike (KNS) of each experimental replication.

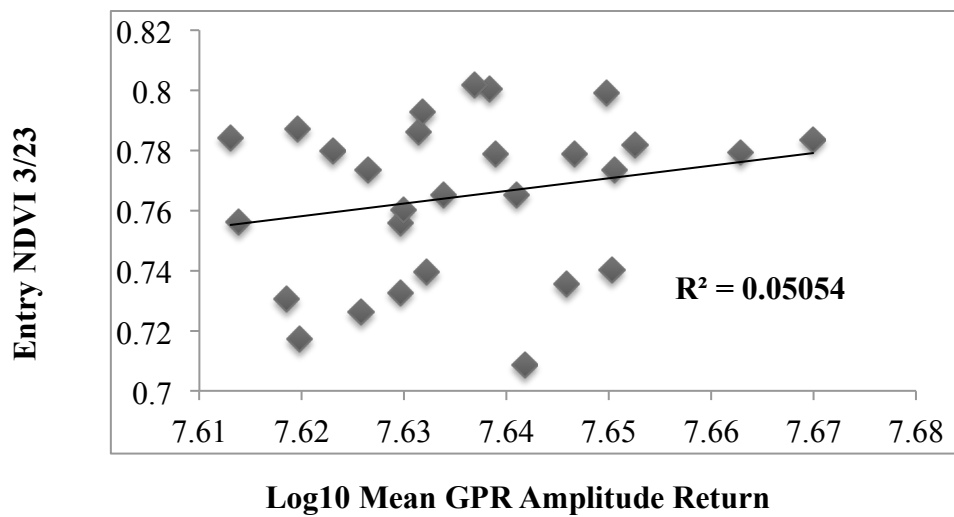


Figure 44. Linear regression between the Log10 of mean ground penetrating radar amplitude returned for the 0-3 ns range and average normalized difference vegetation index (NDVI) of 28 wheat varieties measured on 3/23/2013.

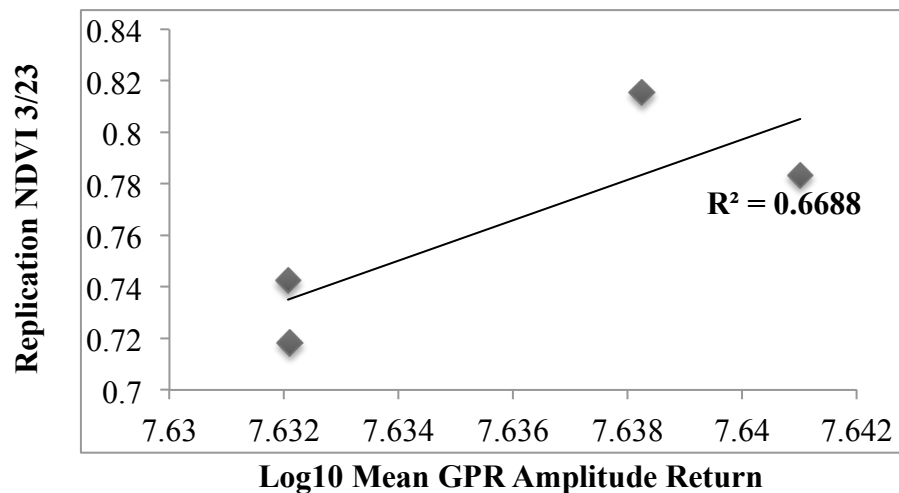


Figure 45. Linear regression between the Log10 of mean ground penetrating radar amplitude returned for the 0-3 ns range and average normalized difference vegetation index (NDVI) of each experimental replication measured on 3/23/2013.

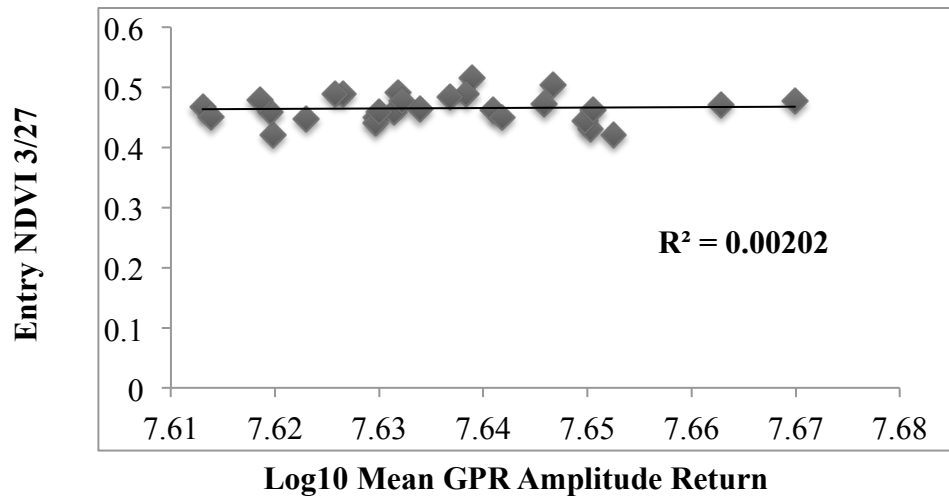


Figure 46. Linear regression between the Log10 of mean ground penetrating radar amplitude returned for the 0-3 ns range and average normalized difference vegetation index (NDVI) of 28 wheat varieties measured on 3/27/2013.

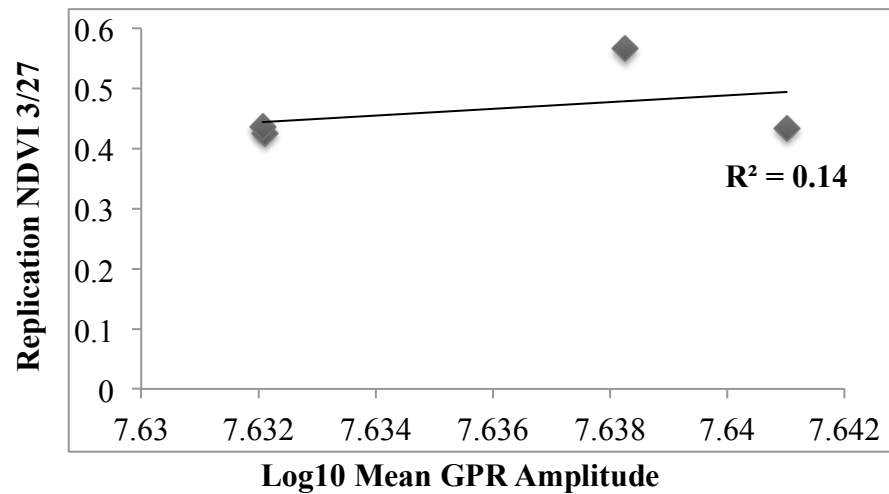


Figure 47. Linear regression between the Log10 of mean ground penetrating radar amplitude returned for the 0-3 ns range and average normalized difference vegetation index (NDVI) of each experimental replication measured on 3/27/2013.

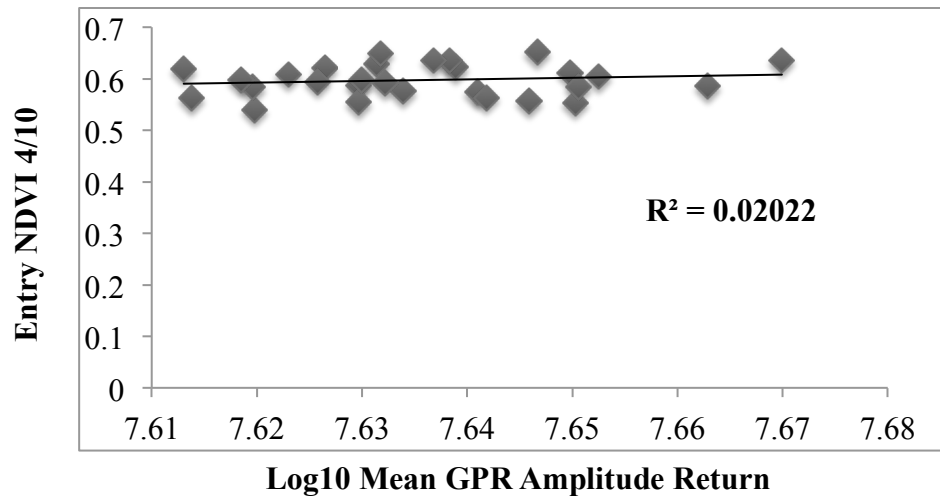


Figure 48. Linear regression between the Log10 of mean ground penetrating radar amplitude returned for the 0-3 ns range and average normalized difference vegetation index (NDVI) of 28 wheat varieties measured on 4/10/2013.

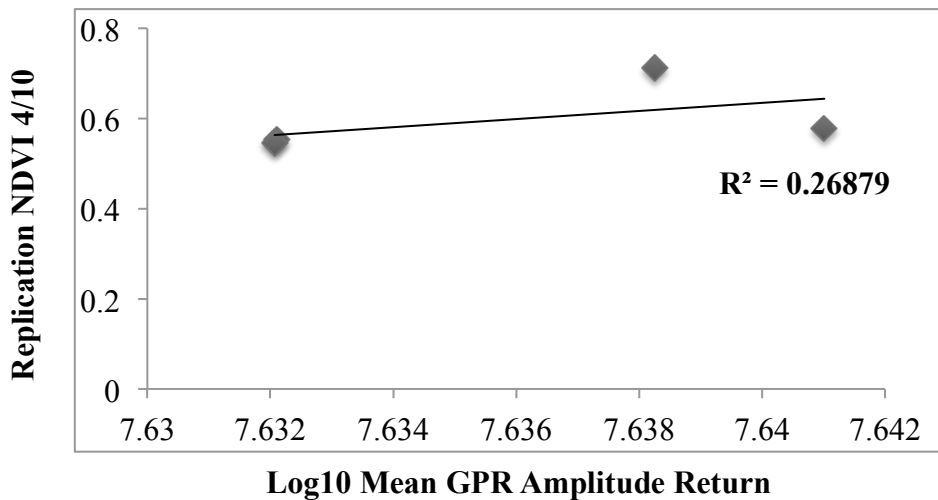


Figure 49. Linear regression between the Log10 of mean ground penetrating radar amplitude returned for the 0-3 ns range and average normalized difference vegetation index (NDVI) of each experimental replication measured on 4/10/2013.

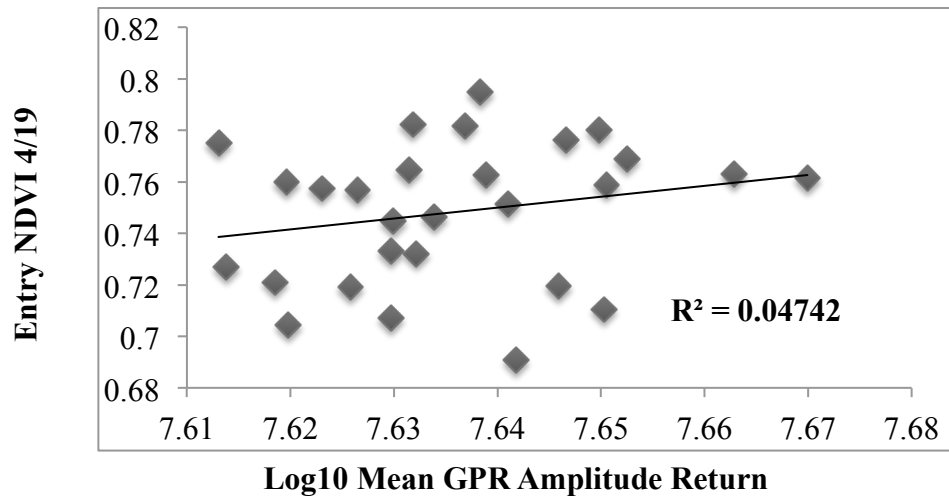


Figure 50. Linear regression between the Log10 of mean ground penetrating radar amplitude returned for the 0-3 ns range and average normalized difference vegetation index (NDVI) of 28 wheat varieties measured on 4/19/2013.

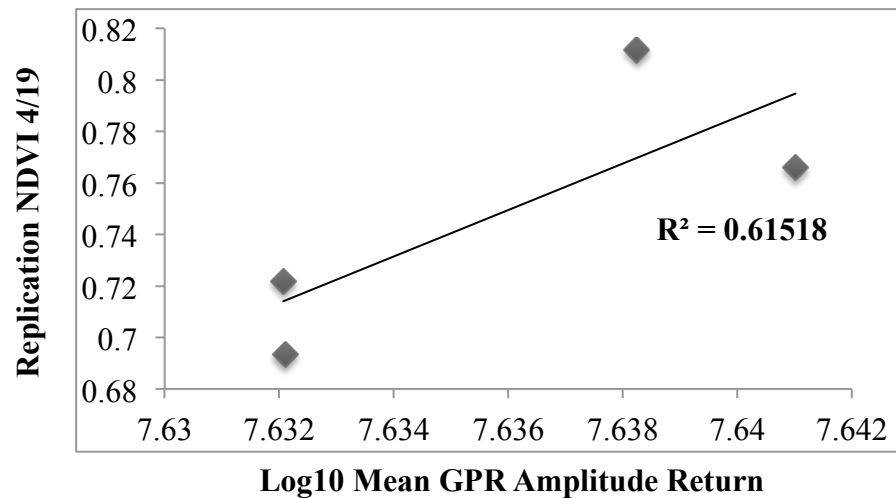


Figure 51. Linear regression between the Log10 of mean ground penetrating radar amplitude returned for the 0-3 ns range and average normalized difference vegetation index (NDVI) of each experimental replication measured on 4/19/2013.



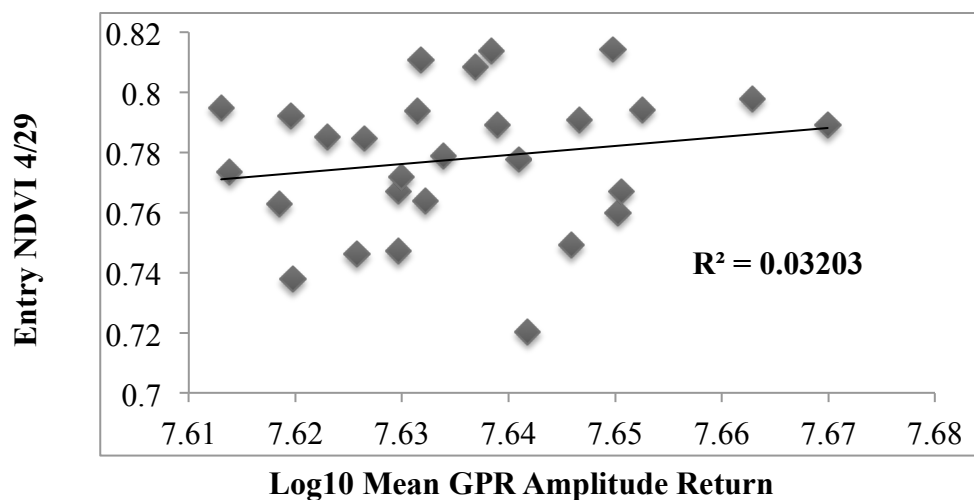


Figure 52. Linear regression between the Log10 of mean ground penetrating radar amplitude returned for the 0-3 ns range and average normalized difference vegetation index (NDVI) of 28 wheat varieties measured on 4/29/2013.

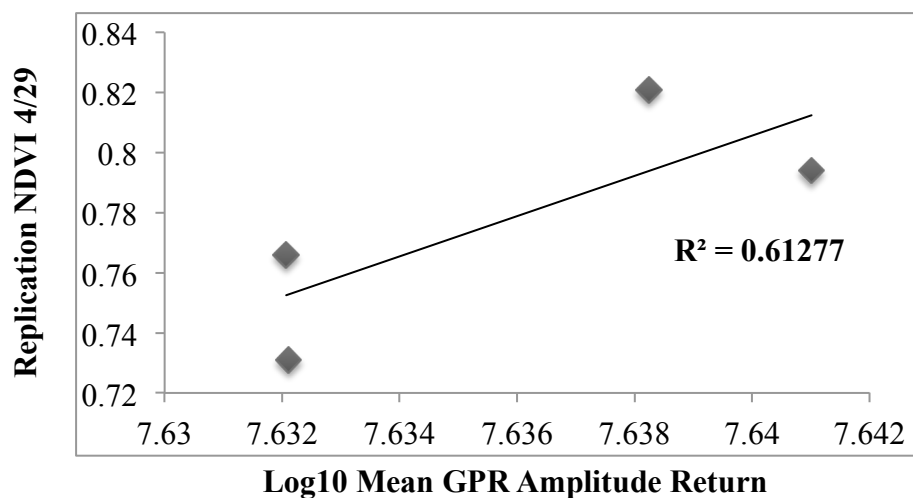


Figure 53. Linear regression between the Log10 of mean ground penetrating radar amplitude returned for the 0-3 ns range and average normalized difference vegetation index (NDVI) of each experimental replication measured on 4/29/2013.

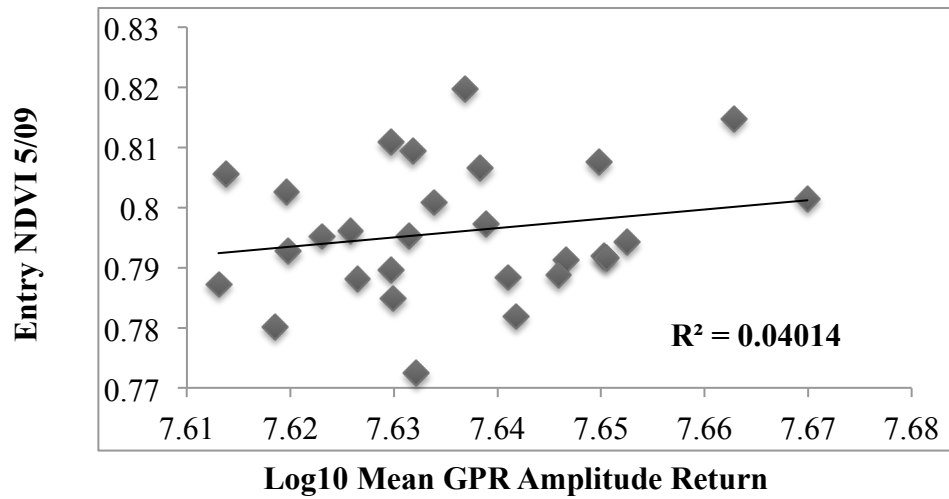


Figure 54. Linear regression between the Log10 of mean ground penetrating radar amplitude returned for the 0-3 ns range and average normalized difference vegetation index (NDVI) of 28 wheat varieties measured on 5/09/2013.

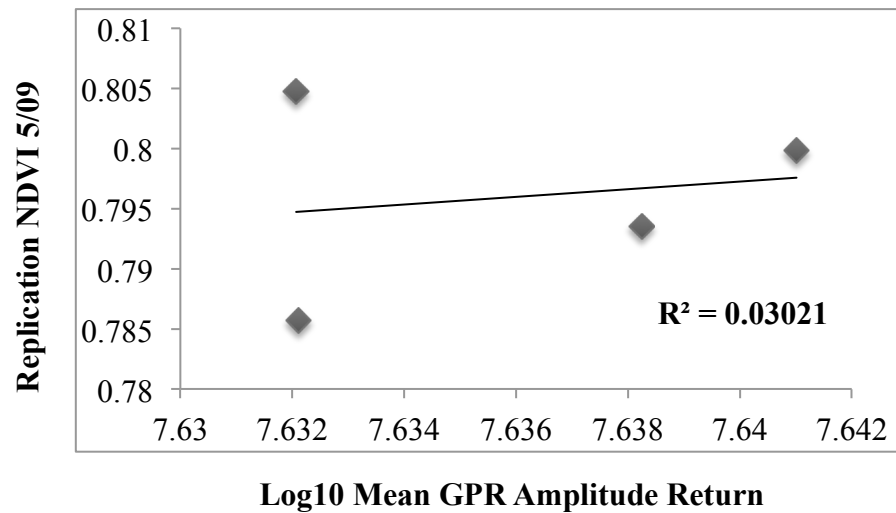


Figure 55. Linear regression between the Log10 of mean ground penetrating radar amplitude returned for the 0-3 ns range and average normalized difference vegetation index (NDVI) of each experimental replication measured on 5/09/2013.

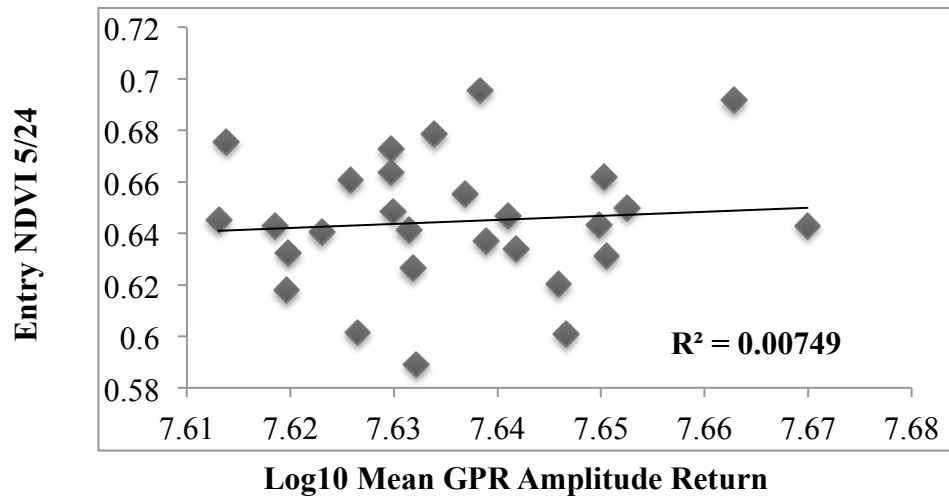


Figure 56. Linear regression between the Log10 of mean ground penetrating radar amplitude returned for the 0-3 ns range and average normalized difference vegetation index (NDVI) of 28 wheat varieties measured on 5/24/2013.

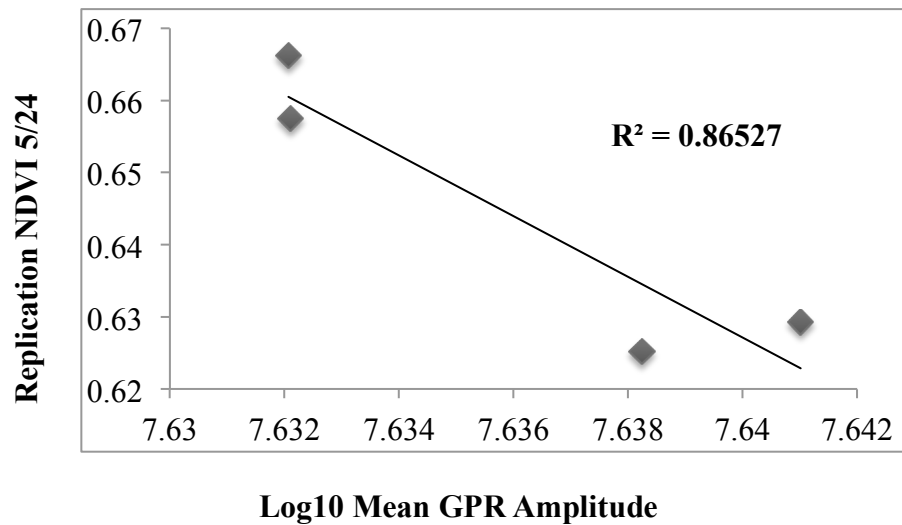


Figure 57. Linear regression between the Log10 of mean ground penetrating radar amplitude returned for the 0-3 ns range and average normalized difference vegetation index (NDVI) of each experimental replication measured on 5/24/2013.

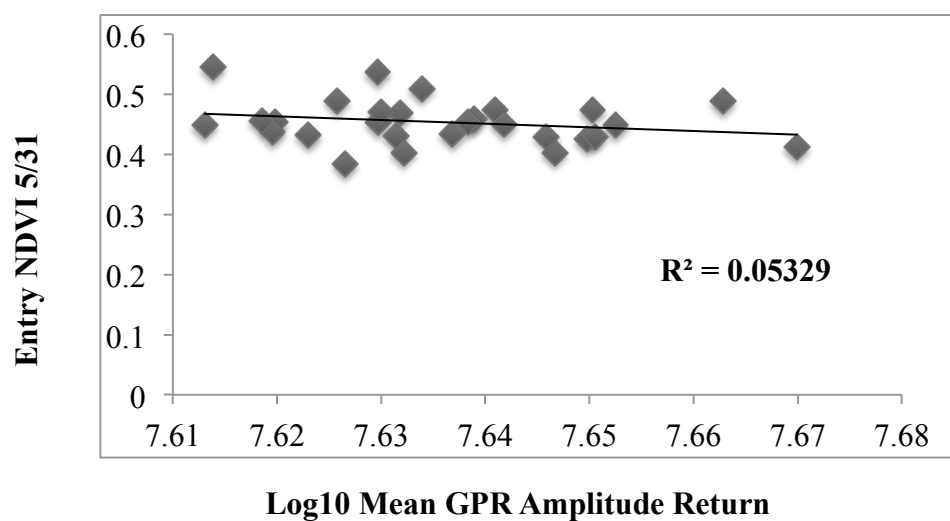


Figure 58. Linear regression between the Log10 of mean ground penetrating radar amplitude returned for the 0-3 ns range and average normalized difference vegetation index (NDVI) of 28 wheat varieties measured on 5/31/2013.

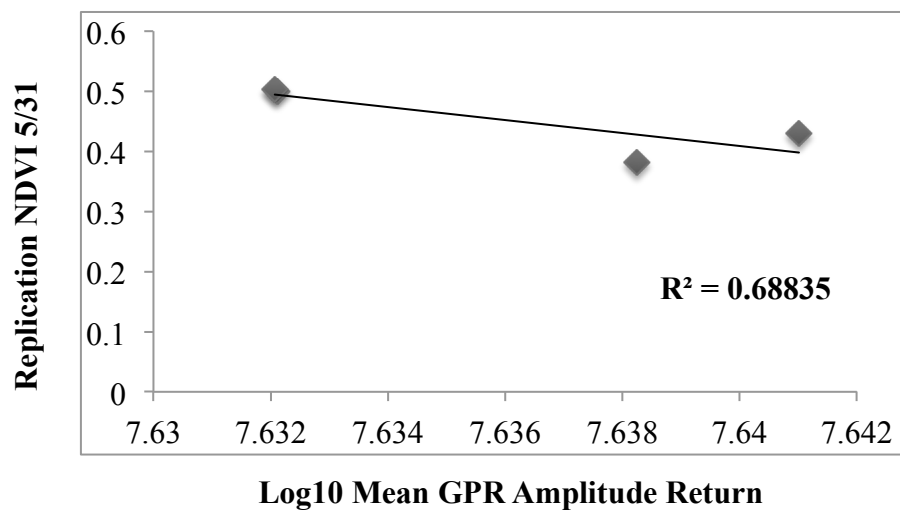


Figure 59. Linear regression between the Log10 of mean ground penetrating radar amplitude returned for the 0-3 ns range and average normalized difference vegetation index (NDVI) of each experimental replication measured on 5/31/2013.

### ***Root biomass measurements***

Linear regression between Log10 of the mean GPR amplitude return for each plot at the 0-3 ns range was compared with fresh weight (FW) and dry weight (DW) root biomass from soil coring. Each trait was evaluated by comparison of the mean of four replications for each of the 28 wheat entries as well each trait was evaluated with by the mean of all entries within each of four replications. FW root biomass from 0-30 cm (Figure 60; 61), 30-60 cm (Figure 62; 63), and total 0-60 cm (Figure 64; 65), were all evaluated. In addition, DW root biomass from 0-30 cm (Figure 66; 67), 30-60 cm (Figure 68; 69), and total 0-60 cm (Figure 70; 71), were also evaluated.

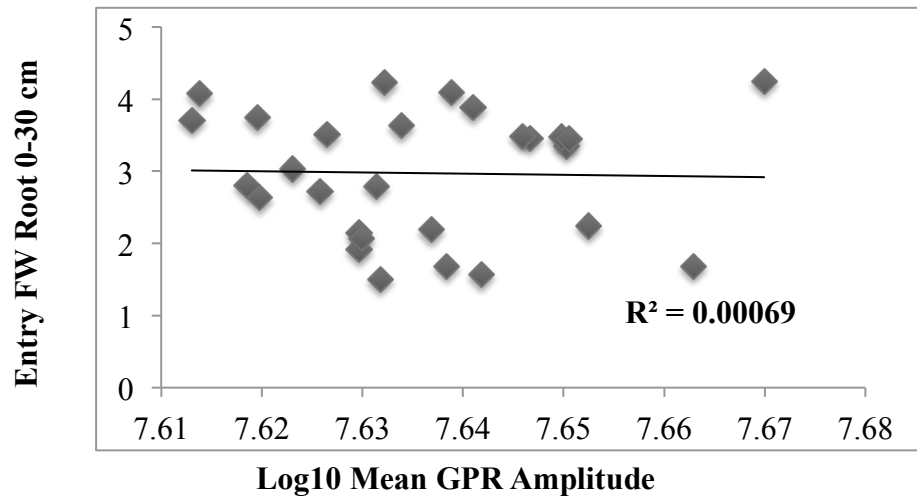


Figure 60. Linear regression between the Log10 of mean ground penetrating radar amplitude returned for the 0-3 ns range and average fresh weight (FW) root biomass collected at 0-30 cm for each wheat variety.

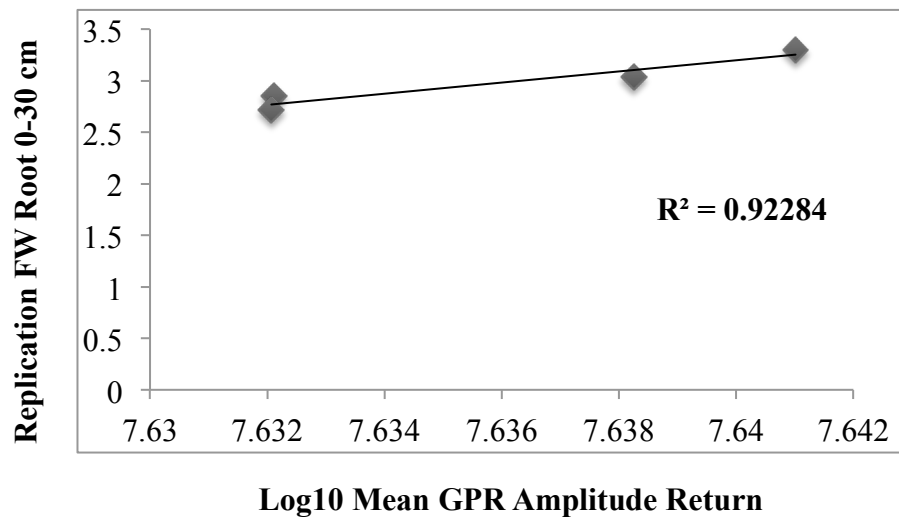


Figure 61. Linear regression between the Log10 of mean ground penetrating radar amplitude returned for the 0-3 ns range and average fresh weight (FW) root biomass collected at 0-30 cm for each experimental replication.

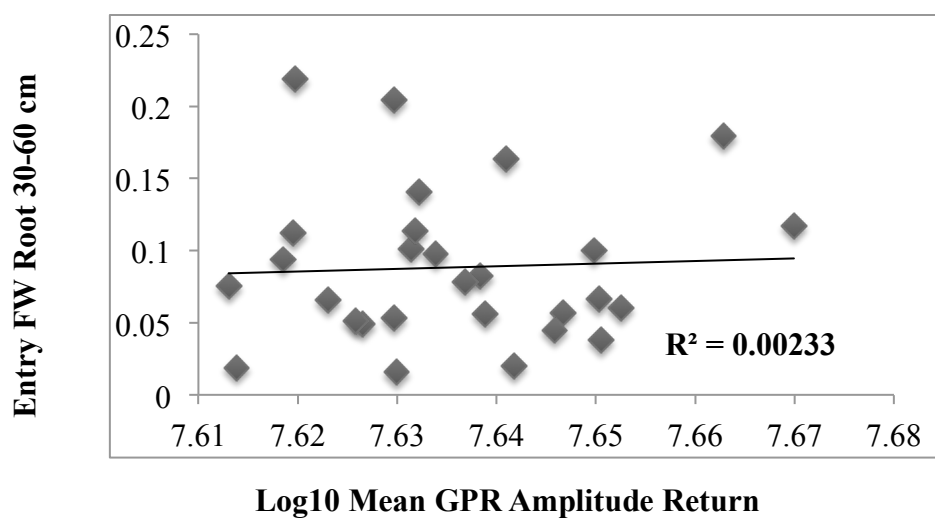


Figure 62. Linear regression between the Log10 of mean ground penetrating radar amplitude returned for the 0-3 ns range and average fresh weight (FW) root biomass collected at 30-60 cm for each wheat variety.

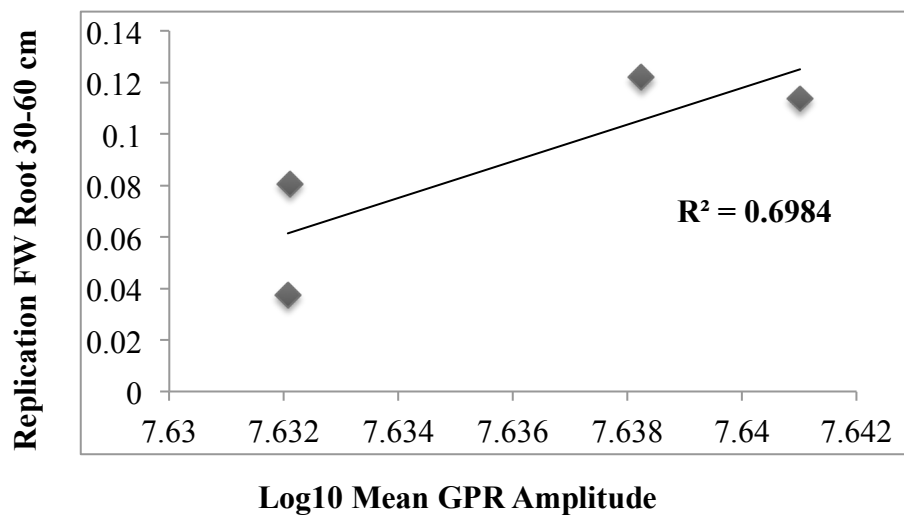


Figure 63. Linear regression between the Log10 of mean ground penetrating radar amplitude returned for the 0-3 ns range and average fresh weight (FW) root biomass collected at 30-60 cm for each experimental replication.

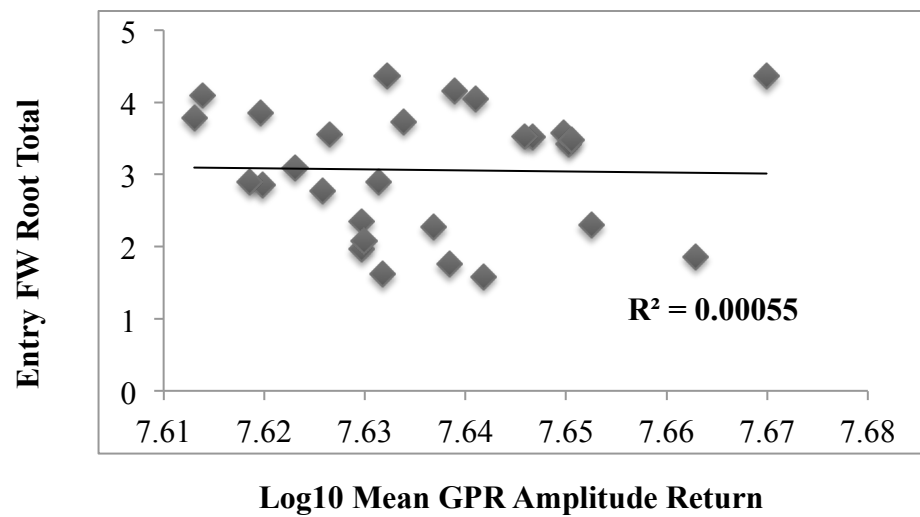


Figure 64. Linear regression between the Log10 of mean ground penetrating radar amplitude returned for the 0-3 ns range and average fresh weight (FW) root biomass collected at 0-60 cm for each wheat variety.

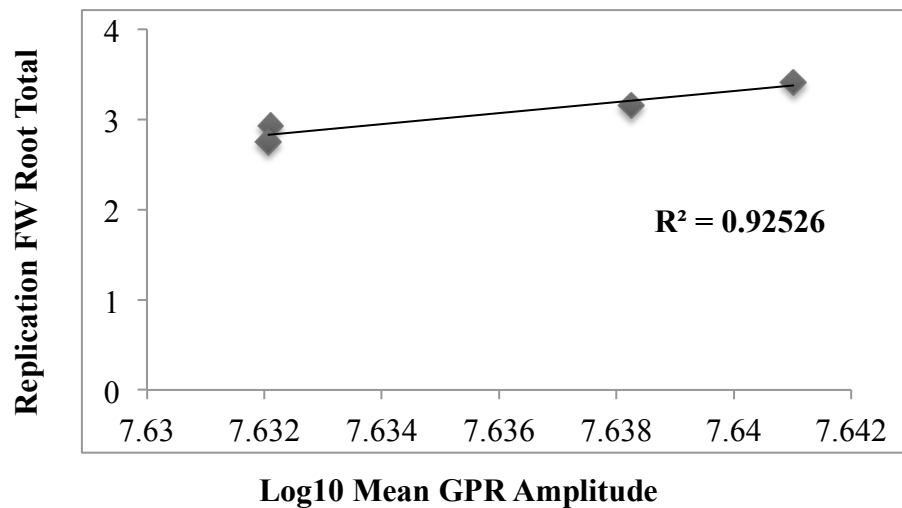


Figure 65. Linear regression between the Log10 of mean ground penetrating radar amplitude returned for the 0-3 ns range and average fresh weight (FW) root biomass collected at 0-60 cm for each experimental replication.



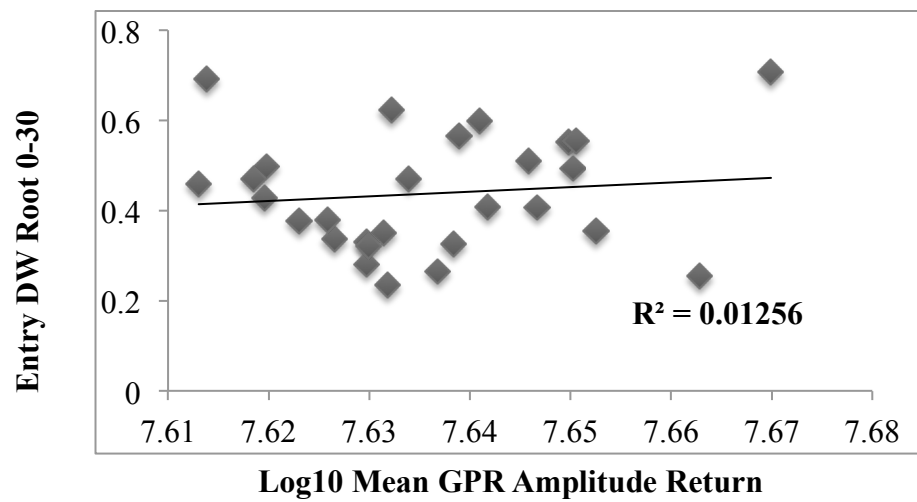


Figure 66. Linear regression between the Log10 of mean ground penetrating radar amplitude returned for the 0-3 ns range and average dry weight (DW) root biomass collected at 0-30 cm for each wheat variety.

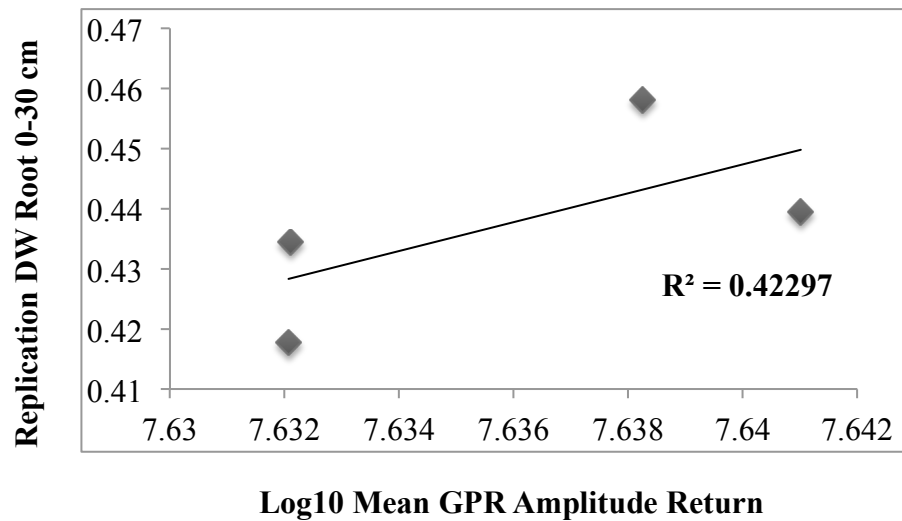


Figure 67. Linear regression between the Log10 of mean ground penetrating radar amplitude returned for the 0-3 ns range and average dry weight (DW) root biomass collected at 0-30 cm for each experimental replication.

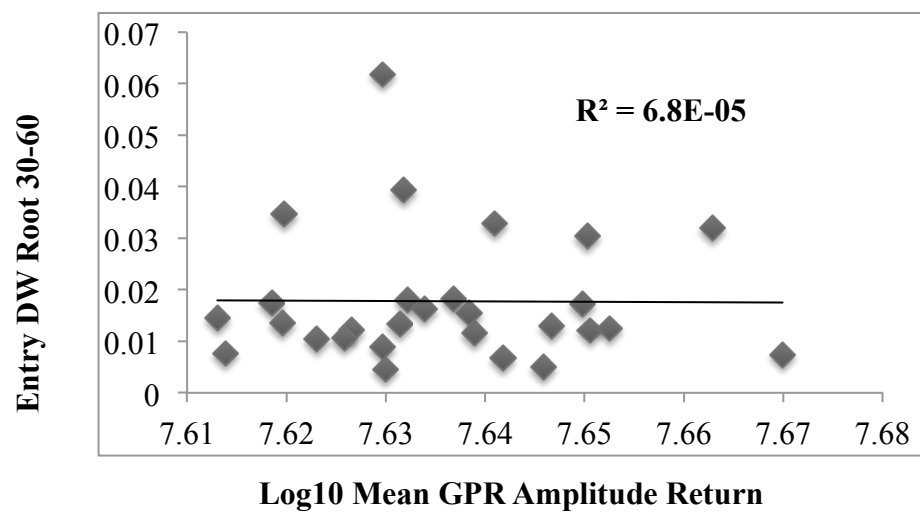


Figure 68. Linear regression between the Log10 of mean ground penetrating radar amplitude returned for the 0-3 ns range and average dry weight (DW) root biomass collected at 30-60 cm for each wheat variety.

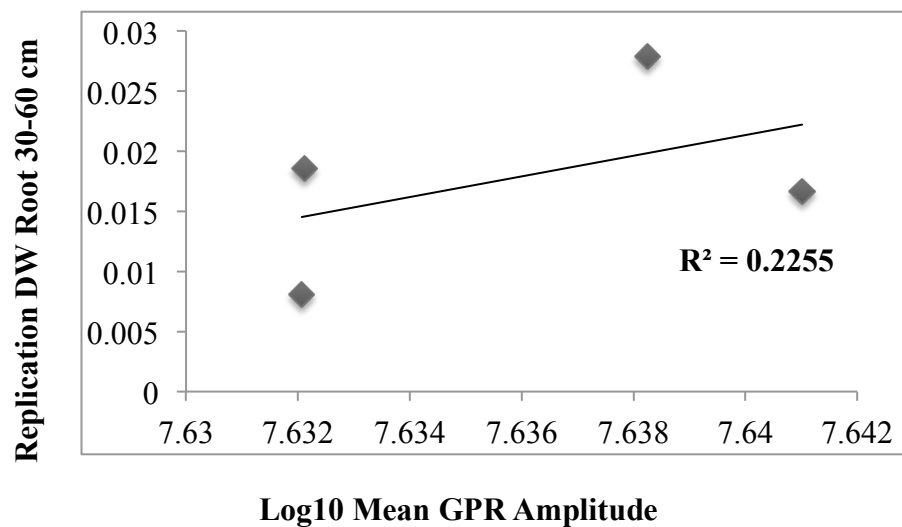


Figure 69. Linear regression between the Log10 of mean ground penetrating radar amplitude returned for the 0-3 ns range and average dry weight (DW) root biomass collected at 30-60 cm for each experimental replication.

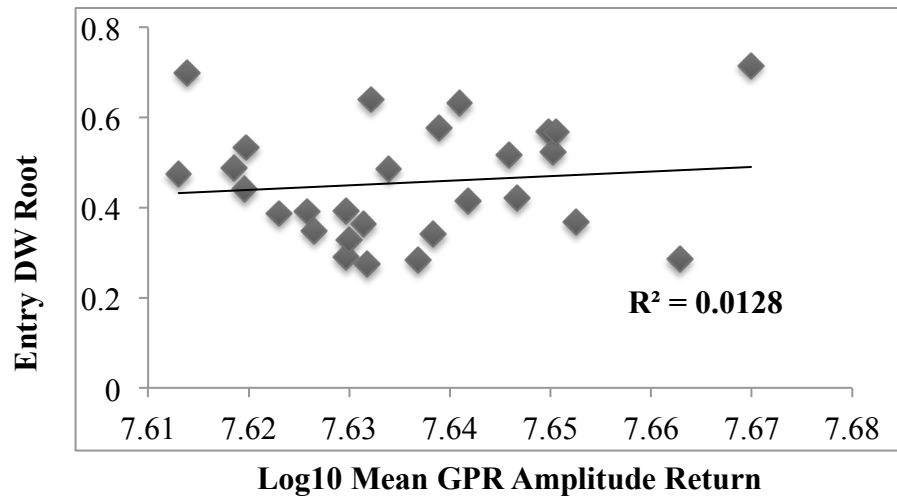


Figure 70. Linear regression between the Log10 of mean ground penetrating radar amplitude returned for the 0-3 ns range and average dry weight (DW) root biomass collected at 0-60 cm for each wheat variety.

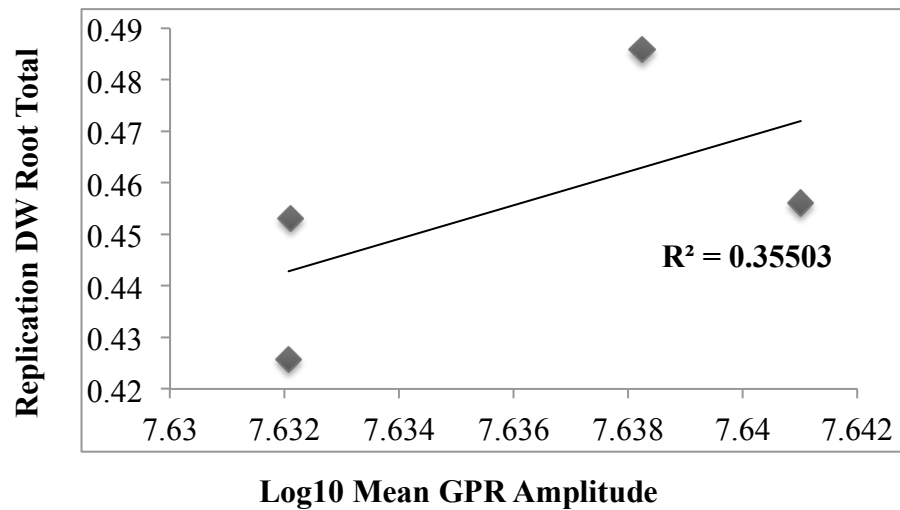


Figure 71. Linear regression between the Log10 of mean ground penetrating radar amplitude returned for the 0-3 ns range and average dry weight (DW) root biomass collected at 0-60 cm for each experimental replication.

### ***Electrical conductivity mapping***

EC was mapped using GPS coordinates in ArcGIS (ESRI, Redlands, CA, USA).

Kriging was used to develop an EC prediction for the experimental trial (Figure 72).

Field spatial variability is classified into six contours differing in soil EC.

## **Discussion**

### ***GPR wheat root discrimination***

The ability of GPR to non-destructively identify spatially identify tree roots has been established (Hruska et al., 1999). Site specific soils have been shown to limit the root prediction ability of GPR based largely on differences in soil conductivity (Butnor et al., 2003). The use of GPR to non-destructively evaluate crop roots has been neglected in part limited by the expected poor response of highly conductive type agricultural soils. Using a 1.6 GHz antenna we were able to spatially predict plot root interactions of wheat (Figure 33). GPR radar grams collected for each plot revealed a clearly defined area of increased amplitude return within the 0-3 ns range. This area is thought to represent the root cap of the wheat plant. High amplitude returns were spatially consistent with known plot and ally length. High amplitude return was observe for the areas of expected roots below the plot locations while no amplitude return was observed below the trail alleyways where all growth was controlled by herbicide. Combining the four

radiograms collected across each experimental plot provided clear field level distribution of plots based on GPR amplitude return as compared to those of low amplitude return (Figure 34). GPR is capable of identifying root interactions in crop production clay type soils.

GPR was able to predict root presence and absence comparing known plot location and with amplitude return intensity for each position within the experimental trail. GPR was able to differentiate root mass from soil significantly ( $\alpha = 0.95$ ,  $t = 1.96022$ ) (Figure 35).

### ***GPR wheat agronomic trait predictability***

Log10 of the mean GPR amplitude return for each plot in the 0-3 ns range was compared with yield, TKW, KWS, and KNS (Figure 33). Each trait was evaluated by comparison of the mean of four replications for each of the 28 wheat entries as well each trait was evaluated with by the mean of all entries within each of four replications. As expected, the prediction ability of GPR increased for each trait when considering the mean for each replication as compared to the mean across four replications for each entry. TKW was the highest correlated trait between log10 of the mean GPR amplitude return and mean for each replication (Figure 39).

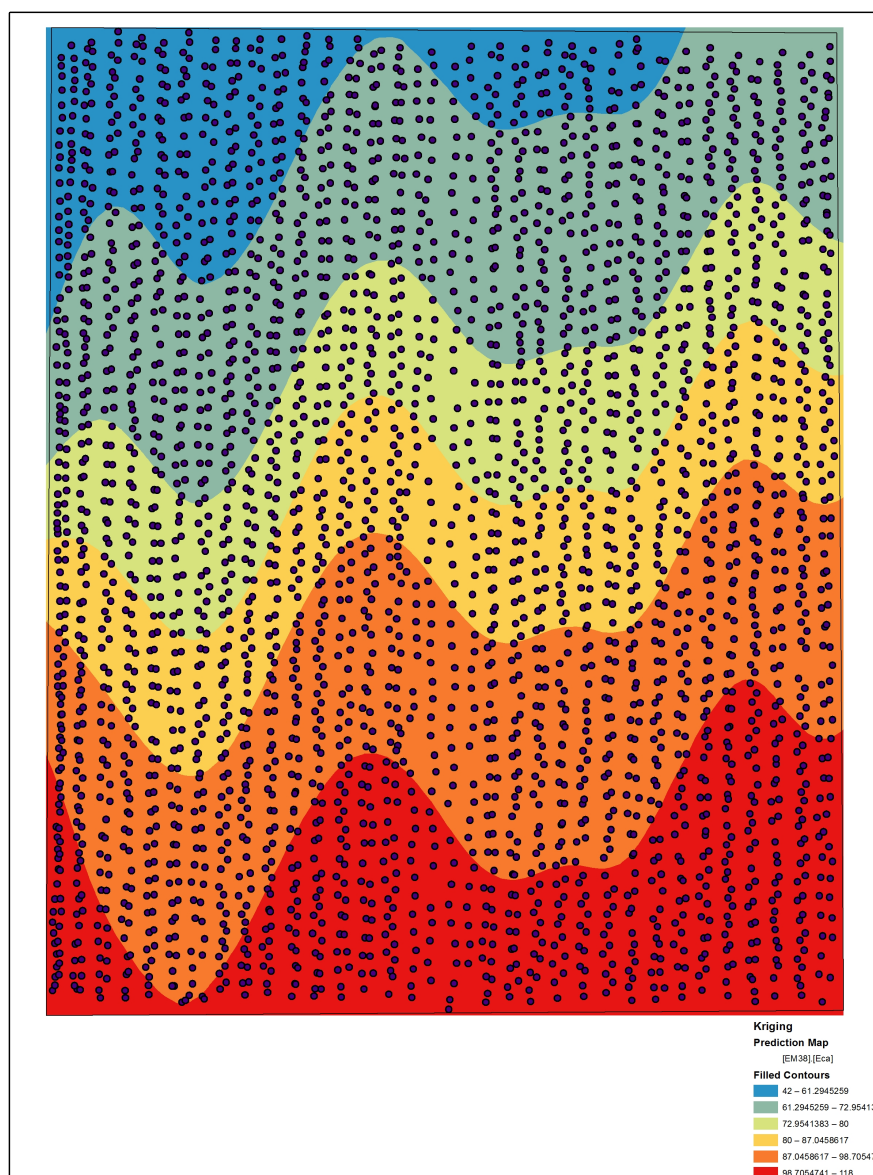


Figure 72. Field soil electrical conductivity map of experimental trial. Differences in electrical conductivity across experimental field trial as predicted by kriging.

KWS was the highest correlated trait between log10 of the mean GPR amplitude return and mean of four replications for each of the 28 wheat entries (Figure 40).

NDVI is capable of evaluating plot establishment and biomass through closure of the crop canopy. Increased biomass is during physiological development can be characterized by increased NDVI indices. Linear regression between NDVI and Log10 of the mean GPR amplitude return for each plot in the 0-3 ns range was evaluated at eight different times during physiological development and maturation. NDVI collected on 4/19/2013 and 4/29/2013 represent vegetative growth and thus a reliable measurement in characterizing establishment and aboveground biomass growth. NDVI collected for both dates was strongly correlated with the log10 of the mean GPR amplitude return against the mean across the four replications for each entry (Figure 51; 53).

### ***Wheat rooting biomass and depth prediction ability***

Log10 of the mean GPR amplitude return for each plot in the 0-3 ns range was compared with FW and DW wheat root biomass of the 0-30, 30-60, and 0-60 cm range of the collected soil cores sampled. The strongest correlation was seen for the combined total of root biomass in both 0-30 and 30-60 cm ranges of the FW samples when compared with the total replication mean ( $R^2 = 0.92526$ ) (Figure 65). Higher correlation was

observed in both the FW and DW samples for the 0-30 cm range as compared to the 30-60 cm range of the soil cores when compared with the total replication means.

### ***Field spatial variability***

Heterogeneity of a testing environment can cause spatial autocorrelation violating the errors assumption of the experimental design being used confounding analysis. The phenotyping environment characterization is essential to reduce error variances ultimately negatively impacting collected data (Araus and Cairns, 2013). Spatial variability can be caused by many different factors including differences in soil. The EC prediction map depicts the spatial variability of the trail as classified into six contours differing in soil EC (Figure 72). The high variability classified by soil EC is consistent with variability seen between yield and physiological data of the four replications within the trail.



## **Conclusions**

### ***Forward strategies***

GPR data presented here is limited by a lack of radar information between the profiles scanned. In this study a 1.6 GHz antenna was utilized on 50 cm profile spacing. Using this antenna we were able to capture 512 sample returns for each position into the soil as well densely collect information in the direction of the profile. However, information within the plot between profile scans was not measured due to equipment and data sampling design, archaeological GPR surveys suffer from this same sampling bias. Using the collected information requires that missing data between profiles be modeled using software designed to reconstruct a prediction of the subsurface (Novo, 2012). Advances in GPR imaging systems have lead to multi-channel systems utilizing several transmitters and receivers spaced centimeters apart within one antenna are capable of collecting this missing data and ultimately allow for true 3D reconstruction of the subsurface (Novo et al., 2013). Use of multi-channel GPR array systems could improve the predictive ability of GPR to estimate wheat root biomass and rooting depth by increasing the amount of data sampling points.

### ***Multi-channel ground penetrating radar systems***

Development of multi-channel GPR systems and data analysis platforms has improved data acquisition speed (Novo et al., 2013). Multi-channel GPS systems allow for complete data collection limiting the need for interpolation between widely spaced profiles as with traditional GPR platforms. Archeological sites previously mapped using single antenna GPR systems have been evaluated using the STREAM X multi-channel GPR platform with improved results (Novo et al., 2013).

### ***Advances in ground penetrating radar data analysis***

GPR analysis software has improved allowing for collection, processing, and 3D visualization of multi-channel highly dense datasets (Novo et al., 2013). The highly dense datasets produced by the multi-channel systems requires additional processing however the time required to do so is comparable to standard formats.

## **CHAPTER V**

### **SUMMARY**

#### **Field-based high-throughput phenotyping**

Rapid advances in agricultural technology have been transformative in recent decades leading one to view innovation as silver bullet capable of meeting the world's needs. However sustainable advances in agriculture will not be seen through individual discoveries and innovations. It is important to consider the enormous effort that has grown wheat yield to current benchmarks as well understand the scientific basis for these incremental advances over time. The speed advantage sought by plant breeding through field-based high-throughput platforms is possible only in the context of facilitating an already proven science.

#### **Terrestrial laser scanning**

Terrestrial laser scanning (TLS) has a potential to be used in wheat breeding for identification of aboveground characteristics. Limited variation between treatments within the experimental plots limited the value of the study evident from the lack of correlation between plot forage yield and traditional sampling methodologies. However, we were able to identify possible TLS data components with increased ability to correlate against traditional methodologies driving a need for further study.

## **Ground penetrating radar**

Ground penetrating radar (GPR) has shown strong potential for use in non-destructive characterization of wheat roots. The ability of GPR to non-invasively predict root presence absence is promising in allowing breeders the ability to evaluate root traits. Soil spatial variability will need to be considered in future studies, as this was a major limitation in the ability of GPR to quantify root biomass and depth. Additionally, future studies need to focus on the use of multi array GPR systems allowing for high-throughput dense data collection to remove sampling bias. Data analysis platforms will need to be developed to streamline processing of field data allowing for quick assessment and standardization.

## LITERATURE CITED

Amato M, Bitella G, Rossi R, Gomez JA, Lovelli S, Gomes JJF (2009) Multi-electrode 3D resistivity imaging of alfalfa root zone. *European Journal of Agronomy* 31:213-222

Ammar K, Lage J, Villegas D, Crossa J, Hernandez H, Alvarado G (2008) Association among durum wheat international testing sites and trends in yield progress over the last twenty-two years. *International symposium on wheat yield potential: challenges to international wheat breeding Mexico DF, Mexico: CIMMYT*, pp 108-119

Antonarakis AS, Richards KS, Brasington J, Muller E (2010) Determining leaf area index and leafy tree roughness using terrestrial laser scanning. *Water Resour Res* 46:1-12

Aparicio N, Villegas D, Casadesus J, Araus JL, Royo C (2000) Spectral vegetation indices as nondestructive tools for determining durum wheat yield. *Agronomy Journal* 92:83-91

Araus JL, Cairns JE (2013) Field high-throughput phenotyping: the new crop breeding frontier. *Trends in Plant Science* 19:52-61

Araus JL, Slafer GA, Royo C, Serret MD (2008) Breeding for yield potential and stress adaptation in cereals. *Critical Reviews in Plant Sciences* 27:377-412

Assad MT, Paulsen GM (2002) Genetic changes in resistance to environmental stresses by U.S. Great Plains wheat cultivars. *Euphytica* 128:87-96

Attia al Hagrey S (2006) Geophysical imaging of root-zone, trunk, and moisture heterogeneity. *J Exp Bot* 58:839-854

Bauriegel E, Giebel A, Geyer M, Schmidt U, Herppich WB (2011) Early detection of Fusarium infection in wheat using hyper-spectral imaging. *Comput Electron Agric* 75:304-312

Benfey PN, Mitchell-Olds T (2008) From genotype to phenotype: systems biology meets natural variation. *Science* 320:495-497

Bengough AG, McKenzie BM, Hallett PD, Valentine TA (2011) Root elongation, water stress, and mechanical impedance: a review of limiting stresses and beneficial root tip traits. *J Exp Bot* 62:59-68

Bernardo RN (2010) Breeding for quantitative traits in plants, 2nd edn. Stemma Press, Woodbury, Minn.

Bitá CE, Gerats T (2013) Plant tolerance to high temperature in a changing environment: scientific fundamentals and production of heat stress-tolerant crops. *Front Plant Sci* 4:273

Bohm W (1979) Methods of studying root systems. Springer-Verlag., Gottingen, German

Boopathi NM (2013) Genetic mapping and marker assisted selection. Basics, Practice and Benefits. Springer India, New Delhi ; New York, pp xv, 293 p.

Box JR, EL (1993) Minirhizotron wheat root data: comparisons with soil core root data. *Agronomy Journal* 85:1058-1060

Bragg PL, Govi G, Cannell RQ (1983) A comparison of methods, including angled and vertical minirhizotrons, for studying root growth and distribution in a spring oat crop. *Plant Soil* 73:435-440

Butnor JR, Doolittle JA, Kress L, Cohen S, Johnsen KH (2001) Use of ground-penetrating radar to study tree roots in the southeastern United States. *Tree Physiol* 21:1269-1278

Butnor JR, Kress L, Johnsen KH, Samuelson L, Doolittle JA, Stokes T (2003) Utility of ground-penetrating radar as a root biomass survey tool in forest systems. *Soil Science Society of America Journal* 67:1607-1615

Cabrera-Bosquet L, Crossa J, von Zitzewitz J, Serret MD, Araus JL (2012) High-throughput phenotyping and genomic selection: the frontiers of crop breeding converge. *J Integr Plant Biol* 54:312-320

Cassman KG, Dobermann A, Walters DT, Yang H (2003) Meeting cereal demand while protecting natural resources and improving environmental quality. *Annu Rev Env Resour* 28:315-358

Chow TE, Hodgson ME (2009) Effects of lidar post-spacing and DEM resolution to mean slope estimation. *International Journal of Geographical Information Science* 23:1277-1295

Collard BC, Mackill DJ (2008a) Marker-assisted selection: an approach for precision plant breeding in the twenty-first century. *Philosophical transactions of the Royal Society of London Series B, Biological sciences* 363:557-572

Collard BCY, Jahufer MZZ, Brouwer JB, Pang ECK (2005) An introduction to markers, quantitative trait loci (QTL) mapping and marker-assisted selection for crop improvement: The basic concepts. *Euphytica* 142:169-196

Collard BCY, Mackill DJ (2008b) Marker-assisted selection: an approach for precision plant breeding in the twenty-first century. *Philosophical Transactions of the Royal Society B: Biological Sciences*, pp 557-572

Cossani CM, Reynolds MP (2012) Physiological traits for improving heat tolerance in wheat. *Plant Physiol* 160:1710-1718

Daniels JJ (2000) Ground penetrating radar fundamentals. U.S. EPA Report, Appendix 1–21

Davey JW, Hohenlohe PA, Etter PD, Boone JQ, Catchen JM, Blaxter ML (2011) Genome-wide genetic marker discovery and genotyping using next-generation sequencing. *Nat Rev Genet* 12:499-510

Durlless H, Stanjek H (1997) Capability and limits of a DGPS supported EM38 survey for the fast estimation of the spatial variation of clay and water contents of soils. *Field Screening Europe*:73-76

Easson DL, Pickles SJ, White EM (1995) A study of the tensile force required to pull wheat roots from soil. *Ann Appl Biol* 127:363-373

Eitel JUH, Vierling LA, Long DS (2010) Simultaneous measurements of plant structure and chlorophyll content in broadleaf saplings with a terrestrial laser scanner. *Remote Sensing of Environment* 114:2229-2237

Eizenberg H (2005) A new method for in-situ monitoring of the underground development of orobanche cumana in sunflower (*Helianthus annuus*) with a mini-rhizotron. *Ann Bot-London* 96:1137-1140

Evans LT, Fischer RA (1999) Yield potential: Its definition, measurement, and significance. *Crop Sci* 39:1544-1551

FAO (2013) The State of Food and Agriculture 2013 - Executive Summary. pp 1-6

FAO, IFAD, WFP (2013) The State of Food Insecurity in the World 2013. The multiple dimensions of food security, Rome

Ferris R, Ellis RH, Wheeler TR, Hadley P (1998) Effect of high temperature stress at anthesis on grain yield and biomass of field-grown crops of wheat. *Ann Bot-London* 82:631-639

Franks AM (2013) Small grains forage management and evaluation in central texas. Department of Soil and Crop Sciences. Texas A&M University, 2013

Freeland RS, Yoder RE, Ammons JT (1998) Mapping shallow underground features that influence site-specific agricultural production. *J Appl Geophys* 40:19-27

Garrigues E, Doussan C, Pierret A (2006) Water Uptake by plant roots: I –formation and propagation of a water extraction front in mature root systems as evidenced by 2D light transmission imaging. *Plant Soil* 283:83-98

Gewin V (2010) An underground revolution. *Nature* 466:552-553



Goodman D (1994) Ground-penetrating radar simulation in engineering and archaeology. *Geophysics* 59:224-232

Goodman D, Piro S (2013) *GPR remote sensing in archaeology*. Springer

Guo L, Chen J, Cui X, Fan B, Lin H (2012) Application of ground penetrating radar for coarse root detection and quantification: a review. *Plant Soil* 362:1-23

Haro von Mogel K (2013) Taking the phenomics revolution into the field. *CSA News* 58:4-10

Hays DB, Do JH, Mason RE, Morgan G, Finlayson SA (2007) Heat stress induced ethylene production in developing wheat grains induces kernel abortion and increased maturation in a susceptible cultivar. *Plant Science* 172:1113-1123

Hemingway E (1964) *A moveable feast*. Scribner, New York,

Hodson DP, White JW (2007) Use of spatial analyses for global characterization of wheat-based production systems. *J Agric Sci* 145:115

Hofle B, Pfeifer N (2007) Correction of laser scanning intensity data: data and model-driven approaches. *Isprs J Photogramm* 62:415-433

Hosoi F, Omasa K (2009) Estimating vertical plant area density profile and growth parameters of a wheat canopy at different growth stages using three-dimensional portable lidar imaging. *ISPRS Journal of Photogrammetry and Remote Sensing* 64:151-158

Hruska J, Cermak J, Šustek S (1999) Mapping tree root systems with ground-penetrating radar. *Tree Physiol* 19:125-130

IPCC (2007) *Climate Change 2007 : impacts, adaptation and vulnerability : contribution of Working Group II to the fourth assessment report of the Intergovernmental Panel on Climate Change*. In: M.L. Parry OFC, J.P. Palutikof, P.J. van der Linden and C.E., Hanson (eds). Cambridge University Press, Cambridge ; UK, pp ix, 976 p.

Jones HG, Serraj R, Loveys BR, Xiong L, Wheaton A, Price AH (2009) Thermal infrared imaging of crop canopies for the remote diagnosis and quantification of plant responses to water stress in the field. *Functional Plant Biol* 36:978

Kell DB (2011) Breeding crop plants with deep roots: their role in sustainable carbon, nutrient and water sequestration. *Ann Bot-London* 108:407-418

Large EC (1954) Growth stages in cereals illustration of the feekes scale. *Plant pathology* 3:128-129

Lemmens M (2011) *Terrestrial laser scanning*. Springer

Leucci G (2010) The use of three geophysical methods for 3D images of total root volume of soil in urban environments. *Explor Geophys* 41:268

Lipiec J, Doussan C, Nosalewicz A, Kondracka K (2013) Effect of drought and heat stresses on plant growth and yield: a review. *International Agrophysics* 27

Lobell DB, Ortiz-Monasterio JI, Asner GP, Matson PA, Naylor RL, Falcon WP (2005) Analysis of wheat yield and climatic trends in Mexico. *Field Crop Res* 94:250-256

Lopes MS, Reynolds MP (2010) Partitioning of assimilates to deeper roots is associated with cooler canopies and increased yield under drought in wheat. *Funct Plant Biol* 37:147

Lumme J, Karjalainen M, Kaartinen H, Kukko A, Hyypä J, Hyypä H, Jaakkola A, Kleemola J (2008) Terrestrial laser scanning of agricultural crops. *The International Achieves of the Photogrammetry, Remote Sensing and Spatial Information Sciences* 47:563-566

Majdi H, Nylund J-E (1996) Does liquid fertilization affect fine root dynamics and lifespan of mycorrhizal short roots? *Plant Soil* 185:305-309

Mason R, Singh R (2014) Considerations when deploying canopy temperature to select high yielding wheat breeding lines under drought and heat stress. *Agronomy* 4:191-201

- Mba C, Guimaraes EP, Ghosh K (2012) Re-orienting crop improvement for the changing climatic conditions of the 21st century. *Agric Food Secur* 1:7
- Miglietta F, Bindi M, Vaccari FP, Schapendonk A, Wolf J, Butterfield RE (2000) Crop ecosystem responses to climatic change: root and tuberous crops
- Msangi S, Tokgoz S, Batka M, Rosegrant M (2009) Investment requirements under new demands on world agriculture: feeding the world with bioenergy and climate change:1-18
- Neal A (2004) Ground-penetrating radar and its use in sedimentology: principles, problems and progress. *Earth-Sci Rev* 66:261
- Neumann G, George TS, Plassard C (2009) Strategies and methods for studying the rhizosphere—the plant science toolbox. *Plant Soil* 321:431-456
- Novo (2012) From pseudo-3D to full-resolution GPR imaging of a complex Roman site. NSG
- Novo A, Leckebusch J, Goodman D, Morelli G, Piro S, Catanzariti G (2013) Advances in GPR imaging with multi-channel radar systems. *Journal of Surveying and Mapping Engineering*
- NRCS U (2009) Web soil survey. URL <http://www.websoilsurvey.nrcs.usda.gov/app/>[verified October 29, 2009]
- Pask AJD, Pietragalla J, Mullan DM, Reynolds MP (2012) Physiological breeding II: a field guide to wheat phenotyping. CIMMYT
- Passioura JB (2012) Phenotyping for drought tolerance in grain crops: when is it useful to breeders? *Funct Plant Biol* 39:851-859
- Pesci A, Teza G (2008) Effects of surface irregularities on intensity data from laser scanning: an experimental approach. *Ann Geophys-Italy* 51:839-848

Pierret A, Moran CJ, Doussan C (2005) Conventional detection methodology is limiting our ability to understand the roles and functions of fine roots. *New Phytologist* 166:967-980

Pinchak WE, Worrall WD, Caldwell SP, Hunt LJ, Worrall NJ, Conoly M (1996) Interrelationships of forage and steer growth dynamics on wheat pasture. *J Range Manage* 49:126-130

Poland JA, Rife TW (2012) Genotyping-by-sequencing for plant breeding and genetics. *Plant Genome-U*s 5:92-102

Polomski J, Kuhn N, Waisel Y, Eshel A, Kafkafi U (2002) Root research methods. *Plant Roots: The Hidden Half*;295-321

Reynolds M, Bonnett D, Chapman SC, Furbank RT, Manes Y, Mather DE, Parry MAJ (2010) Raising yield potential of wheat. I. overview of a consortium approach and breeding strategies. *J Exp Bot* 62:439-452

Reynolds M, Manes Y, Izanloo A, Langridge P (2009) Phenotyping approaches for physiological breeding and gene discovery in wheat. *Ann Applied Biology* 155:309-320

Reynolds MP (2010) *Climate Change & Crop Production*, 1 edn. CABI,, Wallingford

Reynolds MP, Balota M, Delgado MIB, Amani I, Fischer RA (1994) Physiological and morphological traits associated with spring wheat yield under hot, irrigated conditions. *Aust J Plant Physiol* 21:717-730

Reynolds MP, Pask A, Mullan DM (2012) Physiological breeding I: interdisciplinary approaches to improve crop adaptation. *CIMMYT* (free PDF download)

Ronald P (2011) Plant genetics, sustainable agriculture and global food security. *Genetics* 188:11-20

Rutherford MC, Curran B (1981) A root observation chamber for replicated use in a natural plant community. *Plant Soil* 63:123-129

Sayre KD, Rajaram S, FISCHER RA (1997) Yield potential progress in short bread wheats in northwest Mexico. *Crop Sci* 37:36-42

Schmidhuber J, Tubiello FN (2007) Global food security under climate change. *P Natl Acad Sci USA* 104:19703-19708

Schroth G, Kolbe D (1994) A method of processing soil core samples for root studies by subsampling. *Biology and Fertility of Soils* 18:60-62

Shinozaki K, Yamaguchi-Shinozaki K (2007) Gene networks involved in drought stress response and tolerance. *J Exp Bot* 58:221-227

Sleper DA, Poehlman JM (2006) *Breeding field crops*, 5th edn. Blackwell Pub., Ames, Iowa

Sui R, Fisher DK, N Reddy K (2012) Cotton yield assessment using plant height mapping system. *JAS* 5

Tester M, Langridge P (2010) Breeding technologies to increase crop production in a changing world. *Science* 327:818-822

Trachsel S, Kaeppler SM, Brown KM, Lynch JP (2010) Shovelomics: high throughput phenotyping of maize (*Zea mays* L.) root architecture in the field. *Plant Soil* 341:75-87

Trethowan RM, van Ginkel M, Rajaram S (2002) Progress in breeding wheat for yield and adaptation in global drought affected environments. *Crop Sci* 42:1441-1446

Wang G (2005) Agricultural drought in a future climate: results from 15 global climate models participating in the IPCC 4th assessment. *Clim Dyn* 25:739-753

Wardlaw IF, Wrigley CW (1994) Heat tolerance in temperate cereals - an overview. *Aust J Plant Physiol* 21:695-703

Whan BR, Carlton GP, Anderson WK (1991) Potential for increasing early vigour and total biomass in spring wheat. I. Identification of genetic improvements. *Crop Pasture Sci* 42:347-361

White JW, Andrade-Sanchez P, Gore MA, Bronson KF, Coffelt TA, Conley MM, Feldmann KA, French AN, Heun JT, Hunsaker DJ, Jenks MA, Kimball BA, Roth RL, Strand RJ, Thorp KR, Wall GW, Wang G (2012) Field-based phenomics for plant genetics research. *Field Crop Res* 133:101-112

## APPENDIX A

### FEELKS SCALE

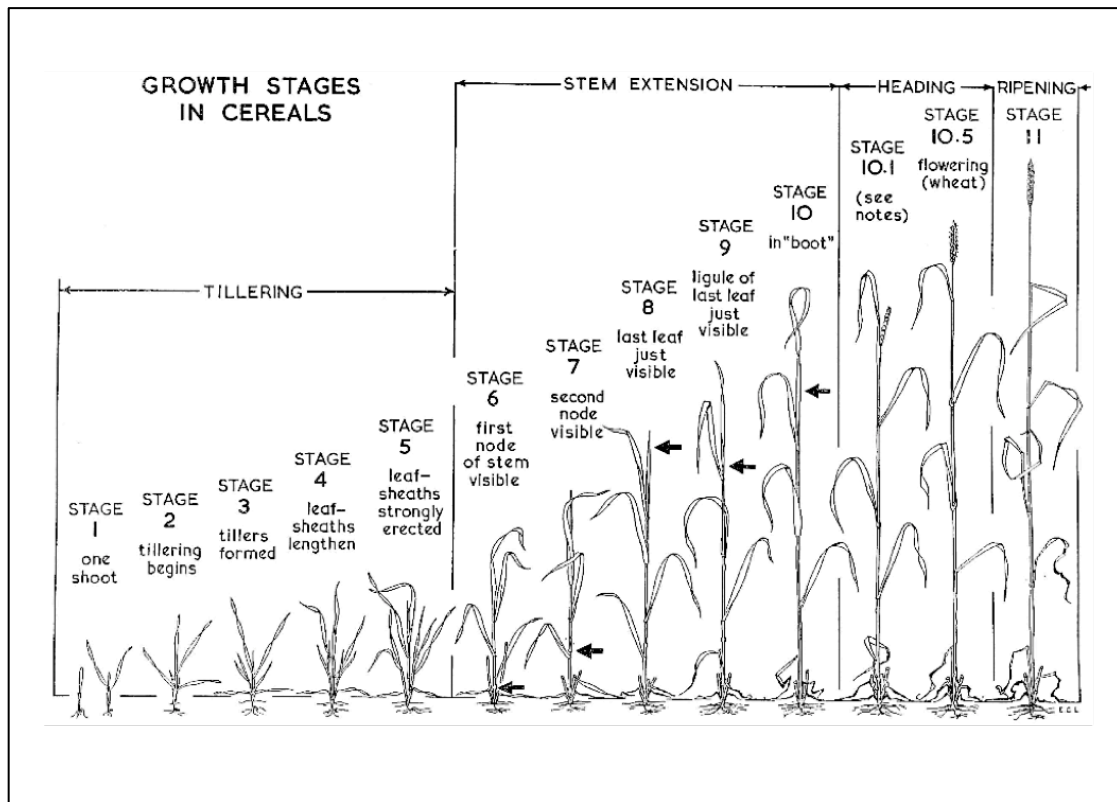


Figure 73. Illustration of the Feekes scale of growth stages in cereals (Large, 1954).

Description of the Feekes scale as described by E. C. Large (Large, 1954).

Stage: Tillering

- 1 One shoot (number of leaves can be added) = "brairding"
- 2 Beginning of tillering
- 3 Tillers formed, leaves often twisted spirally. In some varieties of winter wheats, plants may be "creeping" or prostrate
- 4 Beginning of the erection of the pseudo-stem, leaf sheaths beginning to lengthen
- 5 Pseudo-stem (formed by sheaths of leaves) strongly erected

Stage: Stem Extension

- 6 First node of stem visible at base of shoot
- 7 Second node of stem formed, next-to-last leaf just visible
- 8 Last leaf visible, but still rolled up, ear beginning to swell
- 9 Ligule of last leaf just visible
- 10 Sheath of last leaf completely grown out, ear swollen but not yet visible

Stage: Heading

- 10.1 First ears just visible (awns just showing in barley, ear escaping through split of sheath in wheat or oats)
- 10.2 Quarter of heading process completed
- 10.3 Half of heading process completed
- 10.4 Three-quarters of heading process completed
- 10.5 All ears out of sheath

Stage: Flowering (Jones et al.)

- 10.5.1 Beginning of flowering (Jones et al.)
- 10.5.2 Flowering complete to top of ear
- 10.5.3 Flowering over at base of ear
- 10.5.4 Flowering over, kernel watery ripe

Stage: Ripening

- 11.1 Milky ripe
- 11.2 Mealy ripe, contents of kernel soft but dry
- 11.3 Kernel hard (difficult to divide by thumb-nail)
- 11.4 Ripe for cutting. Straw dead



## **APPENDIX B**

### **STUTT GART SOIL**

#### **Stuttgart Soil**

Stuttgart soils are named for the City of Stuttgart in Southeast Arkansas. They are used primarily for cropland with the dominant crops being rice, soybeans, small grains, and corn. The Stuttgart area is famous for its large fall and winter population of ducks and geese. These waterfowl feed heavily on the crops grown on the Stuttgart soils. Stuttgart soils have been mapped on about 200,000 acres in Arkansas. The Stuttgart series consists of very deep moderately well to somewhat poorly drained soils formed in silty and clayey alluvium. These level to gently sloping soils are on Prairie terraces in the Lower Mississippi Valley. Stuttgart's silt loam surface texture and the slow permeability in its clayey subsoil makes the soil ideal for rice production (NRCS, 2009).

#### **Typical Stuttgart Soil Profile**

Surface:	0 to 11 inches - dark grayish brown and grayish brown silt loam
Subsurface:	11 to 23 inches - yellowish brown silt loam
Subsoil:	23 - 35 inches - red silty clay; 35 - 80 inches - grayish brown and light brownish gray silty clay loam.

## **Soil Family Classification**

Fine, smectitic, thermic Albaquultic Hapludalfs

Stuttgart soils are in the Alfisols soil order. Alfisols are mostly soils of intermediate age.

The "Albaquultic" subgroup implies that the soil has an abrupt textural change, has a moderately high water table during part of the year, and that the base saturation is less than 60 percent at 50 inches below the top of the subsoil. The term "fine" indicates that the upper subsoil averages between 35 and 60 percent clay. The term "smectitic" implies that the clay in the subsoil is dominated by minerals that expand upon wetting and contract upon drying. "Thermic" refers to an average annual soil temperature of between 15° to 22°C (59° to 72°F) (NRCS, 2009).